

## **What is this document?**

This is a comparison of two documents. The two documents are interleaved such that the left document is displayed on even pages and the right document is displayed on odd pages.

## **Is there a specific way I should view this file?**

This document is intended to be viewed in Two Page Continuous mode (or sometimes called 'Two Page Scrolling'). It should open in this mode by default when using Adobe Acrobat and most popular PDF readers.

If the document opens in a different view, you can often change this in the settings. In Adobe Acrobat, go to **View > Page Display > Two Page Scrolling**.

## **Why are there blank pages?**

Blank pages are inserted to keep both documents as aligned as much as possible.

## **How do I read the changes?**

Text deleted from the left document and, hence, not in right document is highlighted red. Text added to the right document and, hence, not in left document is highlighted green.

## **Tip for printing**

When printing this document, we recommend printing double-sided and include this first page. This will result in the matching text being displayed on different pages and easily readable, much like a book.

# Transport coefficients in standard Kappa distributed plasmas

Mahmood J. Jwailes , Imad A. Barghouthi , and Qusay S. Atawnah

Department of physics, Al-Quds university, Jerusalem, Palestine.

**Correspondence:** Mahmood J. Jwailes (mahmood.jwailes@students.alquds.edu)

**Abstract.** This study presents a systematic derivation of transport coefficients—including electrical conductivity, thermoelectric, diffusion, and mobility coefficients—for a Lorentz plasma described by a standard Kappa distribution function. The analysis is implemented within the framework of the five-moment transport equations, in which the standard Kappa distribution is adopted as the zeroth-order function. Momentum and energy collision terms are then evaluated using the Boltzmann collision integral for several types of collisions, including Coulomb collisions, hard-sphere interactions, and Maxwell molecules. These collision terms are incorporated into the momentum equation to construct expressions for the generalized Ohm's law and extended Fick's law, from which the transport coefficients are obtained. The influence of the kappa parameter on the collision terms and transport coefficients is examined in detail, revealing that low kappa values reduce the effective collision frequency and enhance transport coefficients in the standard Kappa distribution, in contrast to the behavior reported for the modified Kappa distribution. Finally, in the asymptotic limit of large kappa values, the transport coefficients consistently recover their Maxwellian forms.

## 1 Introduction

Transport processes in plasma can be analyzed using transport equations, which provide a macroscopic description of the spatial and temporal evolution of the velocity moments of the particles velocity distribution function. These moments (e.g. number density, drift velocity, temperature, pressure tensor, stress tensor, and heat flow vector) capture the collective behavior of plasma particles and interactions that determine their dynamics (Schunk, 1977; Schunk and Nagy, 2009; Bittencourt, 2004). The transport equations are based on linear relationships between the fluxes (e.g., particle flux, heat flux, and current density), the external forces and gradients (e.g., in density, temperature, and pressure) that drive those fluxes. The constants of proportionality in these linear relations are called transport coefficients—namely, the diffusion coefficient, electrical conductivity, mobility coefficient, thermoelectric coefficient, and thermal conductivity—which quantify how particles and energy move through a plasma under the influence of gradients, external forces, and applied electromagnetic forces. Each coefficient characterizes a different aspect of transport, that is, the diffusion coefficient measures the flux of particles driven by spatial variations in density, providing insight into how species spread within the plasma. The mobility coefficient describes how charged particles drift in response to an applied electric field, and it is directly related to the electrical conductivity, which connects the current density to the electric field. The thermoelectric coefficient links electric fields to temperature gradients and characterizes the generation of electric voltages and currents in non-uniform thermal environments. Finally, the thermal conductivity

# Transport coefficients in standard Kappa distributed plasmas: A comparative study

Mahmood J. Jwailes , Imad A. Barghouthi , and Qusay S. Atawnah

Department of physics, Al-Quds university, Jerusalem, Palestine.

**Correspondence:** Mahmood J. Jwailes (mahmood.jwailes@students.alquds.edu)

**Abstract.** This study systematically derives transport coefficients—electrical conductivity, thermoelectric, diffusion, and mobility—for a Lorentz plasma described by a standard Kappa distribution function. Within the five-moment transport framework, the standard Kappa distribution serves as the zeroth-order function. Momentum and energy collision terms are obtained via the Boltzmann collision integral for Coulomb, hard-sphere, and Maxwell molecule interactions, and incorporated into the momentum equation to formulate generalized Ohm's and extended Fick's laws, yielding the transport coefficients. This study also compares the standard Kappa, modified Kappa, and Maxwellian distributions in terms of their influence on plasma behavior. The results show that for velocity-dependent collisions, such as Coulomb collisions, significant differences arise between the standard and modified Kappa distributions. For low kappa parameter  $\kappa$  values, the standard Kappa distribution reduces collision frequency and thermalization, making it suitable for collisionless or weakly collisional plasmas. In contrast, the modified Kappa distribution increases these effects, indicating its relevance for more collisional environments. Consequently, in Coulomb collisions, the standard distribution weakens momentum and energy exchange compared to the Maxwellian case, while the modified distribution enhances them. Transport properties are also affected differently: as  $\kappa$  decreases, the standard distribution enhances conductivity, mobility, diffusion, and thermoelectric effects, whereas the modified distribution reduces conductivity, mobility, and diffusion, with no change in the thermoelectric coefficient.

## 1 Introduction

Transport processes in plasma can be described using transport equations, which provide a macroscopic representation of the system through velocity moments of the particle distribution function (Schunk, 1977; Schunk and Nagy, 2009; Bittencourt, 2004). These equations are based on linear relationships between the fluxes (e.g., particle flux, heat flux, and current density) and the external forces and gradients (e.g., in density, temperature, and pressure) that drive those fluxes.

The constants of proportionality in these linear relations are known as transport coefficients—namely, the diffusion coefficient, electrical conductivity, mobility coefficient, thermoelectric coefficient, and thermal conductivity—which quantify how particles and energy move through a plasma under the influence of gradients, and applied external forces. Each coefficient characterizes a different aspect of transport, that is, the diffusion coefficient measures the flux of particles driven by spatial variations in density, providing insight into how species spread within the plasma. The mobility coefficient describes how charged particles drift in response to an applied electric field, and it is directly related to the electrical conductivity, which con-



determines the heat flux produced by temperature gradients and governs the rate of thermal energy transport within the plasma (Du, 2013; Wang and Du, 2017; Ebne Abbasi et al., 2017; Ebne Abbasi and Esfandyari-Kalejahi, 2019; Guo and Du, 2019; Husidic et al., 2021).

30 For plasmas near thermal equilibrium, the Maxwellian distribution is commonly used to evaluate transport coefficients. However, space and astrophysical plasmas often contain nonthermal particle populations that cause particle velocity distributions to deviate from the Maxwellian form. In these nonthermal environments, such distributions are well fitted by the Kappa velocity distribution functions (Marsch, 2006). Kappa distributions are considered powerful class of non-Maxwellian distributions, characterized by a power-law tail that captures the presence of suprathermal particles, features that the Maxwellian distribution 35 fails to describe.

Consequently, several studies have extensively investigated transport coefficients in nonequilibrium plasmas using the Kappa velocity distribution functions. In particular, studies such as Du (2013); Wang and Du (2017); Ebne Abbasi et al. (2017); Ebne Abbasi and Esfandyari-Kalejahi (2019); Guo and Du (2019); Jwailes et al. (2025) derived diffusion, mobility, electrical conductivity, thermoelectric coefficients, and thermal conductivity based on modified Kappa distributions, which assume a  $\kappa$ - 40 independent effective temperature and therefore produce a stronger low-energy core and enhanced suprathermal tails relative to a Maxwellian. Here, the kappa parameter  $\kappa$ , controls the population of high-energy suprathermal particles. However, this modified form differs fundamentally from the standard (Olbertian) Kappa distribution, introduced by Olbert (1968) and Vasylunas (1968), in which the effective temperature is  $\kappa$ -dependent, leading to weaker core and more pronounced high-energy tails. This motivated Husidic et al. (2021) to evaluate the same transport coefficients for the standard Kappa distribution, demonstrating 45 that distinctions between the two forms are crucial because the choice of distribution impacts the resulting transport coefficients and their physical interpretation.

All of the reviewed studies used simplified collision models rather than the full Boltzmann collision integral. The simplest models appear in Wang and Du (2017), Ebne Abbasi and Esfandyari-Kalejahi (2019), and Husidic et al. (2021) which used Krook-type or BGK operators, offering computational simplicity but limited accuracy. More physically based models—such as 50 those proposed by Du (2013) and Guo and Du (2019)—used macroscopic transport equations derived from idealized relaxation assumptions. The most advanced work, presented by Ebne Abbasi et al. (2017), used the Fokker-Planck equation to model Coulomb collisions. While this captures cumulative small-angle scattering and better represents long-range Coulomb forces, it remains an approximation of the Boltzmann collision integral. Thus, all reviewed works share the same limitation: reliance on simplified collision models. To overcome this limitation, Jwailes et al. (2025) recently introduced a comprehensive re- 55 evaluation of the transport coefficients based on the modified Kappa distribution, using the five-moment approximation of the transport equations with the Boltzmann collision integral as the collision model. In this approach, a new transport theory is developed by deriving the five-moment approximation and the corresponding collision terms for various types of collisions for the modified Kappa distribution. The five-moment momentum equation is then linked to the generalized Ohm's law and the extended Fick's law, from which the transport coefficients are determined.

60 This study is inspired by the work of Husidic et al. (2021) and follows the same methodology and steps introduced by Jwailes et al. (2025). As in Husidic et al. (2021), we focus on evaluating the transport coefficients for the standard Kappa distribution,

nects the current density to the electric field. The thermoelectric coefficient links electric fields to temperature gradients and characterizes the generation of electric voltages and currents in nonuniform thermal environments. Finally, the thermal conductivity determines the heat flux produced by temperature gradients and governs the rate of thermal energy transport within the plasma (Du, 2013; Wang and Du, 2017; Ebne Abbasi et al., 2017; Ebne Abbasi and Esfandyari-Kalejahi, 2019; Husidic et al., 2021).

For plasmas near thermal equilibrium, the Maxwellian distribution is commonly used to evaluate transport coefficients. However, space and astrophysical plasmas often contain nonthermal particle populations that cause particle velocity distributions to deviate from the Maxwellian form. In these nonthermal environments, such distributions are well fitted by the Kappa velocity distribution functions (Marsch, 2006). Unlike the Maxwellian distribution, the Kappa distributions introduce a power-law tail that decays more slowly than the exponential tail of the Maxwellian, making them able to capture the presence of suprathermal particles, a feature that the Maxwellian distribution fails to describe. The shape of this tail is controlled by the kappa parameter  $\kappa$ , which determines the strength of the high-energy tail: larger  $\kappa$  values approach the Maxwellian limit, while smaller values emphasize suprathermal populations. With typical  $\kappa$  values ranging between 2 and 6, Kappa distributions have been observed across diverse plasma environments, including the solar wind, Earth's magnetosheath, and Jupiter's magnetosphere, supported by direct measurements from satellite missions such as Ulysses, Cluster, and Voyager 2, see (Vasyliunas, 1968; Pierrard et al., 2001; Maksimovic et al., 1997; Qureshi et al., 2003; Formisano et al., 1973; Collier and Hamilton, 1995) for details on these missions and their observations of the Kappa distributions.

Consequently, several studies have extensively investigated transport coefficients in nonequilibrium plasmas using the Kappa velocity distribution functions. In particular, studies such as Du (2013), Wang and Du (2017), Ebne Abbasi et al. (2017), Ebne Abbasi and Esfandyari-Kalejahi (2019) and Guo and Du (2019) derived diffusion, mobility, electrical conductivity, thermoelectric coefficients, and thermal conductivity based on modified Kappa distributions, which assume a  $\kappa$ -independent effective temperature and therefore produce a stronger low-energy core and enhanced suprathermal tails relative to the Maxwellian distribution.

However, this modified form differs fundamentally from the standard (Olbertian) Kappa distribution, introduced by Olbert (1968) and Vasyliunas (1968), in which the effective temperature is  $\kappa$ -dependent, leading to a weaker thermal core and more pronounced high-energy tails. As a result, the standard Kappa distribution is widely used in space plasma studies and is particularly suitable for modeling collisionless or weakly collisional plasmas, as it accurately fits spacecraft observations and captures the nonthermal heating of suprathermal populations. Beyond observational fitting, Lazar, M. et al. (2015); Lazar et al. (2016) showed that the modified Kappa approach may yield results in linear dispersion and instability analyses that do not always highlight the destabilizing role of suprathermal particles, sometimes indicating reduced growth rates. In contrast, the standard Kappa formalism tends to produce instability thresholds and growth rates that more clearly reflect the destabilizing influence of suprathermal populations in collisionless or weakly collisional plasmas.

This empirical and theoretical success in collisionless plasma regions has motivated the development of transport coefficients based on the standard Kappa formalism, as done by Husidic et al. (2021). Nevertheless, the modified Kappa distribution remains valuable from a theoretical perspective, as it provides a self-consistent framework for describing systems in which deviations

but we adopt the methodology used in Jwailes et al. (2025), particularly in the formulation of the transport equations, the evaluation of the collision integrals, and the derivation of the transport coefficients. However, in contrast to Husidic et al. (2021), we use the Boltzmann collision integral as our collision model rather than the Krook-type collision model. This substitution is essential for obtaining results that more accurately capture the velocity-dependent interaction dynamics inherent to Kappa-distributed plasmas.

This paper is structured as follows: Section 2 provides a brief review of the Kappa distribution family, introducing the mathematical formulations and the physical interpretation of two different types of suprathermal tail distributions: the standard Kappa and the modified Kappa distribution functions. It also explains how their behaviors differ from that of the Maxwellian distribution. Section 3 presents the theoretical framework of this paper, in which we derive the five-moment approximation and the corresponding collision terms for the standard Kappa velocity distribution function, considering arbitrary drift-velocity and temperature differences between the interacting plasma species. This includes three types of collisions: Coulomb collisions, hard-sphere interactions, and Maxwell-molecule collisions. The section concludes with the derivation of the transport coefficients using the five-moment approximation and the derived collision terms. Section 4 discusses the derived results presented in Section 3 for the standard Kappa distribution and compares them with the corresponding results for both the modified Kappa distribution and the Maxwellian distribution. Three aspects are considered in the comparison: (i) the effective collision frequency and thermalisation rate; (ii) the behavior of the collision terms in the case of Coulomb collisions, with a focus on how collisions affect both the momentum and the energy of the interacting particles; and (iii) the transport coefficients and their dependence on the kappa parameter. The derived formulas are also compared with results from previous studies, highlighting their dependence on the kappa parameter. Finally, Section 5 presents the conclusions.

## 2 Distributions with suprathermal tails

Kappa distributions constitute a broad class of non-Maxwellian velocity distribution functions that effectively describe suprathermal particle populations in space and astrophysical plasmas. Unlike the Maxwellian distribution, they introduce a power-law tail that decays more slowly than the exponential tail of the Maxwellian. This tail is controlled by the kappa parameter  $\kappa$ , which determines the strength of the high-energy tail: larger  $\kappa$  values approach the Maxwellian limit, while smaller values emphasize suprathermal populations. With typical  $\kappa$  values ranging between 2 and 6, Kappa distributions have been observed across diverse plasma environments, including the solar wind, Earth's magnetosheath, and Jupiter's magnetosphere, supported by direct measurements from satellite missions such as Ulysses, Cluster, and Voyager 2 (see (Vasyliunas, 1968; Pierrard et al., 2001; Maksimovic et al., 1997; Qureshi et al., 2003; Formisano et al., 1973; Collier and Hamilton, 1995) for details on these missions and their observations of the Kappa distributions). Among the various formulations proposed in the literature, two main types are commonly used: the standard Kappa distribution and the modified Kappa distribution. While both distributions share the general objective of characterizing plasmas with high-energy tails, they differ in their mathematical structure, parameter definitions, and physical interpretations.

from equilibrium redistribute particles between the core and suprathermal tails, and with presence of collisional plasmas. Importantly, as highlighted by Husidic et al. (2021), distinctions between the modified Kappa and standard Kappa distributions are crucial because the choice of distribution directly affects the resulting transport coefficients and their physical interpretation.

All reviewed studies employed simplified collision models rather than the full Boltzmann collision integral in evaluating the transport coefficients. The simplest models appear in Wang and Du (2017), Ebne Abbasi and Esfandiyari-Kalejahi (2019), and Husidic et al. (2021) which used a Krook-type operator, offering computational simplicity but limited accuracy. More physically based models—such as those proposed by Du (2013) and Guo and Du (2019)—used macroscopic transport equations derived from idealized relaxation assumptions. The most advanced work, presented by Ebne Abbasi et al. (2017), used the Fokker-Planck equation to model Coulomb collisions. While this captures cumulative small-angle scattering and better represents long-range Coulomb forces, it remains an approximation of the Boltzmann collision integral. Thus, all reviewed works share the same limitation: reliance on simplified collision models. To overcome this limitation, Jwailes et al. (2025) recently introduced a comprehensive re-evaluation of the transport coefficients based on the modified Kappa distribution, using the five-moment transport approximation with the Boltzmann collision integral as the collision model. In this approach, a new transport theory was developed by deriving the five-moment approximation and the corresponding collision terms for various types of collisions for the modified Kappa distribution. The five-moment momentum equation is then linked to the generalized Ohm's law and the extended Fick's law, from which the transport coefficients are determined.

This study is inspired by the work of Husidic et al. (2021) and follows the same methodology introduced by Jwailes et al. (2025). As in Husidic et al. (2021), we focus on evaluating the transport coefficients for the standard Kappa distribution, but we adopt the methodology used in Jwailes et al. (2025), particularly in the formulation of the transport equations, the evaluation of the collision integrals, and the derivation of the transport coefficients. However, in contrast to Husidic et al. (2021), we use the Boltzmann collision integral as our collision model rather than the Krook-type collision model. This substitution is essential for obtaining results that more accurately capture the velocity-dependent interaction dynamics inherent to Kappa-distributed plasmas. The study further examined the transport coefficients derived from both the modified and standard Kappa distributions, highlighting how the selection of a particular Kappa model can markedly alter the magnitude and trends of these coefficients.

This paper is structured as follows: Section 2 provides a brief review of the Kappa distribution family, introducing the mathematical formulations and the physical interpretation of two different types of suprathermal tail distributions: the standard Kappa and the modified Kappa distribution functions. It also explains how their behaviors differ from that of the Maxwellian distribution. Section 3 presents the theoretical framework of this paper, in which we derive the five-moment approximation and the corresponding collision terms for the standard Kappa velocity distribution function, considering arbitrary drift-velocity and temperature differences between the interacting plasma species. This includes three types of collisions: Coulomb collisions, hard-sphere interactions, and Maxwell-molecule collisions. The section concludes with the derivation of the transport coefficients using the five-moment approximation and the derived collision terms. Section 4 discusses the derived results presented in Section 3 for the standard Kappa distribution and compares them with the corresponding results for both the modified Kappa distribution and the Maxwellian distribution. Three aspects are considered in the comparison: (i) the effective collision



The concept of the Kappa distribution was first proposed by Olbert (1968) to explain the presence of high-energy particles observed in the solar wind and magnetospheric plasmas, and was subsequently formalized by Vasyliunas (1968), who provided a more rigorous mathematical formulation. This early version is commonly referred to as the Olbertian or standard Kappa distribution (SK). In velocity space, the drifting standard Kappa distribution is given by (Lazar and Fichtner, 2021)

$$f_s^{\text{SK}}(\mathbf{r}, \mathbf{c}_s, t) = \frac{n_s \xi(\kappa_s)}{\pi^{3/2} w_s^3} \left( 1 + \frac{c_s^2}{\kappa_s w_s^2} \right)^{-\kappa_s - 1}, \quad (1)$$

where  $n_s$  denotes the number density and  $w_s$  is the thermal velocity of species  $s$ , defined as

$$w_s = \sqrt{\frac{2k_B T_s}{m_s}}, \quad (2)$$

with  $m_s$  and  $T_s$  being the particle mass and the absolute temperature, respectively, and  $k_B$  the Boltzmann constant. The random velocity  $\mathbf{c}_s$  is defined in terms of the position  $\mathbf{r}$ , velocity  $\mathbf{v}_s$ , and the drift velocity  $\mathbf{u}_s(\mathbf{r}, t)$  of the species  $s$ ,

$$\mathbf{c}_s(\mathbf{r}, \mathbf{v}_s, t) = \mathbf{v}_s - \mathbf{u}_s, \quad (3)$$

The normalization function  $\xi(\kappa_s)$ , which depends on the kappa parameter  $\kappa_s$ , is given by

$$\xi(\kappa_s) = \kappa_s^{-3/2} \frac{\Gamma(\kappa_s + 1)}{\Gamma(\kappa_s - 1/2)}, \quad (4)$$

The parameter  $\kappa_s$  determines the slope of the power-law tails. Within this framework, the effective temperature  $T_\kappa$ , obtained via the second velocity moment, depends on the kappa parameter  $\kappa_s$  and is written as

$$T_\kappa = \frac{\kappa_s}{\kappa_s - 3/2} \frac{m_s w_s^2}{2k_B} = \frac{\kappa_s}{\kappa_s - 3/2} T_s. \quad (5)$$

As  $\kappa_s$  increases, the effective temperature decreases until it reaches the Maxwellian temperature  $T_s$ . This dependence implies that the enhanced presence of suprathermal particles contributes additional energy to the system, effectively heating the plasma. Moreover, the expression for the effective temperature in equation 5 imposes a condition on the kappa parameter, namely  $\kappa_s > 3/2$ ; below this value the effective temperature diverges and is therefore undefined (Pierrard and Lazar, 2010).

Decades later, inspired by the principles of non-extensive statistical mechanics introduced by Tsallis (2012), Livadiotis (2017) developed a new theoretical perspective reformulated the Kappa distribution into what is now known as the modified Kappa distribution (MK). In velocity space, the modified Kappa distribution is given by (Livadiotis, 2018; Davis et al., 2023)

$$f_s^{\text{MK}}(\mathbf{r}, \mathbf{c}_s, t) = \frac{n_s \eta(\kappa_s)}{\pi^{3/2} w_s^3} \left( 1 + \frac{c_s^2}{\kappa_{0s} w_s^2} \right)^{-\kappa_s - 1}, \quad (6)$$

where  $w_s$  is defined as in equation 2. The normalization function in this case takes the form

$$\eta(\kappa_s) = \kappa_{0s}^{-3/2} \frac{\Gamma(\kappa_s + 1)}{\Gamma(\kappa_s - 1/2)}, \quad \kappa_{0s} = \kappa_s - \frac{3}{2}. \quad (7)$$

Here,  $\kappa_{0s}$  represents the invariant Kappa index, while  $\kappa_s$  is the shape parameter that governs the slope of the suprathermal tails. As before, the condition  $\kappa_s > 3/2$  must be satisfied to ensure that the modified Kappa distribution function in equation (7)

frequency and thermalisation rate; (ii) the behavior of the collision terms in the case of Coulomb collisions, with a focus on how collisions affect both the momentum and the energy of the interacting particles; and (iii) the transport coefficients and their dependence on the kappa parameter. The derived formulas are also compared with results from previous studies, highlighting their dependence on the kappa parameter. Finally, Section 5 presents the conclusions, summarizing the main findings of this study,

## 2 Distributions with suprathermal tails

Kappa distributions constitute a broad class of non-Maxwellian velocity distribution functions that effectively describe suprathermal particle populations in space and astrophysical plasmas. Among the various formulations proposed in the literature, two main types are commonly used: the standard Kappa distribution and the modified Kappa distribution. While both distributions share the general objective of characterizing plasmas with high-energy tails, they differ in their mathematical structure, parameter definitions, and physical interpretations.

The concept of the Kappa distribution was first proposed by Olbert (1968) to explain the presence of high-energy particles observed in the solar wind and magnetospheric plasmas, and was subsequently formalized by Vasyliunas (1968), who provided a more rigorous mathematical formulation. This early version is commonly referred to as the Olbertian or standard Kappa distribution (SK). In velocity space, the drifting standard Kappa distribution is given by Lazar and Fichtner (2021) as,

$$f_s^{\text{SK}}(\mathbf{r}, \mathbf{c}_s, t) = \frac{n_s \xi(\kappa_s)}{\pi^{3/2} w_s^3} \left( 1 + \frac{c_s^2}{\kappa_s w_s^2} \right)^{-\kappa_s - 1}, \quad (1)$$

where  $n_s$  denotes the number density and  $w_s$  is the thermal speed of species  $s$ , defined as

$$w_s = \sqrt{\frac{2k_B T_s}{m_s}}, \quad (2)$$

with  $m_s$  and  $T_s$  being the particle mass and the absolute temperature, respectively, and  $k_B$  the Boltzmann constant. The random velocity  $\mathbf{c}_s$  is defined in terms of the position  $\mathbf{r}$ , velocity  $\mathbf{v}_s$ , and the drift velocity  $\mathbf{u}_s(\mathbf{r}, t)$  of the species  $s$ ,

$$\mathbf{c}_s(\mathbf{r}, \mathbf{v}_s, t) = \mathbf{v}_s - \mathbf{u}_s, \quad (3)$$

The kappa dependent function  $\xi(\kappa_s)$  is given by

$$\xi(\kappa_s) = \kappa_s^{-3/2} \frac{\Gamma(\kappa_s + 1)}{\Gamma(\kappa_s - 1/2)}, \quad (4)$$

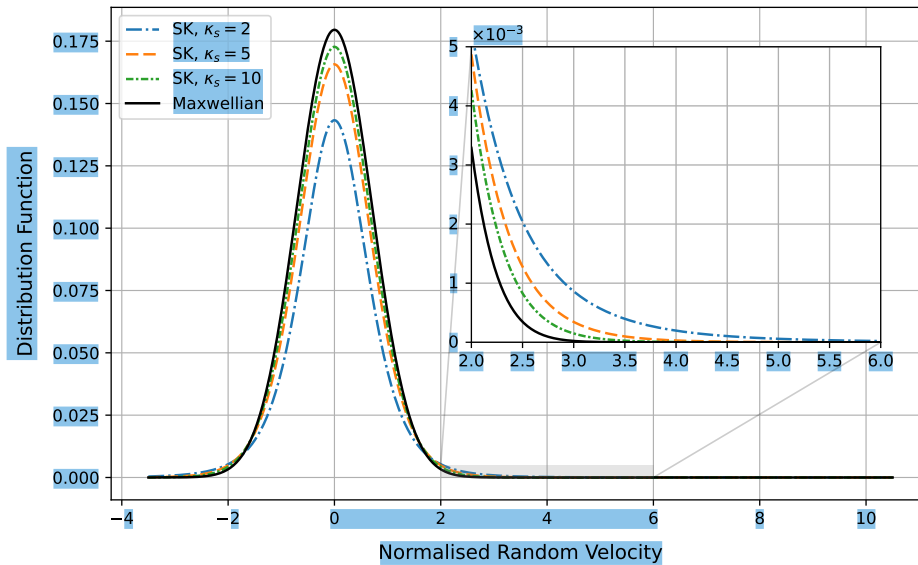
where  $\kappa_s$  is the kappa parameter that determines the slope of the power-law tails. Within this framework, the effective temperature  $T_s^\kappa$ , obtained via the second velocity moment, depends on the kappa parameter  $\kappa_s$  and is written as,

$$T_s^\kappa = \frac{\kappa_s}{\kappa_s - 3/2} \frac{m_s w_s^2}{2k_B} = \frac{\kappa_s}{\kappa_s - 3/2} T_s. \quad (5)$$

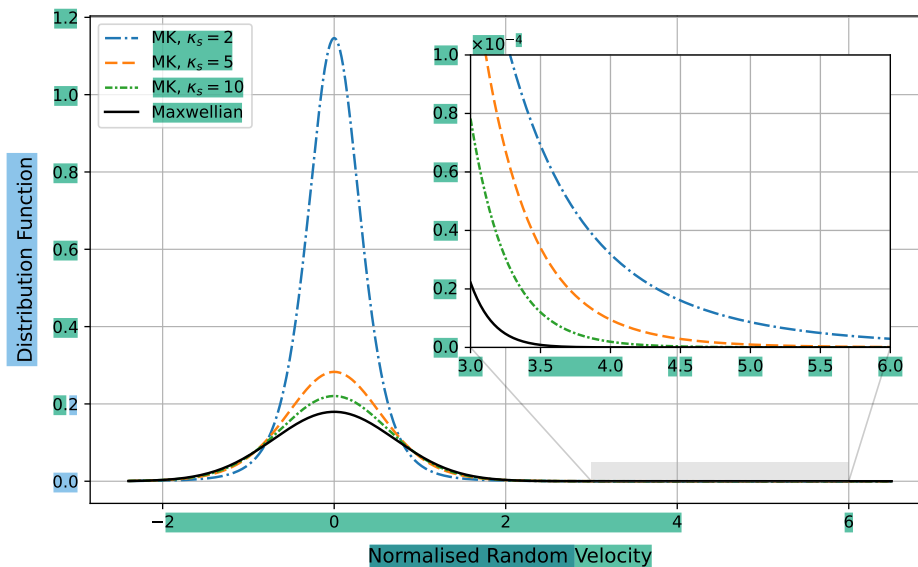
As  $\kappa_s$  increases, the effective temperature decreases until it approaches the Maxwellian temperature  $T_s$  (Lazar et al., 2016). This dependence implies that the enhanced presence of suprathermal particles contributes additional energy to the system,



effectively heating the plasma. Moreover, the expression for the effective temperature in Eq. (5) imposes a condition on the kappa parameter, namely  $\kappa_s > 3/2$ ; below this value the effective temperature diverges and is therefore undefined (Pierrard and Lazar, 2010).



(a)



(b)

**Figure 1.** A schematic comparison between (a) standard Kappa, (b) modified Kappa velocity distributions for  $\kappa_s$  values 2, 5, and 10, with the Maxwellian velocity distribution as a functions of the normalised random velocity,  $c_s/w_s$ .



remains well defined. This modified version introduces a stronger thermodynamic basis by decoupling the effective temperature from the kappa parameter  $\kappa_s$ , making it a kappa independent quantity, as given by

$$T_\kappa = \frac{\kappa_{0s}}{\kappa_s - 3/2} \frac{m_s w_s^2}{2k_B} = T_s, \quad (8)$$

125 which is identical to the Maxwellian temperature and remains constant regardless of the value of  $\kappa_s$ . This ensures that variations in the high-energy tails do not change the overall thermal energy content of the plasma. In this sense, the modified Kappa distribution maintains the same total thermal energy content as a Maxwellian plasma while redistributing the particles between the core and tail regions.

On the similarity side, both the standard and modified Kappa distributions are used to describe particle populations with suprathermal tails, since both distributions retain a power-law form and exhibit suprathermal tails that are higher than those of the Maxwellian distribution. Moreover, both distributions reduce to the Maxwellian distribution in the limiting case where  $\kappa_s$  approaches infinity, (Pierrard and Lazar, 2010).

$$\lim_{\kappa_s \rightarrow \infty} f_s^{\text{SK}} = \lim_{\kappa_s \rightarrow \infty} f_s^{\text{MK}} = \frac{n_s}{\pi^{3/2} w_s^3} \exp\left(-\frac{c_s^2}{w_s^2}\right). \quad (9)$$

This behaviour is illustrated in Figure 1, where increasing  $\kappa_s$  causes both the standard and modified Kappa distributions to converge smoothly toward the Maxwellian distribution. Although the standard and modified Kappa distributions share this common limiting behavior and exhibit similar qualitative features, they differ in their mathematical formulation and physical interpretation. The mathematical distinction between the two forms lies primarily in their parameterization and normalization. The standard distribution employs  $\kappa_s$  in the energy-dependent term, while the modified version replaces it with  $\kappa_s - 3/2$ . While this shift may appear minor, it significantly affects the scaling of the velocity distributions, resulting in slightly flatter high-energy tails in the modified Kappa distribution compared to the standard Kappa distribution for the same  $\kappa_s$  value. Moreover, in the standard Kappa distribution, the effective temperature of the particles depends on  $\kappa_s$ , making it much higher than the temperature in the Maxwellian case. However, for the modified Kappa distribution, the effective temperature is independent of  $\kappa_s$ , making it identical to the Maxwellian temperature.

145 These differences are reflected in how the particle's velocity is distributed. To illustrate how the two Kappa distributions differ from the Maxwellian distribution, Fig. 2 shows a comparison between the Maxwellian, the modified Kappa, and the standard Kappa distributions. The first thing we can notice is that both the modified and the standard Kappa distributions have higher-energy tails than the Maxwellian distribution, which is a defining characteristic of Kappa distributions. At the same time, we can also observe differences in the shape of each distribution, which are directly related to the effective temperature. In the standard Kappa distribution, the effective temperature  $T_\kappa$  is higher than that of both the Maxwellian and the modified Kappa distributions, as shown in equation 5. Consequently, the population of high-energy suprathermal particles (i.e., at large velocity magnitudes) is significantly enhanced compared to the other distributions. At the same time, this increase in high-energy particles is accompanied by a reduction in the particle population within the low-energy core (i.e., at small velocity magnitudes). On the other hand, in the modified Kappa distribution, the effective temperature is the same as in the Maxwellian distribution.

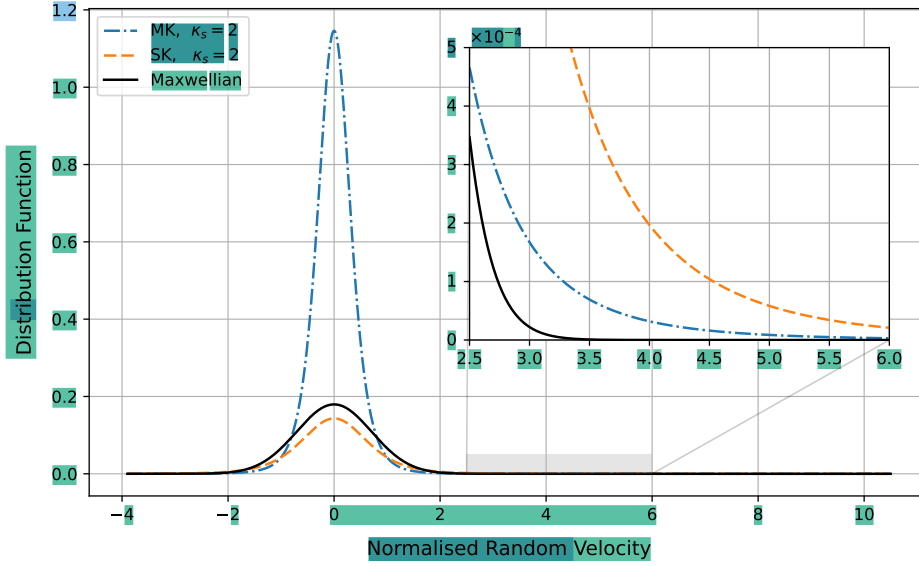


**Figure 2.** A schematic comparison of the standard Kappa distribution, the modified Kappa distribution for  $\kappa_s = 2$ , and the Maxwellian velocity distribution as a functions of the normalised random velocity,  $c_s/w_s$ .

Decades later, inspired by the principles of non-extensive statistical mechanics introduced by Tsallis (2012), Livadiotis (2017) developed a new theoretical perspective and reformulated the Kappa distribution into what is now known as the modified Kappa distribution (MK). In velocity space, the modified Kappa distribution is given by Livadiotis (2018) and Davis et al. (2023) as,

$$f_s^{\text{MK}}(\mathbf{r}, \mathbf{c}_s, t) = \frac{n_s \eta(\kappa_s)}{\pi^{3/2} w_s^3} \left( 1 + \frac{c_s^2}{\kappa_{0_s} w_s^2} \right)^{-\kappa_s - 1}, \quad (6)$$

where  $w_s$  is defined as in Eq. (2). The kappa dependent function in this case takes the form

$$\eta(\kappa_s) = \kappa_{0_s}^{-3/2} \frac{\Gamma(\kappa_s + 1)}{\Gamma(\kappa_s - 1/2)}, \quad \kappa_{0_s} = \kappa_s - \frac{3}{2}. \quad (7)$$

Here,  $\kappa_{0_s}$  represents the invariant kappa index, while  $\kappa_s$  is the shape parameter that governs the slope of the suprathermal tails.

As before, the condition  $\kappa_s > 3/2$  must be satisfied to ensure that the modified Kappa distribution function in Eq. (7) remains well defined. This modified version introduces a stronger thermodynamic basis by decoupling the effective temperature from the kappa parameter  $\kappa_s$ , making it a kappa independent quantity, as given by

$$T_s^\kappa = \frac{\kappa_{0_s}}{\kappa_s - 3/2} \frac{m_s w_s^2}{2k_B} = T_s, \quad (8)$$

which is identical to the Maxwellian temperature and remains constant regardless of the value of  $\kappa_s$  (Lazar et al., 2016).

This ensures that variations in the high-energy tails do not change the overall thermal energy of the plasma. In this sense, the modified Kappa distribution maintains the same total thermal energy content as a Maxwellian plasma while redistributing the particles between the core and tail regions.



On the similarity side, both the standard and modified Kappa distributions are used to describe particle populations with suprathermal tails, since both distributions retain a power-law form and exhibit suprathermal tails that are higher than those of the Maxwellian distribution.

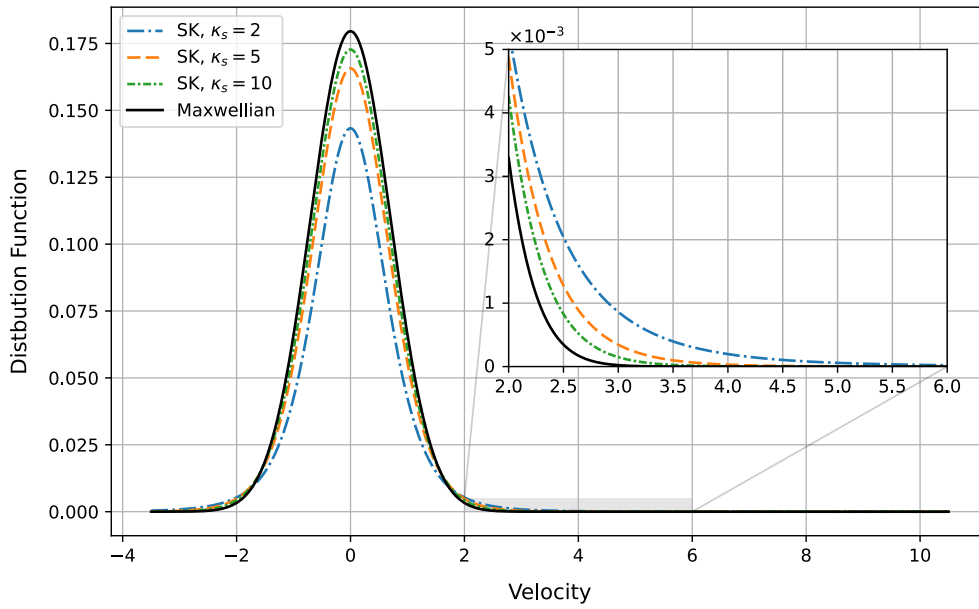
Moreover, both distributions reduce to the Maxwellian distribution in the limiting case where  $\kappa_s$  approaches infinity, (Pierard and Lazar, 2010).

$$\lim_{\kappa_s \rightarrow \infty} f_s^{\text{SK}} = \lim_{\kappa_s \rightarrow \infty} f_s^{\text{MK}} = \frac{n_s}{\pi^{3/2} w_s^3} \exp\left(-\frac{c_s^2}{w_s^2}\right). \quad (9)$$

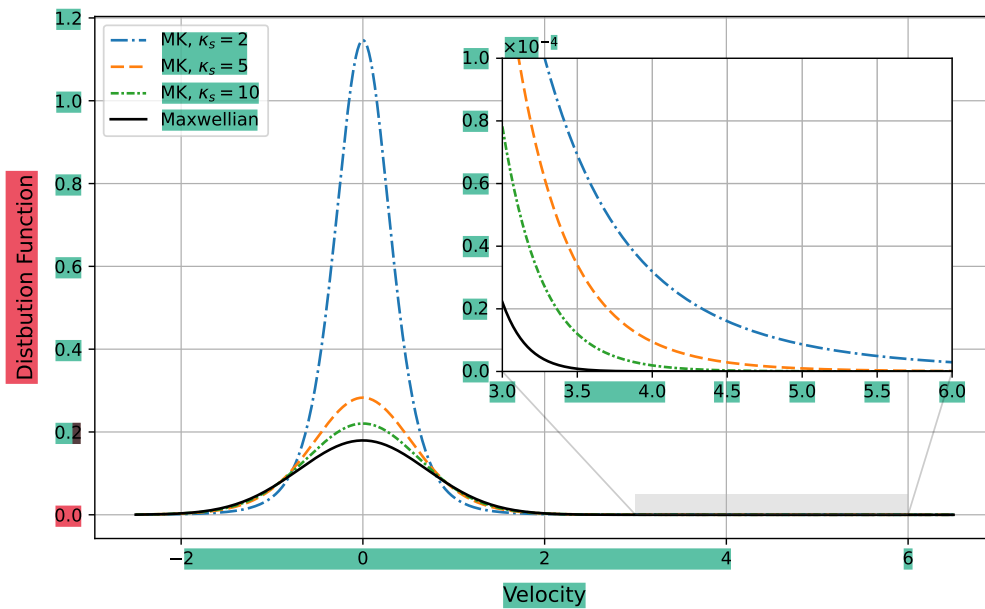
This behaviour is illustrated in Figure 1, where increasing  $\kappa_s$  causes both the standard and modified Kappa distributions to converge smoothly toward the Maxwellian distribution. Although the standard and modified Kappa distributions share this common limiting behavior and exhibit similar qualitative features, they differ in their mathematical formulation and physical interpretation. The mathematical distinction between the two forms is mainly due to their parameterization and normalization. The standard distribution employs  $\kappa_s$  in the energy-dependent term, while the modified version replaces it with  $\kappa_s - 3/2$ . While this shift may appear minor, it significantly affects the scaling of the velocity distributions, resulting in slightly flatter high-energy tails in the modified Kappa distribution compared to the standard Kappa distribution for the same  $\kappa_s$  value. Moreover, in the standard Kappa distribution, the effective temperature of the particles depends on  $\kappa_s$ , making it much higher than the temperature in the Maxwellian case. However, for the modified Kappa distribution, the effective temperature is independent of  $\kappa_s$ , making it identical to the Maxwellian temperature.

**Table 1.** Mathematical and physical comparison of Maxwellian, standard Kappa, and modified Kappa velocity distribution functions

Feature	Maxwellian (M)	Standard Kappa (SK)	Modified Kappa (MK)
Statistical nature	Thermal equilibrium	Non-equilibrium	Non-equilibrium
Theoretical basis	Boltzmann statistics	Empirical (space data)	Non-extensive statistics
Mathematical form	$f_s^{\text{M}} \propto \exp\left(-\frac{c_s^2}{w_s^2}\right)$	$f_s^{\text{SK}} \propto \left(1 + (c_s^2/\kappa_s w_s^2)\right)^{-\kappa_s - 1}$	$f_s^{\text{MK}} \propto \left(1 + (c_s^2/\kappa_{0s} w_s^2)\right)^{-\kappa_s - 1}$
Key shape parameter	—	$\kappa_s$	$\kappa_s, \kappa_{0s} = \kappa_s - 3/2$
Parameter constraint	—	$\kappa_s > 3/2$	$\kappa_s > 3/2$
Limit as $\kappa_s \rightarrow \infty$	—	Maxwellian distribution	Maxwellian distribution
Tail behavior	Exponential	Power-law	Power-law
Dominant region	Core-dominated	Tail-dominated	Core-dominated + tail
High-energy population	Lowest	Highest	Intermediate
Low-energy population	Intermediate	Lowest	Highest
Effective temperature, $T_{\text{eff}}$	$T_s$	$\frac{\kappa_s}{\kappa_s - 3/2} T_s$	$T_s$
Dependence of $T_{\text{eff}}$ on $\kappa_s$	Independent of $\kappa_s$	Increases as $\kappa_s$ decreases	Independent of $\kappa_s$
Total thermal energy	Baseline	Higher than Maxwellian	Same as Maxwellian



(a)



(b)

**Figure 1.** A schematic comparison between (a) standard Kappa, (b) modified Kappa velocity distributions for  $\kappa_s$  values 2, 5, and 10, with the Maxwellian velocity distribution.

160 These differences are reflected in how the particle velocities are distributed. To illustrate how the two Kappa distributions differ from the Maxwellian distribution, Fig. 2 shows a comparison between the Maxwellian, the modified Kappa, and the standard Kappa distributions. The first thing we can notice is that both the modified and the standard Kappa distributions exhibit enhanced tails compared to the Maxwellian distribution, which is a defining characteristic of Kappa distributions. At the same time, we can also observe differences in the shape of each distribution, which are directly related to the effective temperature.

165 In the standard Kappa distribution, the effective temperature  $T_s^{\kappa}$  is higher than that of both the Maxwellian and the modified Kappa distributions, as shown in Eq. (5). Consequently, the population of high-energy suprathermal particles (i.e., at large velocity magnitudes) is significantly enhanced compared to the other distributions. At the same time, this increase in high-energy particles is accompanied by a reduction in the particle population within the low-energy core (i.e., at small velocity magnitudes). On the other hand, in the modified Kappa distribution, the effective temperature is the same as in the 170 Maxwellian distribution. To maintain this equality in temperature, particles are redistributed between the low-energy core and the high-energy tail without changing the system's total thermal energy. As a result, the high-energy tail of the modified Kappa distribution is lower than that of the standard Kappa distribution, while the particle population in the low-energy core becomes significantly higher. The mathematical and physical properties of the Maxwellian, standard Kappa, and modified Kappa velocity distribution functions, discussed above, are summarized in Table 1.

175 Both the standard and modified Kappa distributions are used in different contexts. The standard Kappa distribution is the most commonly used tool in space plasma studies, where it provides excellent fits to spacecraft observations from the solar wind and planetary magnetospheres (Vasyliunas, 1968; Olbert, 1968; Collier and Hamilton, 1995; Collier et al., 1996; Maksimovic et al., 1997; Lazar and Fichtner, 2021). It captures the empirical relationship between suprathermal particle populations and the observed nonthermal heating of plasmas. On the other hand, the modified Kappa distribution, is mainly used in theoretical and 180 statistical modeling, particularly in studies of systems governed by non-extensive entropy, long-range interactions, and quasi-stationary states (Lima et al., 2001; Livadiotis, 2015; Yoon, 2014; Livadiotis, 2017). It provides a self-consistent description of plasma systems that exhibit deviations from classical thermodynamic equilibrium without requiring an increase in thermal energy.

### 3 Theoretical Formulation

185 In this section, we present the five-moment approximation of the transport equation system, along with the corresponding collision terms and transport coefficients, using the standard Kappa distribution as the velocity distribution function. The derivation follows the same mathematical framework and analytical steps established in Jwailes et al. (2025). While the full detailed calculations are not repeated here, the essential assumptions and methodological structure remain the same.

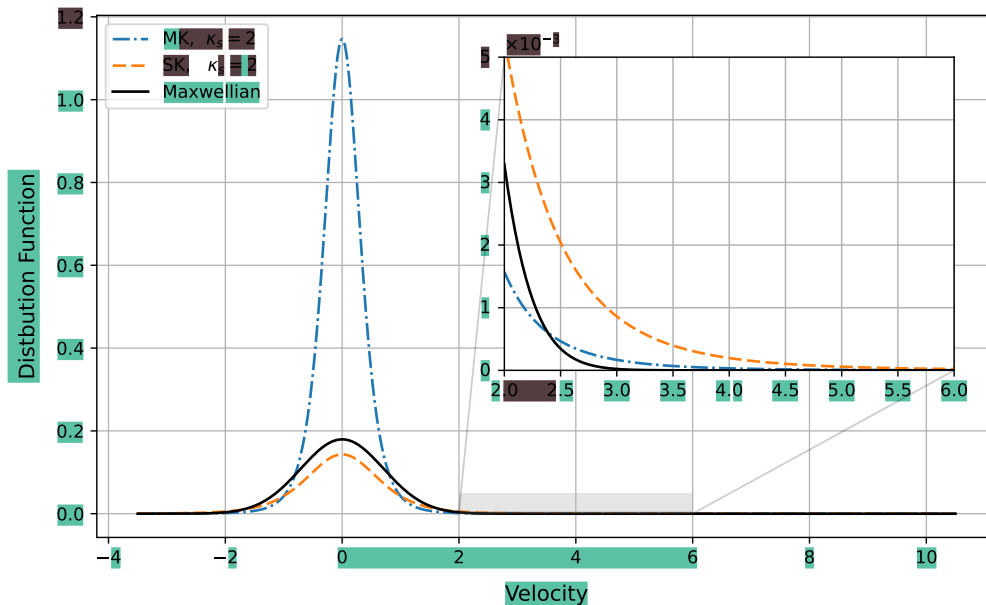


**Figure 2.** A schematic comparison of the standard Kappa distribution, the modified Kappa distribution for  $\kappa_s = 2$ , and the Maxwellian velocity distribution.

To maintain this equality in temperature, particles are redistributed between the low-energy core and the high-energy tail without changing the system's total thermal energy. As a result, the high-energy tail of the modified Kappa distribution is lower than that of the standard Kappa distribution, while the particle population in the low-energy core becomes significantly higher.

Both the standard and modified Kappa distributions are used in different contexts. The standard Kappa distribution is the most commonly used tool in space plasma studies, where it provides excellent fits to spacecraft observations from the solar wind, planetary magnetospheres, and the heliosheath. It captures the empirical relationship between suprathermal particle populations and the observed nonthermal heating of plasmas. On the other hand, the modified Kappa distribution, is mainly used in theoretical and statistical modeling, particularly in studies of systems governed by non-extensive entropy, long-range interactions, and quasi-stationary states. It provides a self-consistent description of plasma systems that exhibit deviations from classical thermodynamic equilibrium without requiring an increase in thermal energy.

Finally, Table 1 summarizes the main mathematical and physical properties of the Maxwellian, standard Kappa, and modified Kappa velocity distribution functions discussed above, providing a compact overview of their key characteristics, parameter definitions, and limiting behavior, and allowing for an easy and direct comparison among the three distributions.

### 3.1 Transport equations

190 The transport equations describe the spatial and temporal evolution of the physically significant velocity moments, such as number density, drift velocity, temperature, pressure tensor, stress tensor, and heat flow vector. These equations are obtained by multiplying the Boltzmann equation by an appropriate velocity-dependent function and then integrating over the velocity space, as presented in Schunk (1977), Schunk and Nagy (2009), and Bittencourt (2004). However, the general transport equations do not constitute a closed system since each moment equation depends on a higher-order moment. To close the system, the velocity

195 distribution function, is approximated by expanding it into a complete orthogonal series around an appropriate zeroth-order distribution function  $f_s^{(0)}$  (Grad, 1949; Mintzer, 1965). When only the first term of this expansion is retained, the species distribution function  $f_s$ , is represented by the zeroth-order function,  $f_s^{(0)}$ . The general system of transport equations then reduces to the so-called five-moment approximation, in which the stress, heat flux, and all higher-order moments are neglected. At this level of approximation, the properties of each species are described by five parameters: the number density, three

200 components of drift velocity, and temperature. If the chosen zeroth-order distribution function  $f_s^{(0)}$  has a stress tensor  $\tau_s$  and a heat flux vector  $\mathbf{q}_s$  equal to zero, as in the drifting Maxwellian, drifting modified Kappa, and drifting standard Kappa distributions (Scherer et al., 2019), and if the main external forces acting on the charged particles are gravitational and Lorentz forces, the five-moment approximation equations become (Schunk, 1977; Jwailes et al., 2025),

$$\frac{\delta n_s}{\delta t} = \frac{\partial n_s}{\partial t} + \nabla \cdot (n_s \mathbf{u}_s), \quad (10)$$

$$205 \quad \frac{\delta \mathbf{M}_s}{\delta t} = n_s m_s \frac{D_s \mathbf{u}_s}{Dt} + \nabla p_s^\kappa - n_s m_s \mathbf{G} - n_s e_s \left( \mathbf{E} + \frac{\mathbf{u}_s \times \mathbf{B}}{c} \right), \quad (11)$$

$$\frac{\delta E_s}{\delta t} = \frac{3}{2} \frac{D_s p_s^\kappa}{Dt} + \frac{5}{2} p_s^\kappa (\nabla \cdot \mathbf{u}_s). \quad (12)$$

In these equations, the symbol  $\nabla$  denotes the gradient in spatial coordinates. The operator  $D_s/Dt$ , is defined as

$$\frac{D_s}{Dt} = \frac{\partial}{\partial t} + \mathbf{u}_s \cdot \nabla. \quad (13)$$

210 The partial pressure associated with the species  $s$  can be expressed as

$$p_s^\kappa = n_s k_B T_s^\kappa, \quad (14)$$

with  $n_s(\mathbf{r}, t)$  being the number density and  $T_s^\kappa(\mathbf{r}, t)$  the effective temperature associated with the standard Kappa distribution given in Eq.(5). The charge and the mass of the species  $s$  are denoted by  $e_s$  and  $m_s$ , respectively. The vectors  $\mathbf{E}$  and  $\mathbf{B}$  correspond to the electric and magnetic fields, while  $\mathbf{G}$  represents the gravitational acceleration. Finally,  $c$  is the speed of light

215 in vacuum.

The five-moment approximation given in Eqs. (10–12) differs from the approximations obtained for the Maxwellian and modified Kappa distributions (Jwailes et al., 2025). In particular, the partial pressure here depends explicitly on the Kappa



**Table 1.** Mathematical and physical comparison of Maxwellian, standard Kappa, and modified Kappa velocity distribution functions

Feature	Maxwellian (M)	Standard Kappa (SK)	Modified Kappa (MK)
Statistical nature	Thermal equilibrium	Non-equilibrium	Non-equilibrium
Theoretical basis	Boltzmann statistics	Empirical (space data)	Non-extensive statistics (Tsallis, 2012)
Primary application	Classical plasma theory	Space plasma fitting	Non-equilibrium plasma modeling with long-range interactions
Mathematical form	$f_s^M \propto \exp\left(-\frac{c_s^2}{w_s^2}\right)$	$f_s^{SK} \propto \left(1 + (c_s^2/\kappa_s w_s^2)\right)^{-\kappa_s - 1}$	$f_s^{MK} \propto \left(1 + (c_s^2/\kappa_{0_s} w_s^2)\right)^{-\kappa_s - 1}$
Normalization factor	$\frac{n_s}{\pi^{3/2} w_s^3}$	$\frac{n_s \kappa_s^{-3/2}}{\pi^{3/2} w_s^3} \frac{\Gamma(\kappa_s + 1)}{\Gamma(\kappa_s - 1/2)}$	$\frac{n_s \kappa_{0_s}^{-3/2}}{\pi^{3/2} w_s^3} \frac{\Gamma(\kappa_s + 1)}{\Gamma(\kappa_s - 1/2)}$
Key shape parameter	—	$\kappa_s$	$\kappa_s, \kappa_{0_s} = \kappa_s - 3/2$
Parameter constraint	—	$\kappa_s > 3/2$	$\kappa_s > 3/2$
Limit as $\kappa_s \rightarrow \infty$	—	Maxwellian distribution	Maxwellian distribution
Tail behavior	Exponential	Power-law	Power-law
Dominant region	Core-dominated	Tail-dominated	Core-dominated + tail
High-energy population	Lowest	Highest	Intermediate
Low-energy population	Intermediate	Lowest	Highest
Effective temperature	$T_\kappa = T_s$	$T_\kappa = \frac{\kappa_s}{\kappa_s - 3/2} T_s$	$T_\kappa = T_s$
Dependence of $T_\kappa$ on $\kappa_s$	Independent of $\kappa_s$	Increases as $\kappa_s$ decreases	Independent of $\kappa_s$
Total thermal energy	Baseline	Higher than Maxwellian	Same as Maxwellian

### 3 Theoretical Formulation

In this section, we derive the five-moment approximation of the system of transport equations, along with the corresponding collision terms and transport coefficients, using the standard Kappa distribution as the velocity distribution function. The derivation follows the same mathematical framework and procedural steps established in Jwailes et al. (2025). While the full detailed calculations are not repeated here, the essential assumptions and methodological structure remain the same.

#### 3.1 Transport equations

The transport equations describe the spatial and temporal evolution of the physically significant velocity moments, such as number density, drift velocity, temperature, pressure tensor, stress tensor, and heat flow vector. These equations are obtained by multiplying the Boltzmann equation by an appropriate velocity-dependent function and then integrating over the velocity space, as presented in Schunk (1977), Schunk and Nagy (2009), and Bittencourt (2004). The general transport equations do not constitute a closed system because the equation governing the moment of order  $l$  contains the moment of order  $l + 1$ . That is, while the continuity equation describes the evolution of the density, it also contains the drift velocity, and similar dependencies





occur in the higher-order moment equations. To close the system, the velocity distribution function  $f_s$ , is approximated by expanding it into a complete orthogonal series around an appropriate zeroth-order distribution function  $f_s^{(0)}$ , which is chosen such that the series converges rapidly (Grad, 1949; Mintzer, 1965). When only the first term of this expansion is retained, the species distribution function  $f_s$ , is represented by the zeroth-order function,  $f_s^{(0)}$ . The general system of transport equations then reduces to the so-called five-moment approximation, in which the stress, heat flux, and all higher-order moments are neglected. At this level of approximation, the properties of each species are described by five parameters: the number density, three components of drift velocity, and temperature. If the chosen zeroth-order distribution function  $f_s^{(0)}$  has a stress tensor  $\tau_s$  and a heat flux vector  $\mathbf{q}_s$  equal to zero, as in the drifting Maxwellian, drifting modified Kappa, and drifting standard Kappa distributions (Scherer et al., 2019), and if the main external forces acting on the charged particles are gravitational and Lorentz forces, the five-moment approximation equations become (Schunk, 1977),

$$\frac{\delta n_s}{\delta t} = \frac{\partial n_s}{\partial t} + \nabla \cdot (n_s \mathbf{u}_s), \quad (10)$$

$$\frac{\delta \mathbf{M}_s}{\delta t} = n_s m_s \frac{D_s \mathbf{u}_s}{Dt} + \nabla p_s - n_s m_s \mathbf{G} - n_s e_s \left( \mathbf{E} + \frac{\mathbf{u}_s \times \mathbf{B}}{c} \right), \quad (11)$$

$$\frac{\delta E_s}{\delta t} = \frac{3}{2} \frac{D_s p_s}{Dt} + \frac{5}{2} p_s (\nabla \cdot \mathbf{u}_s). \quad (12)$$

In these equations, the symbol  $\nabla$  denotes the gradient in coordinate space. The operator  $D_s/Dt$ , is defined as

$$\frac{D_s}{Dt} = \frac{\partial}{\partial t} + \mathbf{u}_s \cdot \nabla. \quad (13)$$

The partial pressure associated with this species is given by

$$p_s = n_s k_B T_s, \quad (14)$$

with  $n_s(\mathbf{r}, t)$  being the number density and  $T_s(\mathbf{r}, t)$  the temperature. The parameters  $e_s$  and  $m_s$  denote the charge and mass of species  $s$ , respectively. The vectors  $\mathbf{E}$  and  $\mathbf{B}$  correspond to the electric and magnetic fields, while  $\mathbf{G}$  represents the gravitational acceleration. Finally,  $c$  is the speed of light, and  $k_B$  stands for the Boltzmann constant.

### 200 3.2 Collision terms

The terms appearing on the left-hand side of the five-moment approximation, equations (10–12), are called the collision terms, also known as the transfer collision integral. These terms represent the moments of the Boltzmann collision integral and





describe the rate of change of density, momentum, and energy due to collisions, and they are defined as follows

$$\frac{\delta n_s}{\delta t} = \int_{\mathbb{R}^3} \frac{\delta f_s}{\delta t} d\mathbf{c}_s, \quad (15)$$

$$205 \quad \frac{\delta \mathbf{M}_s}{\delta t} = m_s \int_{\mathbb{R}^3} \mathbf{c}_s \frac{\delta f_s}{\delta t} d\mathbf{c}_s, \quad (16)$$

$$\frac{\delta E_s}{\delta t} = \frac{m_s}{2} \int_{\mathbb{R}^3} c_s^2 \frac{\delta f_s}{\delta t} d\mathbf{c}_s, \quad (17)$$

where the term  $(\delta f_s/\delta t)$ , represents the rate of change of the velocity distribution function  $f_s$ , in a given region of phase space as a result of collisions, and its form depends on the type of collision process considered. The appropriate expression in the case of binary elastic collisions between particles (collisions governed by inverse power laws, and resonant charge exchange collisions) is the Boltzmann collision integral (Schunk, 1977; Schunk and Nagy, 2009), given by

$$210 \quad \frac{\delta f_s}{\delta t} = \sum_t \int_{\mathbb{R}^3 \times \Omega} [f'_s f'_t - f_s f_t] g_{st} \sigma_{st}(g_{st}, \theta) d\Omega d\mathbf{c}_t, \quad (18)$$

where  $d\mathbf{c}_t$  is the random velocity space volume element for the target species  $t$ ,  $g_{st}$  is the magnitude of the relative velocity of the colliding particles  $s$  and  $t$ , with  $\mathbf{g}_{st}$  defined as

$$\mathbf{g}_{st} = \mathbf{v}_s - \mathbf{v}_t, \quad (19)$$

215  $d\Omega$  is the element of solid angle in the  $s$  particle reference frame,  $\theta$  is the scattering angle,  $\sigma_{st}(g_{st}, \theta)$  is the differential scattering cross-section, defined as the number of particles scattered per solid angle  $d\Omega$ , per unit time, divided by the incident intensity, and the primes denote quantities evaluated after the collision. By evaluating the integrals appearing in equations (15–17), we obtain the general expressions for the collision terms under the assumption that the velocity distribution functions of both interacting species,  $s$  and  $t$ , follow drifting standard Kappa distributions. The results for the three types of collisions—Coulomb collisions, hard-sphere interactions, and Maxwell molecule collisions—are summarized below.

$$220 \quad \frac{\delta n_s}{\delta t} = 0, \quad (20)$$

$$\frac{\delta \mathbf{M}_s}{\delta t} = \sum_t n_s m_s \nu_{st}^{\text{SK}}(\kappa_s, \kappa_t) \Phi(\varepsilon_{st}) \Delta \mathbf{u}_{st}, \quad (21)$$

$$\begin{aligned} \frac{\delta E_s}{\delta t} = \sum_t n_s \left[ \frac{3}{2} k_B \nu_{st,T}^{\text{SK}}(\kappa_s, \kappa_t) \Psi(\varepsilon_{st}) \Delta T_{st}^{\text{SK}} \right. \\ \left. + m_{st} \nu_{st}^{\text{SK}}(\kappa_s, \kappa_t) \Phi(\varepsilon_{st}) |\Delta \mathbf{u}_{st}|^2 \right], \end{aligned} \quad (22)$$

225 where the relative drift velocity  $\Delta \mathbf{u}_{st}$  and relative temperature difference  $\Delta T_{st}^{\text{SK}}$  are defined by

$$\Delta \mathbf{u}_{st} = \mathbf{u}_t - \mathbf{u}_s, \quad (23)$$

$$\Delta T_{st}^{\text{SK}} = H(\kappa_t) T_t - H(\kappa_s) T_s, \quad (24)$$

parameter,  $\kappa_s$ . This dependence arises from the evaluation of the second-order velocity moment, where, for the standard Kappa distribution, the second moment of the random velocity is expressed as

$$220 \quad \langle c_s^2 \rangle = \frac{3k_B T_s^\kappa}{m_s} = \frac{\kappa_s}{\kappa_s - 3/2} \frac{3k_B T_s}{m_s}. \quad (15)$$

In contrast, such a modification does not appear in the modified Kappa distribution, because its temperature is defined consistently with the Maxwellian case. As a result, the second moment retains the familiar Maxwellian form:

$$\langle c_s^2 \rangle = \frac{3k_B T_s}{m_s}. \quad (16)$$

### 3.2 Collision terms

225 The terms appearing on the left-hand side of the five-moment approximation system, Eqs. (10–12), are called the collision terms, also known as the transfer collision integral. These terms represent the rates of change of density, momentum, and energy due to collisions, respectively denoted by  $\delta n_s / \delta t$ ,  $\delta \mathbf{M}_s / \delta t$ , and  $\delta E_s / \delta t$ . The collision terms depend strongly on the collision model being considered. The appropriate expression for the collision model in the case of binary elastic collisions between particles (i.e., collisions governed by inverse power laws and resonant charge exchange) is the Boltzmann collision  
230 integral.

In this study, the Boltzmann collision integral is employed to model three types of collisions: Coulomb collisions, hard-sphere interactions, and Maxwell-molecule collisions. These interactions differ primarily in the range and character of the forces between particles. Coulomb collisions describe long-range electrostatic interactions between charged particles, resulting in cumulative small-angle deflections; in plasmas. In contrast, the hard-sphere model assumes that particles interact only upon  
235 direct contact, with instantaneous collisions determined purely by geometry, making it suitable for neutral gases with short-range interactions. Maxwell molecule collisions, based on a soft repulsive force decreasing with the fifth power of distance, represent an intermediate case with short-range, smooth interactions (Schunk, 1977; Chapman and Cowling, 1990; Schunk and Nagy, 2009).

The general expressions for the collision terms, under the assumption that the velocity distribution functions of both inter-  
240 acting species,  $s$  and  $t$ , follow drifting standard Kappa distributions, are summarized below for the three types of collisions: Coulomb collisions, hard-sphere interactions, and Maxwell molecule collisions. For Coulomb collisions and hard-sphere interactions, the results are implicitly derived in Jwailes et al. (2025) and can be obtained by setting  $\kappa_0 = \kappa$ . In the case of Maxwell molecule collisions, the derivation follows the same procedure as in Jwailes et al. (2025), but with modifications in



and the drift-to-thermal speed ratio  $\varepsilon_{st}$  is given by

$$\varepsilon_{st} = \frac{|\Delta \mathbf{u}_{st}|}{w_{st}}, \quad w_{st} = \sqrt{\frac{2k_B T_{st}}{m_{st}}}, \quad (25)$$

230 with the reduced mass  $m_{st}$  and the reduced temperature  $T_{st}$  are defined as

$$m_{st} = \frac{m_s m_t}{m_s + m_t}, \quad T_{st} = \frac{m_s T_t + m_t T_s}{m_s + m_t}. \quad (26)$$

The kappa-dependent terms  $\nu_{st}^{\text{SK}}$  and  $\nu_{st,T}^{\text{SK}}$  represent, respectively, the effective collision frequency and the thermal equilibration rate (or simply the thermalisation rate) for systems described by the standard Kappa distribution, and they are defined as

$$\nu_{st}^{\text{SK}}(\kappa_s, \kappa_t) = \nu_{st} D(\kappa_s, \kappa_t), \quad (27)$$

$$235 \quad \nu_{st,T}^{\text{SK}}(\kappa_s, \kappa_t) = 2 \frac{m_{st}}{m_t} \nu_{st}^{\text{SK}}, \quad (28)$$

where  $\nu_{st}$  denote the effective collision frequency rate for systems governed by the Maxwellian distribution. The factors  $\nu_{st}$ ,  $\Phi$ ,  $\Psi$ ,  $D$ , and  $H$  forms change depending on the type of collision, such as Coulomb, hard-sphere, or Maxwell molecule collisions, and can be summarized as follows:

**Coulomb collisions**

240 The effective collision frequency for Coulomb collisions in the Maxwellian case is

$$\nu_{st} = \nu_{st}^{\text{Co}} = \frac{4}{3} \frac{n_t}{\pi^{1/2}} \frac{m_t}{m_s + m_t} \left( \frac{1}{2k_B T_{st}} \right)^{3/2} Q_{\text{Co}}, \quad (29)$$

where  $Q_{\text{Co}}$  is defined as

$$Q_{\text{Co}} = 4\pi \left( \frac{e_s e_t}{4\pi \varepsilon_0 m_{st}} \right)^2 \ln \Lambda, \quad (30)$$

with  $e_s$  and  $e_t$  are the charges of species  $s$  and  $t$ , respectively,  $\varepsilon_0$  is the permittivity of free space, and  $\ln \Lambda$  is the Coulomb 245 logarithm. The functions  $\Phi$  and  $\Psi$  are given by

$$\Phi = \Phi_{\text{Co}}(\varepsilon_{st}) = \frac{3\sqrt{\pi} \operatorname{erf}(\varepsilon_{st})}{4 \varepsilon_{st}^3} - \frac{3e^{-\varepsilon_{st}^2}}{2\varepsilon_{st}^2}, \quad (31)$$

$$\Psi = \Psi_{\text{Co}}(\varepsilon_{st}) = e^{-\varepsilon_{st}^2}. \quad (32)$$

The kappa-dependent factors  $D$  and  $H$  are defined as

$$D(\kappa_s, \kappa_t) = \frac{(\kappa_s - 1/2)(\kappa_t - 1/2)}{\kappa_s \kappa_t}, \quad (33)$$

$$250 \quad H(\kappa_\alpha) = \frac{\Gamma(\kappa_\alpha) \kappa_\alpha^{1/2}}{\Gamma(\kappa_\alpha + 1/2)}, \quad \alpha = s, t. \quad (34)$$

the expectation values.

$$245 \quad \frac{\delta n_s}{\delta t} = 0, \quad (17)$$

$$\frac{\delta \mathbf{M}_s}{\delta t} = \sum_t n_s m_s \nu_{st}^{\text{SK}}(\kappa_s, \kappa_t) \Phi(\varepsilon_{st}) \Delta \mathbf{u}_{st}, \quad (18)$$

$$\begin{aligned} \frac{\delta E_s}{\delta t} = \sum_t n_s \left[ \frac{3}{2} k_B \nu_{st,T}^{\text{SK}}(\kappa_s, \kappa_t) \Psi(\varepsilon_{st}) \Delta T_{st}^{\text{SK}} \right. \\ \left. + m_{st} \nu_{st}^{\text{SK}}(\kappa_s, \kappa_t) \Phi(\varepsilon_{st}) |\Delta \mathbf{u}_{st}|^2 \right], \end{aligned} \quad (19)$$

where the relative drift velocity  $\Delta \mathbf{u}_{st}$  and relative temperature difference  $\Delta T_{st}^{\text{SK}}$  are defined by

$$250 \quad \Delta \mathbf{u}_{st} = \mathbf{u}_t - \mathbf{u}_s, \quad (20)$$

$$\Delta T_{st}^{\text{SK}} = H(\kappa_t) T_t - H(\kappa_s) T_s, \quad (21)$$

and the drift-to-thermal speed ratio  $\varepsilon_{st}$  is given by

$$\varepsilon_{st} = \frac{|\Delta \mathbf{u}_{st}|}{w_{st}}, \quad w_{st} = \sqrt{\frac{2k_B T_{st}}{m_{st}}}, \quad (22)$$

with the reduced mass  $m_{st}$  and the reduced temperature  $T_{st}$  are defined as

$$255 \quad m_{st} = \frac{m_s m_t}{m_s + m_t}, \quad T_{st} = \frac{m_s T_t + m_t T_s}{m_s + m_t}. \quad (23)$$

The kappa parameter dependent terms  $\nu_{st}^{\text{SK}}$  and  $\nu_{st,T}^{\text{SK}}$  represent, respectively, the effective collision frequency and the thermal equilibration rate (or simply the thermalisation rate) for systems described by the standard Kappa distribution, and they are defined as

$$\nu_{st}^{\text{SK}}(\kappa_s, \kappa_t) = \nu_{st} D(\kappa_s, \kappa_t), \quad (24)$$

$$260 \quad \nu_{st,T}^{\text{SK}}(\kappa_s, \kappa_t) = 2 \frac{m_{st}}{m_t} \nu_{st}^{\text{SK}}, \quad (25)$$

where  $\nu_{st}$  denote the effective collision frequency rate for systems governed by the Maxwellian distribution. The functional forms of the factors  $\nu_{st}$ ,  $\Phi$ ,  $\Psi$ ,  $D$ , and  $H$  depend on the type of collision considered. The factors  $\nu_{st}$ ,  $\Phi$ , and  $\Psi$  are listed in Jwailes et al. (2025) for all three types of collisions—Coulomb collisions, hard-sphere interactions, and Maxwell molecule collisions. The factors  $D$  and  $H$ , however, are summarized for the three types of collisions as follows, for *Coulomb collisions*

and *hard-sphere interactions*, they are defined as:

$$D(\kappa_s, \kappa_t) = \frac{(\kappa_s - 1/2)}{\kappa_s} \frac{(\kappa_t - 1/2)}{\kappa_t}, \quad (26)$$

$$H(\kappa_\alpha) = \frac{\Gamma(\kappa_\alpha) \kappa_\alpha^{1/2}}{\Gamma(\kappa_\alpha + 1/2)}, \quad \alpha = s, t. \quad (27)$$



### Hard-sphere interactions

The effective collision frequency for Hard-sphere in the Maxwellian case is

$$\nu_{st} = \nu_{st}^{\text{HS}} = \frac{8}{3} \frac{n_t}{\pi^{1/2}} \frac{m_t}{m_s + m_t} \left( 2k_B \frac{T_{st}}{m_{st}} \right)^{1/2} Q_{\text{HS}}, \quad (35)$$

255 where  $Q_{\text{HS}}$  is defined as

$$Q_{\text{HS}} = \pi \sigma^2, \quad (36)$$

with  $\sigma$  represent the sum of the radii of the colliding particles. The functions  $\Phi$  and  $\Psi$  are given by

$$\begin{aligned} \Phi = \Phi_{\text{HS}}(\varepsilon_{st}) = & \frac{3}{8} \left( 1 + \frac{1}{2\varepsilon_{st}^2} \right) e^{-\varepsilon_{st}^2} \\ & + \frac{3\sqrt{\pi}}{8} \left( \varepsilon_{st} + \frac{1}{\varepsilon_{st}} - \frac{1}{4\varepsilon_{st}^3} \right) \text{erf}(\varepsilon_{st}), \end{aligned} \quad (37)$$

$$260 \quad \Psi = \Psi_{\text{HS}}(\varepsilon_{st}) = \frac{\sqrt{\pi}}{2} \left( \varepsilon_{st} + \frac{1}{2\varepsilon_{st}} \right) \text{erf}(\varepsilon_{st}) + \frac{e^{-\varepsilon_{st}^2}}{2}. \quad (38)$$

The kappa-dependent factors D and H are defined the same as in equation (33) and (34).

### Maxwell molecule collisions

The effective collision frequency for Maxwell molecule collisions in the Maxwellian case is

$$\nu_{st} = \nu_{st}^{\text{MC}} = \frac{n_t m_t}{m_s + m_t} Q_{\text{MC}}, \quad (39)$$

265 where  $Q_{\text{MC}}$  is defined as.

$$Q_{\text{MC}} = 0.844 \pi \left( \frac{K_{st}}{m_{st}} \right)^{1/2}, \quad (40)$$

with  $K_{st}$  denotes a proportionality constant that measures the force magnitude between particles. The functions  $\Phi$  and  $\Psi$  are given by

$$\Phi = \Phi_{\text{MC}}(\varepsilon_{st}) = 1, \quad \Psi = \Psi_{\text{MC}}(\varepsilon_{st}) = 1, \quad (41)$$

270 The factors D and H are defined as

$$D(\kappa_s, \kappa_t) = 1, \quad (42)$$

$$H(\kappa_\alpha) = \frac{\kappa_\alpha}{(\kappa_\alpha - 3/2)}, \quad \alpha = s, t. \quad (43)$$

A few remarks related to the collision terms summarized above are worth noting. First, the collision terms for non-drifting standard Kappa distributions can be obtained by setting the drift velocities of both interacting particles  $s$  and  $t$  to zero,  $\mathbf{u}_s =$

For Maxwell molecule collisions, they are defined as

$$D(\kappa_s, \kappa_t) = 1, \quad (28)$$

$$H(\kappa_\alpha) = \frac{\kappa_\alpha}{(\kappa_\alpha - 3/2)}, \quad \alpha = s, t. \quad (29)$$

A few remarks on the collision terms are worth noting. The collision terms for non-drifting standard Kappa distributions can be obtained by setting the drift velocities of both interacting particles  $s$  and  $t$  to zero,  $\mathbf{u}_s = \mathbf{u}_t = 0$ , in Eqs. (17-19). The same result holds when the drift velocities of species  $s$  and  $t$  are equal, i.e.,  $\mathbf{u}_s = \mathbf{u}_t$ . Another point is that, in the limit as  $\kappa$  approaches infinity,  $\kappa = \kappa_s = \kappa_t$ , the collision terms, Eqs. (17–19), exactly recover the same results as those for the Maxwellian distribution (Schunk and Nagy, 2009), with the same definitions of  $\Phi$ ,  $\Psi$ , and  $\nu_{st}$ . That is, the effective collision frequency, the thermalisation rate, and the relative temperature difference, which are the terms that the collision terms depend on the kappa parameter through, reduce to their form in the Maxwellian case

$$\lim_{\kappa \rightarrow \infty} \nu_{st}^{\text{SK}}(\kappa, \kappa) = \nu_{st}, \quad (30)$$

$$\lim_{\kappa \rightarrow \infty} \nu_{st,T}^{\text{SK}}(\kappa, \kappa) = \nu_{st,T}, \quad (31)$$

$$\lim_{\kappa \rightarrow \infty} \Delta T_{st}^{\text{SK}} = T_t - T_s = \Delta T_{st}. \quad (32)$$

Hence,

$$\lim_{\kappa \rightarrow \infty} D(\kappa, \kappa) = \lim_{\kappa \rightarrow \infty} H(\kappa) = 1. \quad (33)$$

With  $\nu_{st,T}$  denoting the thermalisation rate for systems governed by the Maxwellian distribution, defined as

$$\nu_{st,T} = 2 \frac{m_{st}}{m_t} \nu_{st}. \quad (34)$$

Obtaining the Maxwellian result provides a consistency check that the derived collision terms are correct, since the standard Kappa distribution reduces to a Maxwellian distribution when the kappa parameter  $\kappa$  approaches infinity, as discussed in Section 2.

### 3.3 Transport coefficients

A Lorentz plasma is a type of plasma characterized by negligible electron–electron collisions compared to electron–ion collisions, allowing the electrons to be treated as moving through a background of nearly stationary ions (Du, 2013). In this setting, and adopting the standard Kappa distribution, the transport coefficients—namely, the electrical conductivity  $\sigma_e$ , thermoelectric coefficient  $\alpha_e$ , diffusion coefficient  $D_e$ , and mobility coefficient  $\mu_e$ —can be derived using the five-moment approximation. The procedure starts from the momentum equation with a drifting standard Kappa distribution, equation (18), for a simple electron–ion collision. By assuming a steady, low-inertia regime with unmagnetized plasma ( $\mathbf{B} = 0$ ), negligible gravitational



275  $\mathbf{u}_t = 0$ , in equations (20-22). The same result holds when the drift velocities of species  $s$  and  $t$  are equal, i.e.,  $\mathbf{u}_s = \mathbf{u}_t$ . Second, the functions  $\Phi$ 's and  $\Psi$ 's in case of Coulomb collision and hard sphere interaction, given in equations (31, 32, 37, and 38) can be written in terms of the hypergeometric functions, as discussed in Jwailes et al. (2025). Third, in the limit as  $\kappa$  approaches infinity,  $\kappa = \kappa_s = \kappa_t$ , the collision terms, equation (20–22), exactly recover the same results as those for the Maxwellian distribution (Schunk and Nagy, 2009), with the same definitions of  $\Phi$ ,  $\Psi$ , and  $\nu_{st}$ . That is, the effective collision frequency, the thermalisation rate, and the relative temperature difference, which are the terms that the collision terms depend on the kappa parameter through, reduce to their form in the Maxwellian case

$$\lim_{\kappa \rightarrow \infty} \nu_{st}^{\text{SK}}(\kappa, \kappa) = \nu_{st}, \quad (44)$$

$$\lim_{\kappa \rightarrow \infty} \nu_{st,T}^{\text{SK}}(\kappa, \kappa) = \nu_{st,T}, \quad (45)$$

$$\lim_{\kappa \rightarrow \infty} \Delta T_{st}^{\text{SK}} = T_t - T_s = \Delta T_{st}. \quad (46)$$

285 Hence,

$$\lim_{\kappa \rightarrow \infty} D(\kappa, \kappa) = \lim_{\kappa \rightarrow \infty} H(\kappa) = 1. \quad (47)$$

With  $\nu_{st,T}$  denoting the thermalisation rate for systems governed by the Maxwellian distribution, defined as

$$\nu_{st,T} = 2 \frac{m_{st}}{m_t} \nu_{st}. \quad (48)$$

Obtaining the Maxwellian result provides a consistency check that the derived collision terms are correct, since the standard Kappa distribution reduces to a Maxwellian distribution when the kappa parameter  $\kappa$  approaches infinity, as discussed in Section 2.

### 3.3 Transport coefficients

A Lorentz plasma is a type of plasma characterized by negligible electron–electron collisions compared to electron–ion collisions, allowing the electrons to be treated as moving through a background of nearly stationary ions (Du, 2013). In this setting, and adopting the standard Kappa distribution, the transport coefficients—namely, the electrical conductivity  $\sigma_e$ , thermoelectric coefficient  $\alpha_e$ , diffusion coefficient  $D_e$ , and mobility coefficient  $\mu_e$ —can be derived using the five-moment approximation. The procedure starts from the momentum equation with a drifting standard Kappa distribution, equation (21), for a simple electron–ion collision. That is, by assuming a steady and low-inertia regime, unmagnetized plasma ( $\mathbf{B} = 0$ ) with negligible gravitational effects ( $\mathbf{G} = 0$ ), negligible ion drift ( $\mathbf{u}_i \approx 0$ ), and the electron drift velocity is small compared to the thermal velocity ( $\epsilon_{ei} = 0$ ), the electron momentum equation reduces to the following form (Jwailes et al., 2025),

$$-n_e \mathbf{u}_e = \frac{k_B T_e}{m_e \nu_{ei}^{\text{SK}}} \nabla n_e + \frac{n_e k_B}{m_e \nu_{ei}^{\text{SK}}} \nabla T_e + \frac{n_e e}{m_e \nu_{ei}^{\text{SK}}} \mathbf{E}. \quad (49)$$

By setting  $\nabla n_e = 0$ , as in Husidic et al. (2021), equation 49 reduces to the generalized Ohm's law :

$$\mathbf{E} = \frac{\mathbf{J}_e}{\sigma_e} + \alpha_e \nabla T_e. \quad (50)$$





where  $\mathbf{E}$  denotes the electric field and  $\mathbf{J}_e$  is the current density, with  $e$  being the electron charge and  $n_e$  the electron number  
305 density. From this, we can identify the electrical conductivity and thermoelectric coefficient as

$$\sigma_e = \frac{n_e e^2}{m_e \nu_{ei}^{SK}}, \quad (51)$$

$$\alpha_e = -\frac{k_B}{e}. \quad (52)$$

Alternatively, by setting  $\nabla T_e = 0$ , as in Husidic et al. (2021), we obtain the extended Fick's law :

$$\mathbf{\Gamma}_e = -D_e \nabla n_e - \mu_e n_e \mathbf{E}. \quad (53)$$

310 where  $\mathbf{\Gamma}_e$  denotes the particle flux density, and the diffusion and mobility coefficients are identified as

$$D_e = \frac{k_B T_e}{m_e \nu_{ei}^{SK}}, \quad (54)$$

$$\mu_e = \frac{e}{m_e \nu_{ei}^{SK}}. \quad (55)$$

Equations 51, 52, 54, and 55 represent the mathematical forms of the transport coefficients governing electron dynamics in  
a Lorentz plasma with a standard Kappa distribution. Together, they demonstrate that electrical conduction, thermoelectric  
315 effects, diffusion, and mobility coefficients are controlled primarily by the electron–ion collision frequency.

#### 4 Comparison of collision processes and transport coefficients

In this section, we present a comprehensive comparison of the results derived in Section 3 for three types of distributions: the  
standard Kappa, modified Kappa, and Maxwellian distributions. The comparison focuses on three aspects. First, we examine  
the effective collision frequency and the thermalisation rate. Next, we analyze the collision terms, specifically for Coulomb  
320 collisions. Finally, we compare the resulting transport coefficients for each distribution.

##### 4.1 Effective collision frequency and thermalisation rate

The effective collision frequency describes the average rate of how frequently collisions occur, determining the efficiency of  
momentum transfer within the system, while the thermalisation rate measures how rapidly the system approaches thermal  
equilibrium through collisions. Both quantities are essential for understanding the exchange of momentum and energy between  
325 particles due to collisions. Within the five-moment approximation of the transport equations, these quantities are obtained  
directly from the momentum and energy collision terms. Expressions for the standard Kappa distribution are given in equations  
(27) and (28). Corresponding expressions for the modified Kappa distribution can be found in Jwailes et al. (2025), while those  
for the Maxwellian distribution are provided in Schunk and Nagy (2009).

Equations (27) and (28) show that, for the standard Kappa distribution, both the effective collision frequency and the ther-  
330 malisation rate are affected by the kappa-dependent function  $D(\kappa_s, \kappa_t)$ . This function depends on the kappa parameters  $\kappa_s$  and

295 effects ( $\mathbf{G} = 0$ ), and negligible ion drift velocity ( $\mathbf{u}_i \approx 0$ ), as appropriate for a Lorentz plasma, while allowing electrons to retain a small but finite drift velocity relative to the thermal speed (so that  $\epsilon_{ei} = 0$ ), the electron momentum equation reduces to the following form (Jwailes et al., 2025),

$$-n_e \mathbf{u}_e = \frac{k_B T_e^\kappa}{m_e \nu_{ei}^{\text{SK}}} \nabla n_e + \frac{n_e k_B}{m_e \nu_{ei}^{\text{SK}}} \nabla T_e^\kappa + \frac{n_e e}{m_e \nu_{ei}^{\text{SK}}} \mathbf{E}. \quad (35)$$

By setting  $\nabla n_e = 0$ , as in Husidic et al. (2021), and substituting the expression for the effective temperature  $T_e^\kappa$  using Eq.(5), Eq. (35) reduces to the generalized Ohm's law :

$$\mathbf{E} = \frac{\mathbf{J}_e}{\sigma_e} + \alpha_e \nabla T_e. \quad (36)$$

where  $\mathbf{E}$  denotes the electric field and  $\mathbf{J}_e$  is the current density, with  $e$  being the electron charge and  $n_e$  the electron number density. From this, we can identify the electrical conductivity and thermoelectric coefficient as

$$\sigma_e = \frac{n_e e^2}{m_e \nu_{ei}^{\text{SK}}}, \quad (37)$$

$$305 \quad \alpha_e = -\frac{k_B}{e} \left( \frac{\kappa_e}{\kappa_e - 3/2} \right). \quad (38)$$

Alternatively, by setting  $\nabla T_e = 0$ , which consequently implies that  $\nabla T_e^\kappa = 0$ , as in Husidic et al. (2021), we obtain the extended Fick's law :

$$\mathbf{\Gamma}_e = -D_e \nabla n_e - \mu_e n_e \mathbf{E}. \quad (39)$$

where  $\mathbf{\Gamma}_e$  denotes the particle flux density, and the diffusion and mobility coefficients are identified as

$$310 \quad D_e = \frac{k_B T_e^\kappa}{m_e \nu_{ei}^{\text{SK}}}, \quad (40)$$

$$\mu_e = \frac{e}{m_e \nu_{ei}^{\text{SK}}}. \quad (41)$$

Eqs. (37), (38), (40), and (41) represent the mathematical forms of the transport coefficients governing electron dynamics in a Lorentz plasma with a standard Kappa distribution. Together, they demonstrate that electrical conductivity, thermoelectric, diffusion, and mobility coefficients are controlled primarily by the electron-ion effective collision frequency.

#### 315 4 Comparison of collision processes and transport coefficients

In this section, we present a comprehensive comparison of the results derived in Section 3 for three types of distributions: the standard Kappa, modified Kappa, and Maxwellian distributions. The comparison focuses on three aspects. First, we examine the effective collision frequency and the thermalisation rate. Next, we analyze the collision terms, specifically for Coulomb collisions. Finally, we compare the resulting transport coefficients for each distribution.



$\kappa_t$  of the interacting species  $s$  and  $t$  and its form varies with the type of collision process considered. In collision processes such as Maxwell molecule interactions, where the collision frequency is independent of particle velocity, the redistribution of particles' velocities introduced by the standard Kappa distribution has no effect. In this case,  $D = 1$ , and both the effective collision frequency and the thermalisation rate remain identical to the Maxwellian case,

$$335 \quad \nu_{st}^{\text{SK}} = \nu_{st}, \quad \text{and} \quad \nu_{st,T}^{\text{SK}} = \nu_{st,T}. \quad (56)$$

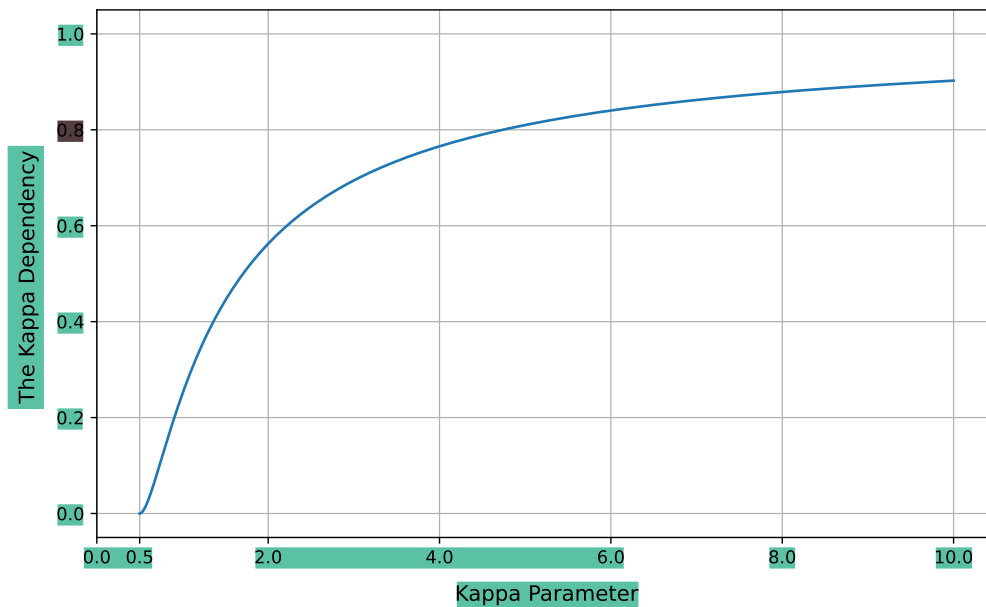


**Figure 3.** The kappa dependency for both the effective collision frequency and the thermalisation rate.

In contrast, for collision processes that strongly depend on particle velocity, the standard Kappa distribution significantly affects both the effective collision frequency and the thermalisation rate. This effect becomes particularly evident in processes such as Coulomb collisions and hard-sphere interactions, where the velocity distribution plays a central role. In these cases, the function  $D$  vary according to the kappa parameters  $\kappa_s$  and  $\kappa_t$ , as given in equation (33). To compare the effective collision frequency and thermalisation rate with the Maxwellian case, and to better understand their behaviour, we consider the special case  $\kappa = \kappa_s = \kappa_t$ , so that the expressions,  $\nu_{st}^{\text{SK}}$  and  $\nu_{st,T}^{\text{SK}}$ , reduce to

$$\nu_{st}^{\text{SK}} = \nu_{st} \left( \frac{\kappa - 1/2}{\kappa} \right)^2, \quad (57)$$

$$\nu_{st,T}^{\text{SK}} = 2 \frac{m_{st}}{m_t} \nu_{st}^{\text{SK}}, \quad (58)$$

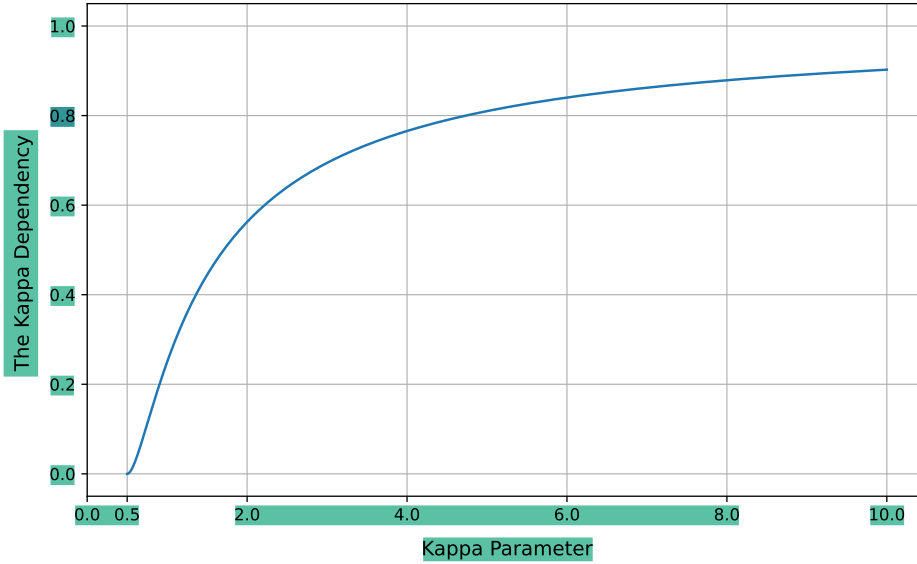


**Figure 3.** Dependence of the effective collision frequency  $\nu_{st}^{\text{SK}}$  and thermalisation rate  $\nu_{st,T}^{\text{SK}}$  on the kappa parameter  $\kappa$  for Coulomb collisions and hard-sphere interactions, as defined in Eq. (43).

#### 320 4.1 Effective collision frequency and thermalisation rate

The effective collision frequency describes the average rate of how frequently collisions occur, determining the efficiency of momentum transfer within the system, while the thermalisation rate measures how rapidly the system approaches thermal equilibrium through collisions. Both quantities are essential for understanding the exchange of momentum and energy between particles due to collisions. Within the five-moment approximation of the transport equations, these quantities are obtained  
 325 directly from the momentum and energy collision terms. Expressions for the standard Kappa distribution are given in Eqs. (24) and (25). Corresponding expressions for the modified Kappa distribution can be found in Jwailes et al. (2025), while those for the Maxwellian distribution are provided in Schunk and Nagy (2009).

Eqs. (24) and (25) show that, for the standard Kappa distribution, both the effective collision frequency and the thermalisation rate are affected by the kappa-dependent function  $D(\kappa_s, \kappa_t)$ . This function depends on the kappa parameters  $\kappa_s$  and  $\kappa_t$  of the  
 330 interacting species  $s$  and  $t$  and its form varies with the type of collision process considered. In collision processes such as Maxwell molecule interactions, where the collision frequency is independent of particle velocity, the redistribution of particles' velocities introduced by the standard Kappa distribution has no effect. In this case,  $D = 1$ , and both the effective collision frequency and the thermalisation rate remain identical to the Maxwellian case,

$$\nu_{st}^{\text{SK}} = \nu_{st}, \quad \text{and} \quad \nu_{st,T}^{\text{SK}} = \nu_{st,T}. \quad (42)$$



345 Equations (57) and (58) show that both the effective collision frequency and the thermalisation rate are reduced at low values of  $\kappa$  and increase as  $\kappa$  increases. As  $\kappa$  goes to infinity, the kappa term in equation (57) approaches 1, and the results converge to those of the Maxwellian distribution, as illustrated in Figure 3. In this figure, we plot the kappa dependency for both the effective collision frequency and the thermalisation rate; in other words, the ratios  $\nu_{st}^{\text{SK}}/\nu_{st}$  and  $\nu_{st,T}^{\text{SK}}/\nu_{st,T}$  as functions of the kappa parameter. This behaviour arises from the redistribution of the particles' velocities in the standard Kappa distribution.

350 As discussed in Section 2, low values of  $\kappa$  correspond to a reduced in the population of particles near the core with a small velocity magnitude compared to a Maxwellian distribution. Since collision frequency in Coulomb collision and hard sphere interactions are inversely proportional to function of velocity, this reduction leads to lower effective collision frequency and thermalisation rates at small  $\kappa$  values.

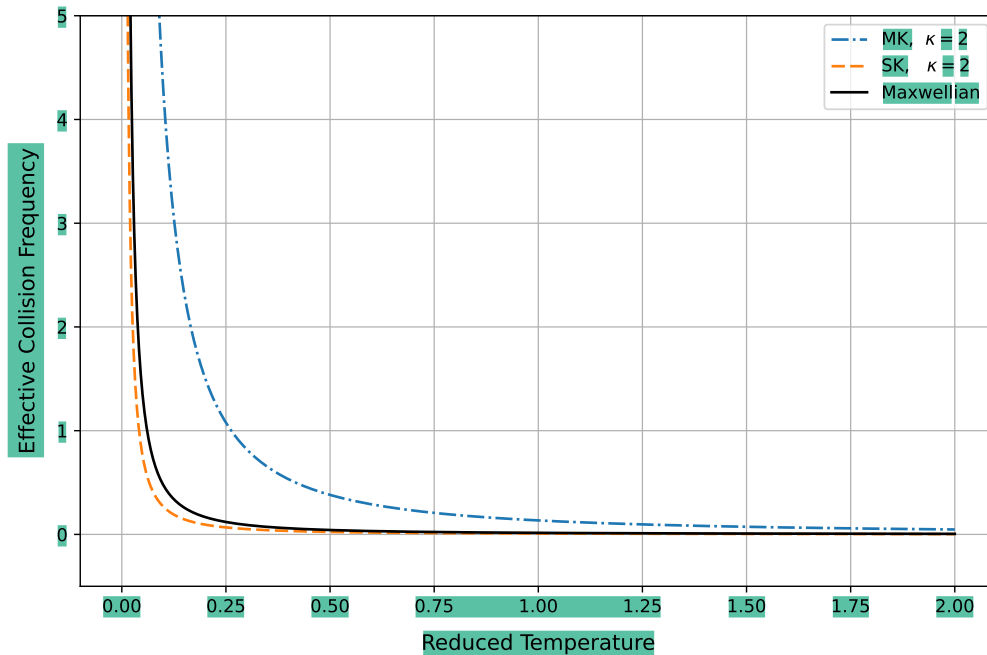


**Figure 4.** The effective collision frequency as a function of reduced temperature  $T_{st}$  for the Maxwellian, modified Kappa, and standard Kappa distributions.

For the modified Kappa distribution, Jwailes et al. (2025) derived both the effective collision frequency and the thermalisation rate. Since both the standard and the modified Kappa distributions primarily redistribute particles' velocities, the effective collision frequency remains unchanged when the collision frequency is independent of velocity. This is the case for Maxwell molecule interaction, for which the collision frequency is constant across Maxwellian, standard Kappa, and modified Kappa distributions

$$\nu_{st}^{\text{SK}} = \nu_{st}^{\text{MK}} = \nu_{st}, \quad \text{and} \quad \nu_{st,T}^{\text{SK}} = \nu_{st,T}^{\text{MK}} = \nu_{st,T}. \tag{59}$$

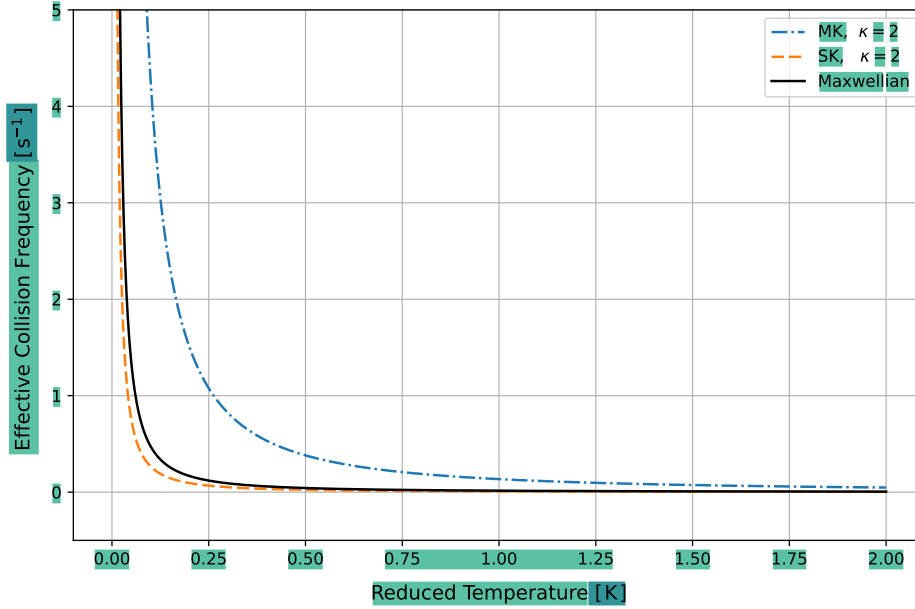


**Figure 4.** The effective collision frequency as a function of reduced temperature  $T_{st}$  for the Maxwellian, modified Kappa, and standard Kappa distributions in case of Coulomb collisions.

335 In contrast, for collision processes that strongly depend on particle velocity, the standard Kappa distribution significantly affects both the effective collision frequency and the thermalisation rate. This effect becomes particularly evident in processes such as Coulomb collisions and hard-sphere interactions, where the velocity distribution plays a central role. In these cases, the function  $D$  vary according to the kappa parameters  $\kappa_s$  and  $\kappa_t$ , as given in Eq. (26). To compare the effective collision frequency and thermalisation rate with the Maxwellian case, and to better understand their behaviour, we consider the special

340 case  $\kappa = \kappa_s = \kappa_t$ , so that the expressions,  $\nu_{st}^{\text{SK}}$  and  $\nu_{st,T}^{\text{SK}}$ , reduce to

$$\nu_{st}^{\text{SK}} = \nu_{st} \left( \frac{\kappa - 1/2}{\kappa} \right)^2, \quad (43)$$

$$\nu_{st,T}^{\text{SK}} = 2 \frac{m_{st}}{m_t} \nu_{st}^{\text{SK}}. \quad (44)$$

Relating Eq. (43) to the Debye length obtained for the standard Kappa distribution in Scherer et al. (2020), we recover exactly the same kappa dependence reported in that work, see Appendix A, thereby confirming the consistency of the present

345 formulation. Eqs. (43) and (44) show that both the effective collision frequency and the thermalisation rate are reduced at low values of  $\kappa$  and increase as  $\kappa$  increases. As  $\kappa$  goes to infinity, the kappa term in Eq. (43) approaches 1, and the results converge to those of the Maxwellian distribution, as illustrated in Figure 3. In this figure, we plot the kappa dependency for both the effective collision frequency and the thermalisation rate; in other words, the ratios  $\nu_{st}^{\text{SK}}/\nu_{st}$  and  $\nu_{st,T}^{\text{SK}}/\nu_{st,T}$  as functions of the kappa parameter. This behaviour arises from the redistribution of the particles' velocities in the standard Kappa distribution.



360 where  $\nu_{st}^{\text{MK}}$  and  $\nu_{st,T}^{\text{MK}}$  represent the effective collision frequency and the thermalisation rate, respectively, for systems described  
by the modified Kappa distribution. For collisions in which the collision frequency depends on particle velocity, such as  
Coulomb collisions or hard-sphere interactions, the choice of distribution strongly affects the effective collision frequency and  
the thermalisation rate. As discussed earlier, in the standard Kappa distribution, low values of  $\kappa$  lead to a reduced effective  
collision frequency compared to the Maxwellian case. However, this is not the case for the modified Kappa distribution, which  
365 predicts the opposite behaviour, showing an increased effective collision frequency at low  $\kappa$  values. Figure 4 illustrates this  
behaviour by showing the effective collision frequency as a function of reduced temperature in the case of Coulomb collision  
for Maxwellian, standard Kappa, and modified Kappa distributions. The figure shows that all three distributions exhibit the  
same general behaviour. However, the standard Kappa distribution shows a lower effective collision frequency compared to  
the Maxwellian distribution, while the modified Kappa distribution shows a significantly higher effective collisions frequency  
370 relative to the Maxwellian case. This behaviour arises from the redistribution of particle velocities in the standard and modified  
Kappa distributions, as discussed in Section 2. At low  $\kappa$  values, the low number of particles near the low energy core in the  
standard Kappa distribution leads to a lower effective collision frequency and thermalisation rate compared to the Maxwellian  
case. For the modified Kappa distribution, the number of particles near the core with small velocity magnitudes is higher than  
in the Maxwellian distribution, which increases the collision frequency for Coulomb collisions and hard sphere interactions.

## 375 4.2 Collision terms

The collision terms for the five-moment approximation, presented in equations (20–22), describe how the density, momentum,  
and energy for species  $s$  change due to collisions. These terms depend on the number density  $n_s$ , drift velocity  $\mathbf{u}_s$ , and  
temperature  $T_s$  for species  $s$ , as well as on the corresponding parameters of species  $t$ , number density  $n_t$ , drift velocity  $\mathbf{u}_t$ ,  
and temperature  $T_t$ . Additionally, two functions of  $\kappa_s$  and  $\kappa_t$ , namely  $D(\kappa_s, \kappa_t)$  and  $H(\kappa_\alpha)$ ,  $\alpha = s, t$ , which contribute to the  
380 effective collision frequency, the thermalisation rate, and the relative temperature difference. The particle masses  $m_s$  and  $m_t$   
are constant and remain unchanged throughout the collision process for all types of collisions; as a result, the density collision  
term vanishes, as shown in equation (20).

In the Maxwellian case, both functions  $D(\kappa_s, \kappa_t)$  and  $H(\kappa_\alpha)$ ,  $\alpha = s, t$ , are set equal to one; see Sub-subsection 3.2. The  
behaviour of the momentum and energy collision terms in this case was studied in detail by Jwailes et al. (2025), providing an  
385 explanation for the physical trends shown in Figures 5a and 5b. Figure 5a shows the isolines of the magnitude of the momentum  
collision term, assuming that the direction of  $\Delta \mathbf{u}_{st}$  along the  $z$ -axis, while Figure 5b shows the isolines of the corresponding  
energy collision term. Both figures display the dependence on  $\Delta \mathbf{u}_{st}$  and  $T_s$ , with all other constants set to 1.0 for simplicity.  
Assuming identical parameters for all  $t$  particles, the summation over  $t$  in equations (20–22) reduces to multiplication by their  
number,  $N_t$ , which is set to 1000 for the sake of comparison with other cases.

390 To understand how the standard Kappa distribution changes the collision terms, we plot the isolines of the momentum and  
energy collision terms as functions of  $\Delta \mathbf{u}_{st}$  and  $T_s$ , as shown in Figure 6. We assume equal kappa values for both species,  $s$   
and  $t$ , i.e.,  $\kappa_s = \kappa_t = \kappa$ , to allow a direct comparison with the Maxwellian case and under the same conditions as in Figure 5a.  
The corresponding cross-sections at  $T_s = 0$  are shown in Figure 7. For the momentum collision term, the behavior closely

350 As discussed in Section 2, low values of  $\kappa$  correspond to a reduction in the population of particles near the core with a small velocity magnitude compared to a Maxwellian distribution. Since collision frequency in Coulomb collisions and hard sphere interactions are inversely proportional to function of velocity, this reduction leads to lower effective collision frequency and thermalisation rates at small  $\kappa$  values.

355 For the modified Kappa distribution, Jwailes et al. (2025) derived both the effective collision frequency and the thermalisation rate. Since both the standard and the modified Kappa distributions primarily redistribute particles' velocities, the effective collision frequency remains unchanged when the collision frequency is independent of velocity. This is the case for Maxwell molecule interaction, for which the collision frequency is constant across Maxwellian, standard Kappa, and modified Kappa distributions

$$\nu_{st}^{\text{SK}} = \nu_{st}^{\text{MK}} = \nu_{st}, \quad \text{and} \quad \nu_{st,T}^{\text{SK}} = \nu_{st,T}^{\text{MK}} = \nu_{st,T}. \quad (45)$$

360 where  $\nu_{st}^{\text{MK}}$  and  $\nu_{st,T}^{\text{MK}}$  represent the effective collision frequency and the thermalisation rate, respectively, for systems described by the modified Kappa distribution. For collisions in which the collision frequency depends on particle velocity, such as Coulomb collisions or hard-sphere interactions, the choice of distribution strongly affects the effective collision frequency and the thermalisation rate. As discussed earlier, in the standard Kappa distribution, low values of  $\kappa$  lead to a reduced effective collision frequency compared to the Maxwellian case. However, this is not the case for the modified Kappa distribution, which predicts the opposite behaviour, showing an increased effective collision frequency at low  $\kappa$  values. Figure 4 illustrates this behaviour by showing the effective collision frequency as a function of reduced temperature in the case of Coulomb collision for Maxwellian, standard Kappa, and modified Kappa distributions. Figure 4, shows that all three distributions exhibit the same general behaviour. However, the standard Kappa distribution shows a lower effective collision frequency compared to the Maxwellian distribution, while the modified Kappa distribution shows a significantly higher effective collisions frequency relative to the Maxwellian case. This behaviour arises from the redistribution of particle velocities in the standard and modified Kappa distributions, as discussed in Section 2. At low  $\kappa$  values, the low number of particles near the low energy core in the standard Kappa distribution leads to a lower effective collision frequency and thermalisation rate compared to the Maxwellian case. For the modified Kappa distribution, the number of particles near the core with small velocity magnitudes is higher than in the Maxwellian distribution, which increases the collision frequency for Coulomb collisions and hard sphere interactions.

## 375 4.2 Collision terms

The collision terms for the five-moment approximation, presented in equations (17–19), describe how the density, momentum, and energy for species  $s$  change due to collisions. These terms depend on the number density  $n_s$ , drift velocity  $\mathbf{u}_s$ , and temperature  $T_s$  for species  $s$ , as well as on the corresponding parameters of species  $t$ , number density  $n_t$ , drift velocity  $\mathbf{u}_t$ , and temperature  $T_t$ . Additionally, two functions of  $\kappa_s$  and  $\kappa_t$ , namely  $D(\kappa_s, \kappa_t)$  and  $H(\kappa_\alpha)$ ,  $\alpha = s, t$ , which contribute to the effective collision frequency, the thermalisation rate, and the relative temperature difference. The particle masses  $m_s$  and  $m_t$  are constant and remain unchanged throughout the collision process for all types of collisions; as a result, the density collision term vanishes, as shown in Eq. (17).



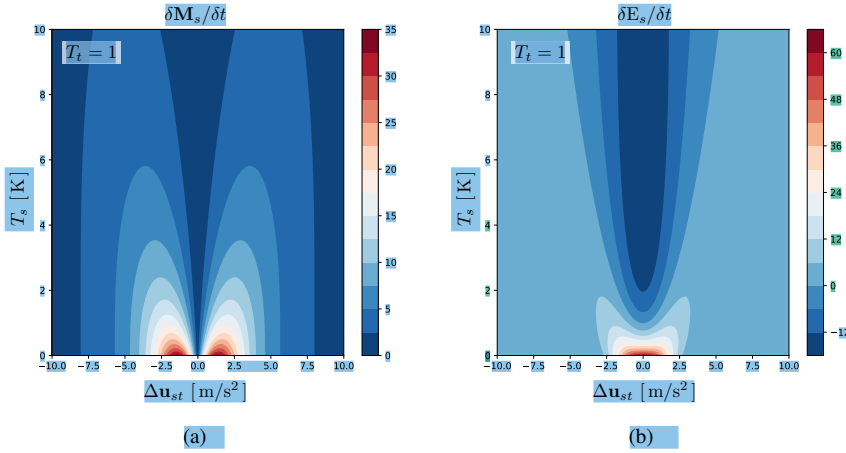


**Figure 5.** (a) The momentum collision term in units of  $[\text{N}/\text{m}^3]$ , and (b) the energy collision term in units of  $[\text{W}/\text{m}^3]$  for the Maxwellian velocity distribution function in the case of Coulomb collisions.

In the Maxwellian case, both functions  $D(\kappa_s, \kappa_t)$  and  $H(\kappa_\alpha)$ ,  $\alpha = s, t$ , are set equal to one; see Sub-subsection 3.2. The behaviour of the momentum and energy collision terms in this case was studied in detail by Jwailes et al. (2025), providing an explanation for the physical trends shown in Figures 5a and 5b. Figure 5a shows the isolines of the magnitude of the momentum collision term, assuming that the direction of  $\Delta \mathbf{u}_{st}$  along the  $z$ -axis, while Figure 5b shows the isolines of the corresponding energy collision term. Both figures display the dependence on  $\Delta \mathbf{u}_{st}$  and  $T_s$ , with all other constants set to 1.0 for simplicity. Assuming identical parameters for all  $t$  particles, the summation over  $t$  in Eqs. (17–19) reduces to multiplication by their number,  $N_t$ , which is set to 1000 for the sake of comparison with other cases.

For the momentum collision term, the behavior closely follows the Maxwellian case, with  $D(\kappa, \kappa)$  scaling the effective collision frequency, as shown in Figures 6 and 7. At low  $\kappa$ , the effective collision frequency decreases, as discussed in Sub-subsection 4.1, leading to reduced momentum transfer. To understand how the standard Kappa distribution changes the collision terms, we plot the isolines of the momentum and energy collision terms as functions of  $\Delta \mathbf{u}_{st}$  and  $T_s$ , as shown in Figure 6. We assume equal kappa values for both species,  $s$  and  $t$ , i.e.,  $\kappa_s = \kappa_t = \kappa$ , to allow a direct comparison with the Maxwellian case and under the same conditions as in Figure 5a. The corresponding cross-sections at  $T_s = 0$  are shown in Figure 7.

For the energy collision term, the function

$$W(\kappa, \kappa) = D(\kappa, \kappa) H(\kappa) \quad (46)$$

appears in the first term of Eq. (19), while  $D(\kappa, \kappa)$  contributes to the second term. The overall behavior is similar to the Maxwellian case, with smaller values of  $\kappa$  yielding a smaller energy collision term. Overall, both collision terms increase with increasing  $\kappa$ , converging toward the Maxwellian result.

follows the Maxwellian case, with  $D(\kappa, \kappa)$  scaling the effective collision frequency, as shown in Figures 6 and 7. At low  $\kappa$ , the effective collision frequency decreases, as discussed in Sub-subsection 4.1, leading to reduced momentum transfer.

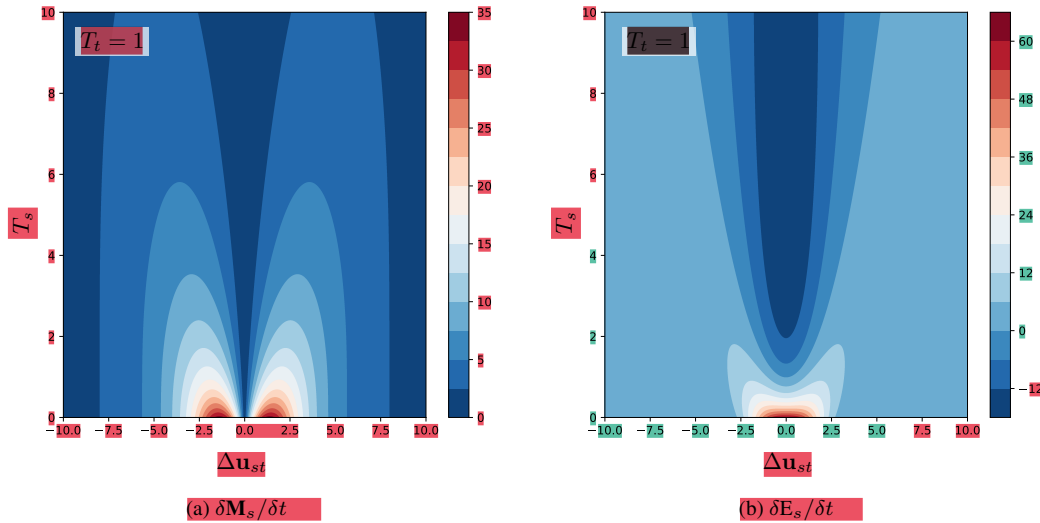


**Figure 5.** The momentum (a) and energy (b) collision terms for the Maxwellian velocity distribution function in the case of Coulomb collisions.

For the energy collision term, the function

$$W(\kappa, \kappa) = D(\kappa, \kappa)H(\kappa) \tag{60}$$

appears in the first term of equation 22, while  $D(\kappa, \kappa)$  contributes to the second term. The overall behavior is similar to the Maxwellian case, with smaller values of  $\kappa$  yielding a smaller energy collision term. Overall, both collision terms increase with increasing  $\kappa$ , converging toward the Maxwellian result.

For the modified Kappa distribution, Jwailes et al. (2025) have studied the behavior of the collision term and compared it with that of the Maxwellian distribution under the same conditions previously applied to the standard Kappa distribution. The results show that the collision terms behave similarly to the standard Kappa and the Maxwellian distribution; however, the modified Kappa distribution amplifies the collision terms at low values of  $\kappa$ . That is, collisions have a stronger influence on momentum and energy exchange between particles due to Coulomb interactions, which is the opposite behavior of the standard Kappa distribution discussed earlier. This significant difference is shown in Figure 8, which presents the cross sections of the momentum and energy collision terms at  $T_s = 0$  as functions of  $\Delta u_{st}$ . It is clear that, at the same value of  $\kappa$ , the collision terms in the modified Kappa distribution are much larger than those in both the standard Kappa and the Maxwellian distributions. This behavior is consistent with the results of Sub-section 4.1, where we found that the effective collision frequency and the thermalization rate are significantly higher for the modified Kappa distribution than for the standard Kappa distribution, as a result of how the particles distribute near the core.

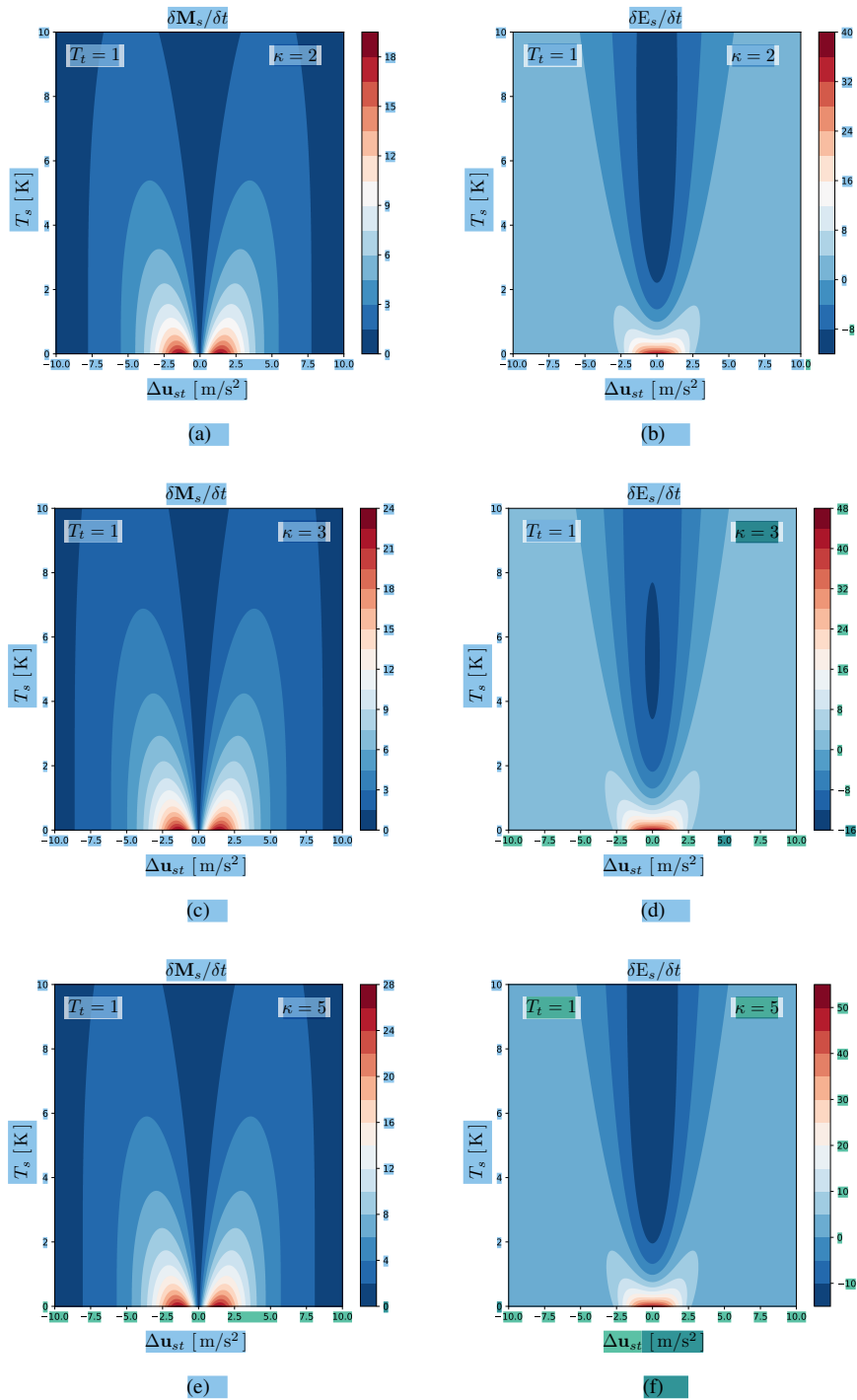


**Figure 6.** (a, c, e) The momentum collision term in units of  $[\text{N/m}^3]$ , and (b, d, f) the energy collision term in units of  $[\text{W/m}^3]$  for the standard Kappa velocity distribution function in the case of Coulomb collisions at different values of  $\kappa$ : 2, 3, and 5.

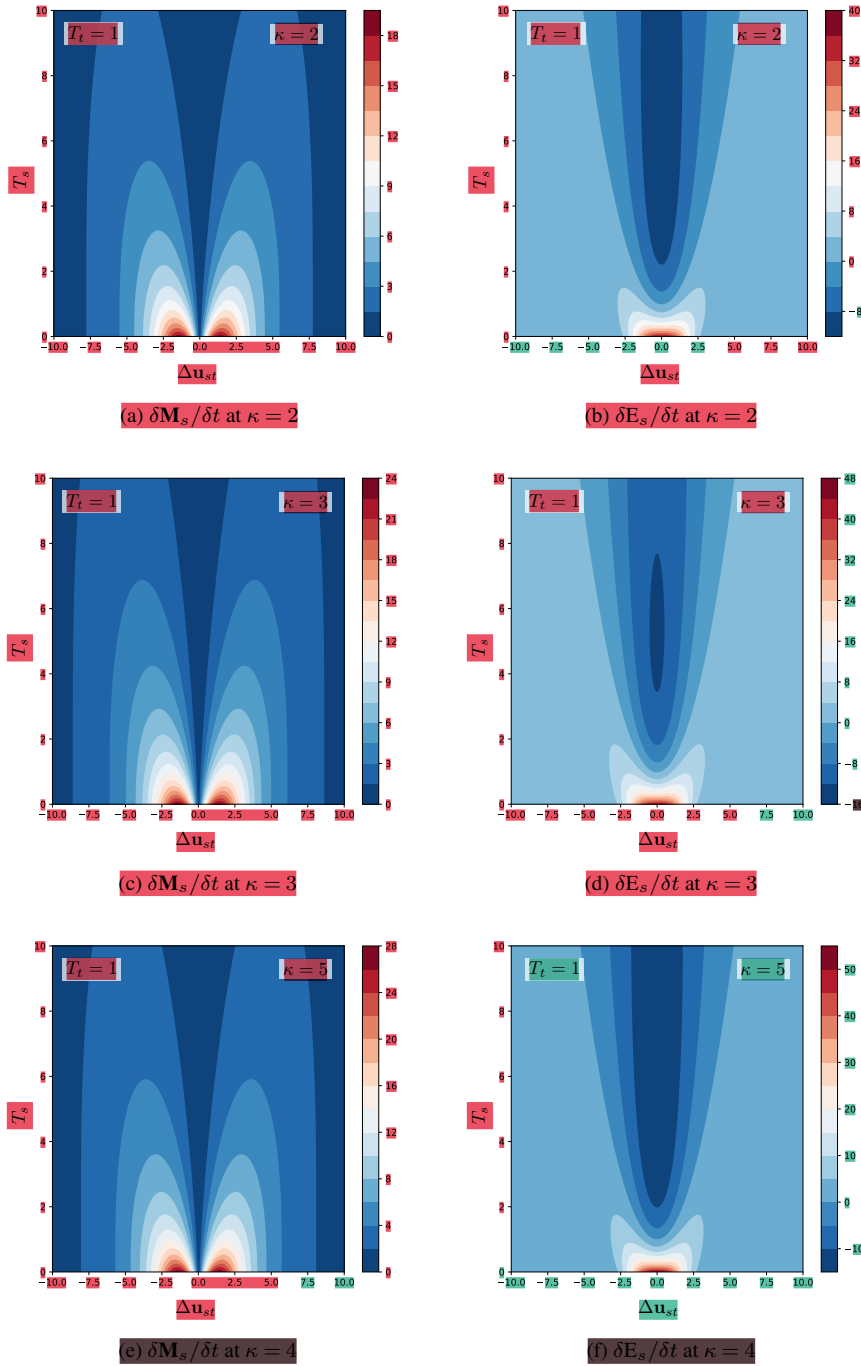


**Figure 6.** The momentum (a, c, e) and energy (b, d, f) collision terms for the standard Kappa velocity distribution function in the case of Coulomb collisions at different values of  $\kappa$ : 2, 3, and 4.

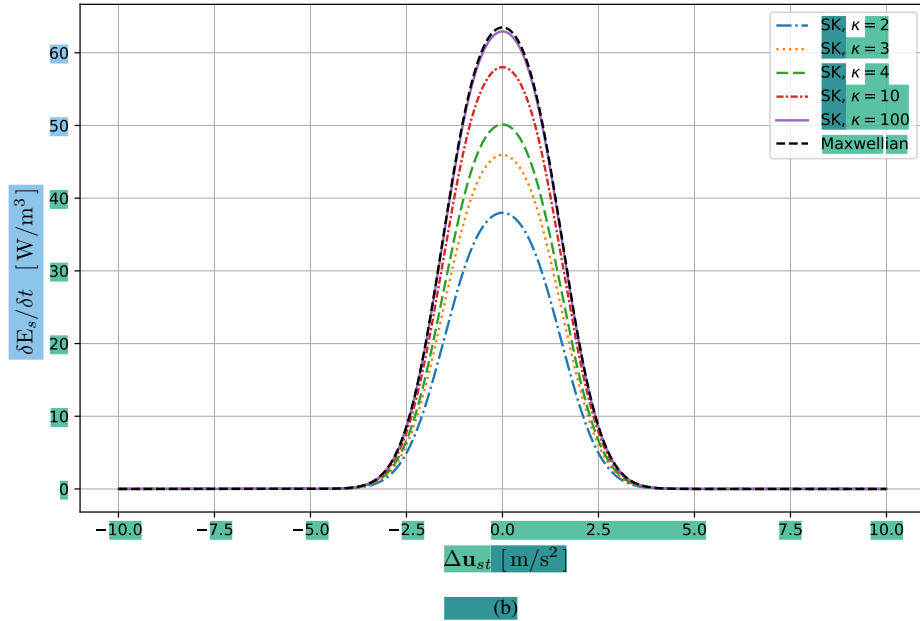
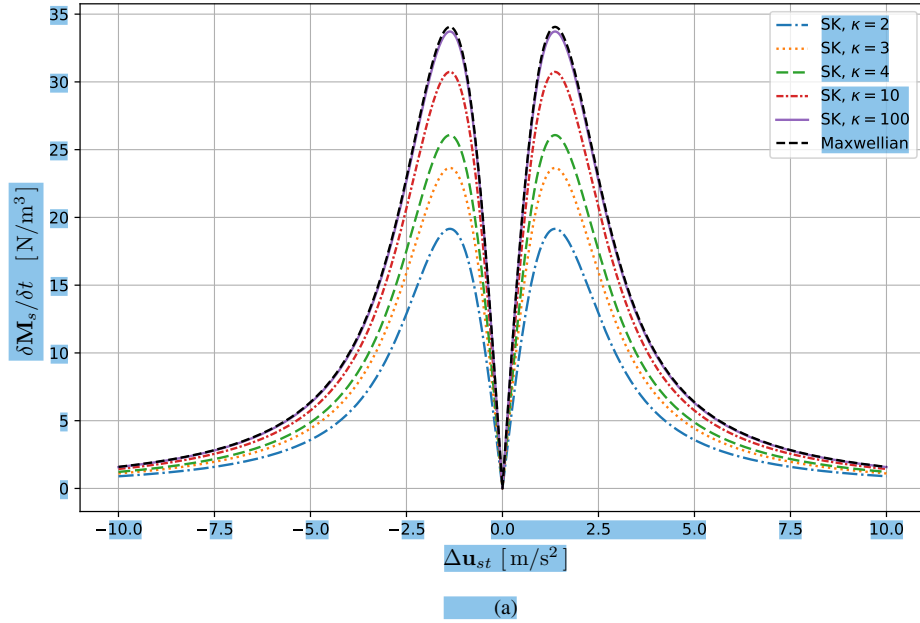
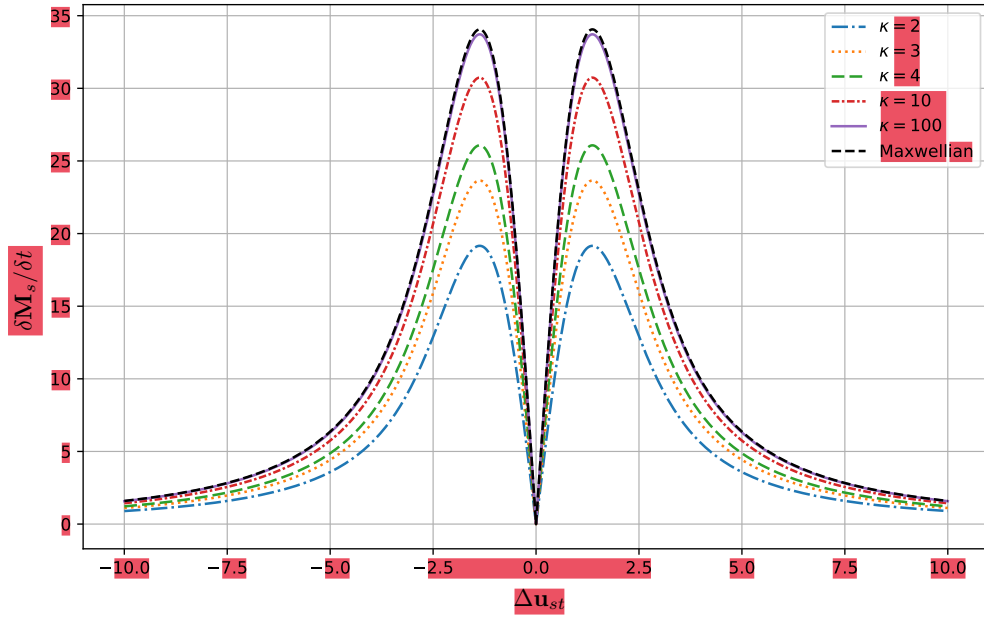
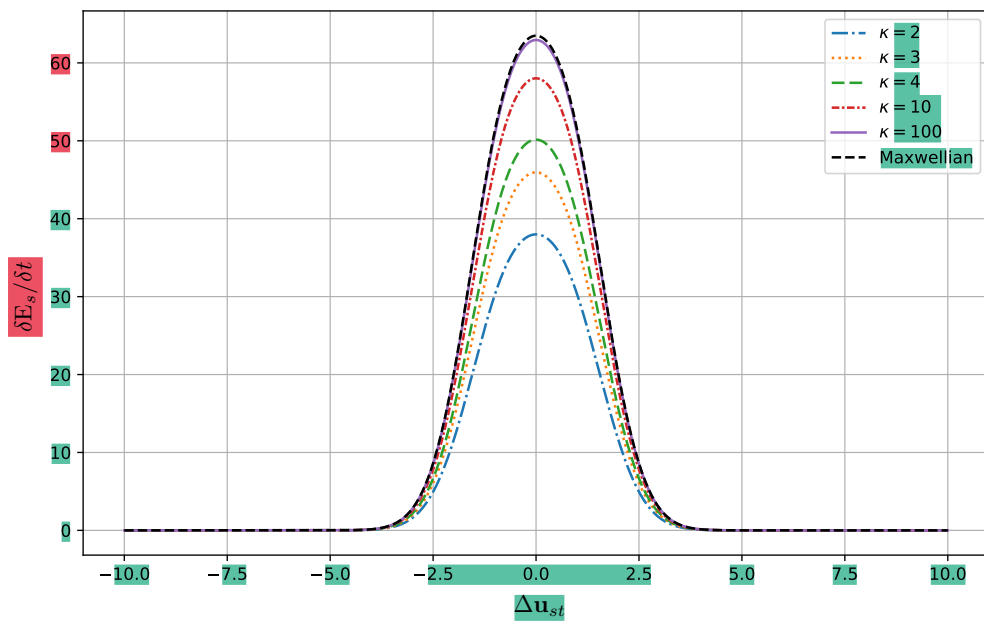


**Figure 7.** The cross-section of the momentum and energy collision terms for the standard Kappa and Maxwellian velocity distribution functions in the case of Coulomb collisions at  $T_s = 0$ .

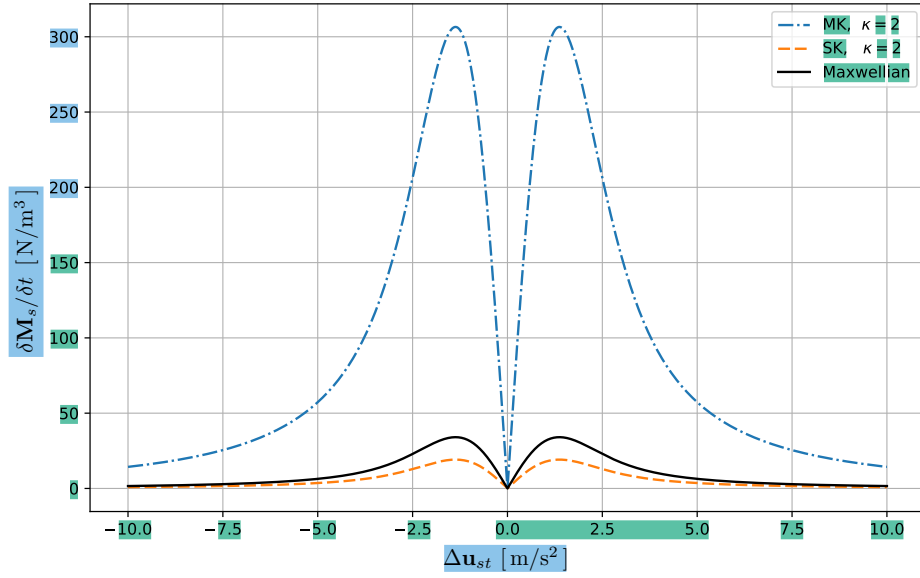


(a)  $\delta M_s / \delta t$  at  $T_s = 0$

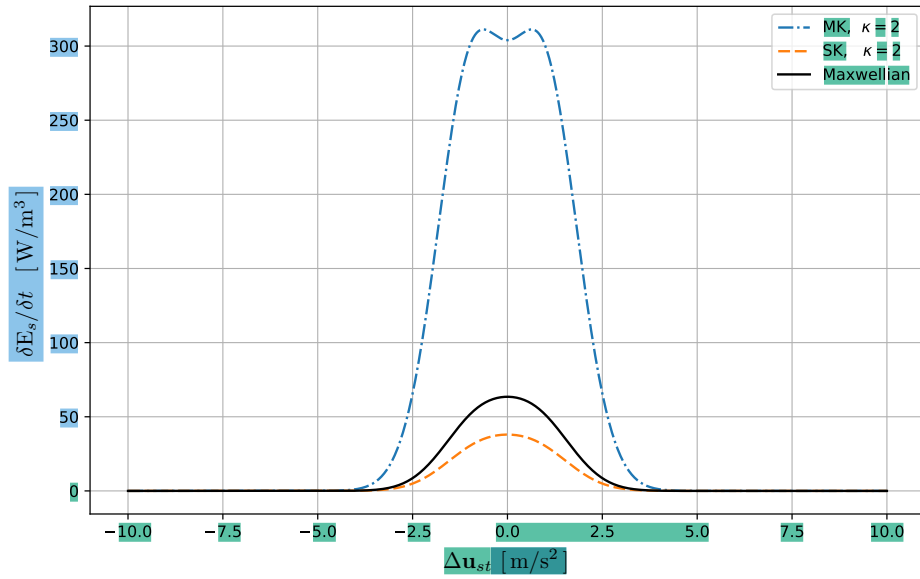


(b)  $\delta E_s / \delta t$  at  $T_s = 0$

**Figure 7.** The cross-section of the momentum and energy collision terms for the standard Kappa and Maxwellian velocity distribution functions in the case of Coulomb collisions at  $T_s = 0$ .



(a)



(b)

**Figure 8.** The cross-section of the momentum and energy collision terms for the standard Kappa and Maxwellian velocity distribution functions in the case of Coulomb collisions at  $T_s = 0$ .

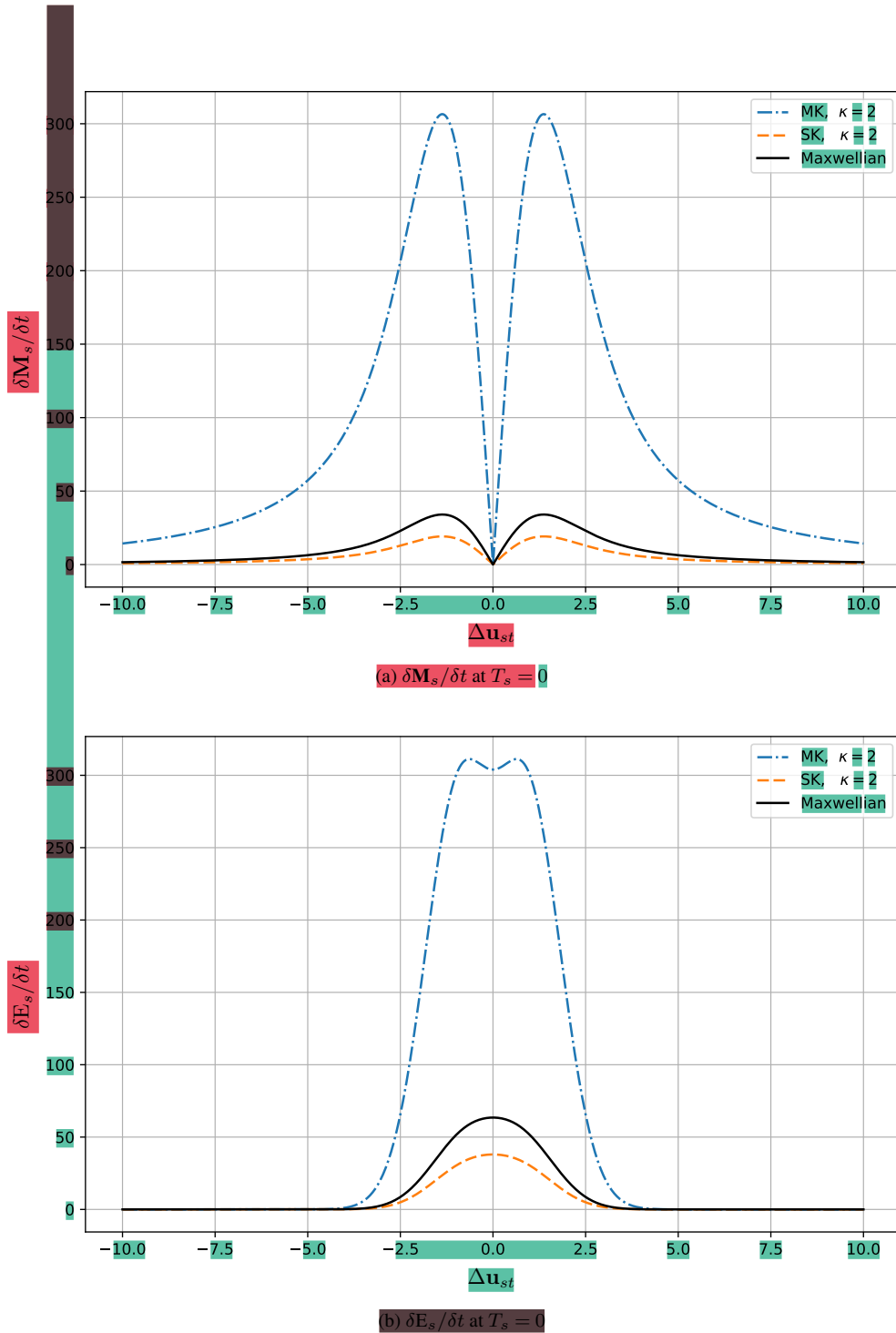


**Figure 8.** The cross-section of the momentum and energy collision terms for the standard Kappa and Maxwellian velocity distribution functions in the case of Coulomb collisions at  $T_s = 0$ .

For the modified Kappa distribution, Jwailes et al. (2025) have studied the behavior of the collision term and compared it with that of the Maxwellian distribution under the same conditions previously applied to the standard Kappa distribution. The results show that the collision terms behave similarly to the standard Kappa and the Maxwellian distribution; however, the modified Kappa distribution amplifies the collision terms at low values of  $\kappa$ . That is, collisions have a stronger influence on momentum and energy exchange between particles due to Coulomb interactions, which is the opposite behavior of the standard Kappa distribution discussed earlier. This significant difference is shown in Figure 8, which presents the cross sections of the momentum and energy collision terms at  $T_s = 0$  as functions of  $\Delta \mathbf{u}_{st}$ . It is clear that, at the same value of  $\kappa$ , the collision terms in the modified Kappa distribution are much larger than those in both the standard Kappa and the Maxwellian distributions. This behavior is consistent with the results of Sub-section 4.1, where we found that the effective collision frequency and the thermalization rate are significantly higher for the modified Kappa distribution than for the standard Kappa distribution, as a result of how the particles distribute near the core.

### 4.3 Transport coefficients

The transport coefficients for the standard Kappa distribution exhibit a clear and systematic dependence on the kappa parameters. This dependence is primarily determined by two factors: the effective electron temperature  $T_e^\kappa$  and the electron-ion effective collision frequency  $\nu_{ei}^{\text{SK}}$ .

In particular, the kappa dependence associated with the effective temperature appears in coefficients that are directly related to the system temperature, specifically the thermoelectric coefficient  $\alpha_e$  and the mobility coefficient  $\mu_e$ . Both of these coefficients are directly influenced by changes in the effective temperature associated with the standard Kappa distribution, where at low values of the kappa parameter, the system temperature increases compared to the Maxwellian case, leading to an increase in both the thermoelectric coefficient  $\alpha_e$  and the mobility coefficient  $\mu_e$ . Because this dependency arises from the effective temperature, it impacts the entire system regardless of the type of interaction between particles (i.e., the effect is the same for all three types of collisions: Coulomb collisions, hard-sphere interactions, and Maxwell molecules).

The second source of kappa dependence arises from the effective collision frequency, whereas the electrical conductivity, diffusion, and mobility all reflect this dependence through  $\nu_{ei}^{\text{SK}}$ , as these transport coefficients are inversely proportional to the effective collision frequency. As discussed earlier, when  $\kappa = \kappa_s = \kappa_t$ , the standard Kappa distribution affects the effective collision frequencies of various collision types differently. For Maxwell molecules, the effective collision frequency is identical to the Maxwellian case, and the kappa dependency of the effective collision frequency does not appear in their transport coefficients. However, for Coulomb collisions and hard-sphere interactions, the effective collision frequency decreases as  $\kappa$  decreases, leading to a increase in the transport coefficients at low values of  $\kappa$  compared to the Maxwellian case.

In Figure 9, we show the kappa dependence of the electrical conductivity, mobility coefficient, thermoelectric coefficient, and diffusion coefficient by plotting the ratios  $\sigma_e/\sigma_e^M$ ,  $\mu_e/\mu_e^M$ ,  $\alpha_e/\alpha_e^M$ , and  $D_e/D_e^M$  as functions of the kappa parameter  $\kappa$ . Here,  $\sigma_e^M$ ,  $\mu_e^M$ ,  $\alpha_e^M$ , and  $D_e^M$  represent, respectively, the electrical conductivity, mobility coefficient, thermoelectric coefficient,



### 4.3 Transport coefficients

From the first look at the derived expressions for the transport coefficients equation, electrical conductivity thermoelectric coefficient the diffusion and mobility coefficients listed in equations (51), (52), (54) and (55) respectively, we can see that they

415 satisfy the familiar relation between the electric conductivity and the mobility coefficient

$$\sigma_e = n_e e \mu_e, \quad (61)$$

and Einstein relation

$$D_e = \frac{k_B T_e}{e} \mu_e. \quad (62)$$

Importantly, both relations are found to hold consistently across all three considered velocity distributions: the standard Kappa, 420 the modified Kappa, and the Maxwellian distributions.

The resulting transport coefficients for the standard Kappa distribution exhibit distinct dependencies on the kappa parameters. In particular, the thermoelectric coefficient  $\alpha_e$  is independent of the kappa parameters, whereas the electrical conductivity, diffusion, and mobility all include the same kappa dependence through the effective collision frequency  $\nu_{ei}^{\text{SK}}$ . These transport coefficients are inversely proportional to the effective collision frequency. As discussed earlier, when  $\kappa = \kappa_s = \kappa_t$ , the effective 425 collision frequency affects different collision types in different ways. As a result, the influence of the standard Kappa distribution on the transport coefficients depends on the collision type. For Maxwell molecules, the effective collision frequency is identical to the Maxwellian case, and the transport coefficients remain unchanged. However, for Coulomb collisions and hard-sphere interactions, the effective collision frequency decreases as  $\kappa$  decreases, leading to an increase in the transport coefficients at low values of  $\kappa$  compared to the Maxwellian case, as shown in Figure 9, which shows the kappa dependence of the electrical 430 conductivity by plotting the ratio  $\sigma_e / \sigma_e^{\text{M}}$  as a function of  $\kappa$ , where  $\kappa = \kappa_t = \kappa_s$ , and

$$\sigma_e^{\text{M}} = \frac{n_e e^2}{m_e \nu_{ei}} \quad (63)$$

As  $\kappa$  approaches infinity, the effective collision frequency  $\nu_{ei}^{\text{SK}}$  reduces to the Maxwellian case  $\nu_{ei}$ , making the transport coefficients recover their Maxwellian limits. In Figure 9, we also compare the dependence of the electrical conductivity on the  $\kappa$  parameter from the present study with the results reported by Husidic et al. (2021). While the figure shows a different dependence on the kappa parameter between the two studies, however, the overall behaviour is the same: at low  $\kappa$  values, the 435 electrical conductivity becomes much larger than in the Maxwellian case, and as  $\kappa$  increases, we approach the Maxwellian case. This confirms that plasmas with smaller  $\kappa$  values conduct more efficiently. Thus, deviations from the Maxwellian limit lead to an increase in electrical conductivity. The difference in the kappa dependence arises from the collision models used in deriving the transport coefficients. While Husidic et al. (2021) employed a Krook-type (BGK) collision model, which provides 440 a simplified representation of collisions, our work uses the full Boltzmann collision integral, which offers a more realistic description, particularly for Coulomb collisions.

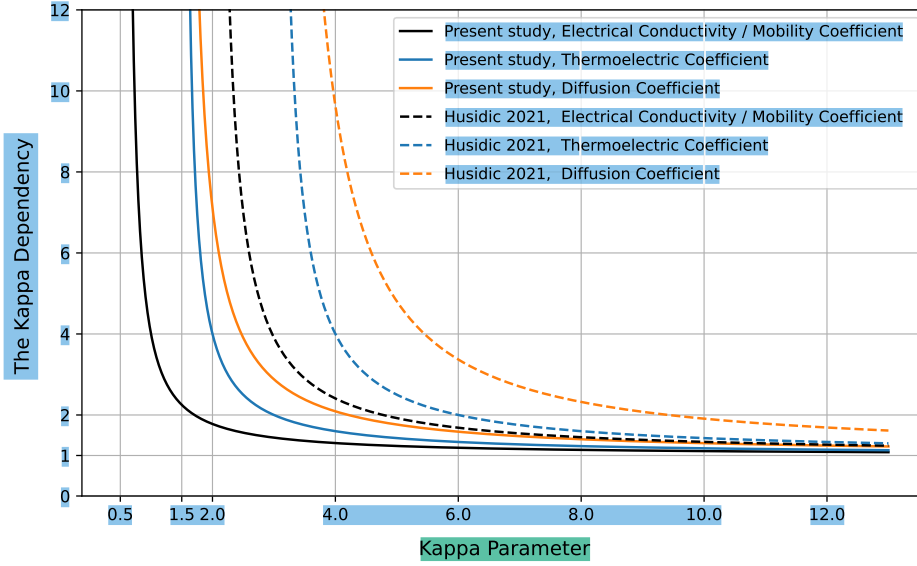


**Figure 9.** Dependence of the electrical conductivity  $\sigma_e$ , mobility coefficient  $\mu_e$ , thermoelectric coefficient  $\alpha_e$ , and diffusion coefficient  $D_e$  on the kappa parameter  $\kappa$  for the standard Kappa distributions in the case of Coulomb collisions.

and diffusion coefficient for the Maxwellian case, and they are defined as:

$$\sigma_e^M = \frac{n_e e^2}{m_e \nu_{ei}}, \quad (47)$$

$$435 \quad \mu_e^M = \frac{k_B T_e}{m_e \nu_{ei}}, \quad (48)$$

$$\alpha_e^M = -\frac{k_B}{e}, \quad (49)$$

$$D_e^M = \frac{e}{m_e \nu_{ei}}. \quad (50)$$

Additionally, the figure also includes a comparison between the present results and those reported by Husidic et al. (2021), highlighting the influence of the kappa parameter on the transport coefficients across different studies.

440 While the figure shows a different dependence on the kappa parameter between the two studies, the overall behaviour is the same: at low  $\kappa$  values, the transport coefficients become much larger than in the Maxwellian case, and as  $\kappa$  increases, they approach the Maxwellian limit. This indicates that plasmas described by a standard Kappa distribution with smaller  $\kappa$  values conduct electric current more efficiently, allow charged particles to move more easily under electric fields, enable particles to diffuse more rapidly, and convert temperature gradients into electric current more effectively.

445 Another similarity between the two studies is that they exhibit the same type of kappa dependence. In both cases, the kappa dependence is identical for the electrical conductivity and mobility coefficients. Additionally, in both studies, the coefficients follow the same general order: the diffusion coefficient shows the strongest kappa dependence, followed by the thermoelectric

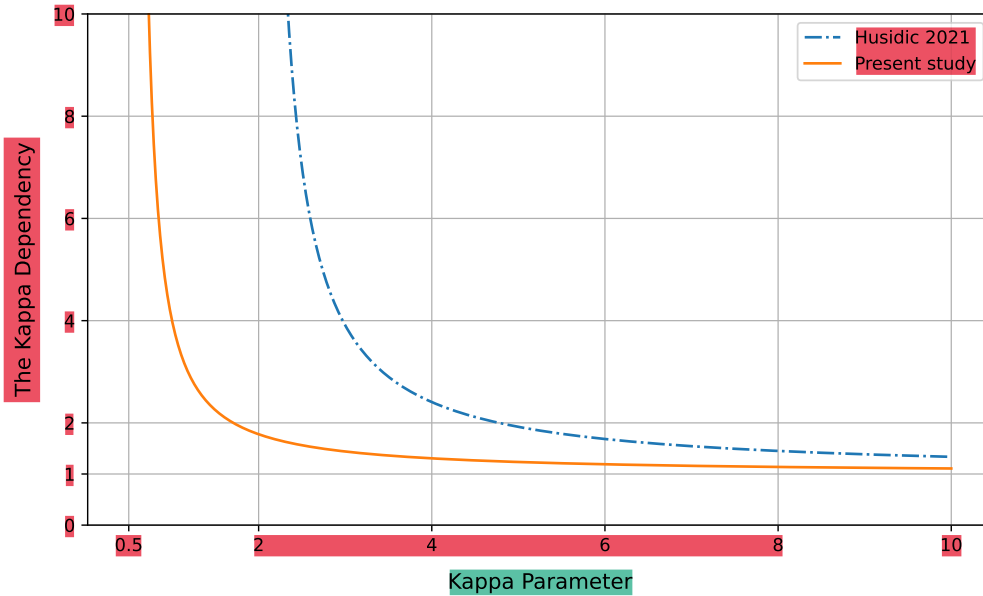


**Figure 9.** The kappa dependency for the electrical conductivity

For the modified Kappa distribution, the transport coefficients were derived by Jwailes et al. (2025). Similar to the standard Kappa distribution, the modified Kappa distribution does not affect the thermoelectric coefficients, and no dependence on the Kappa parameter appears. However, the remaining transport coefficients are influenced through the effective collision frequency, in the same way as for the standard Kappa and Maxwellian distributions. If the collision frequency is independent of particle velocity, the effective collision frequency remains unchanged, and the transport coefficients are identical for the Maxwellian, standard Kappa, and modified Kappa distributions. For collisions in which the collision frequency depends on particle velocity—such as Coulomb collisions or hard-sphere interactions—the effective collision frequency is affected by the modified Kappa distribution. As a result, the transport coefficients acquire a kappa parameter dependence, where the transport coefficient at small kappa values becomes smaller than in the Maxwellian case. This behavior is opposite to that of the standard Kappa distribution, where, as mentioned earlier, small kappa values increase the transport coefficient relative to the Maxwellian case. Figure 10 illustrates this difference by plotting the electrical conductivity as a function of the reduced temperature for the three distributions—Maxwellian, modified Kappa, and standard Kappa. The figure shows that all three distributions exhibit the same general behavior; however, the standard Kappa distribution yields a higher electrical conductivity than the Maxwellian, while the modified Kappa distribution yields a lower value. This difference arises from the redistribution of particle velocities. At low  $\kappa$ , the standard Kappa distribution contains fewer particles in the low-energy core than the Maxwellian, reducing the collision frequency for interactions inversely proportional to velocity, such as Coulomb collisions and hard sphere interactions. This lowers the effective collision frequency and thermalisation rate at low  $\kappa$ . In contrast, the modified Kappa distribution increases the population of core particles, leading to higher collision frequencies for these interactions.

coefficient, and then the electrical conductivity and mobility coefficients, which have the weakest dependence. This ordering arises because the mobility coefficient depends on  $\kappa$  through both the effective temperature and the effective collision frequency, whereas the thermoelectric coefficient depends only on the effective temperature. In contrast, the electrical conductivity and diffusion coefficients depend only on the effective collision frequency.

The difference in the  $\kappa$  dependence between the two studies arises from the collision models used in deriving the transport coefficients. While Husidic et al. (2021) employed a Krook-type collision model, which provides a simplified representation of collisions, our work uses the full Boltzmann collision integral, which offers a more realistic description, particularly for Coulomb collisions.

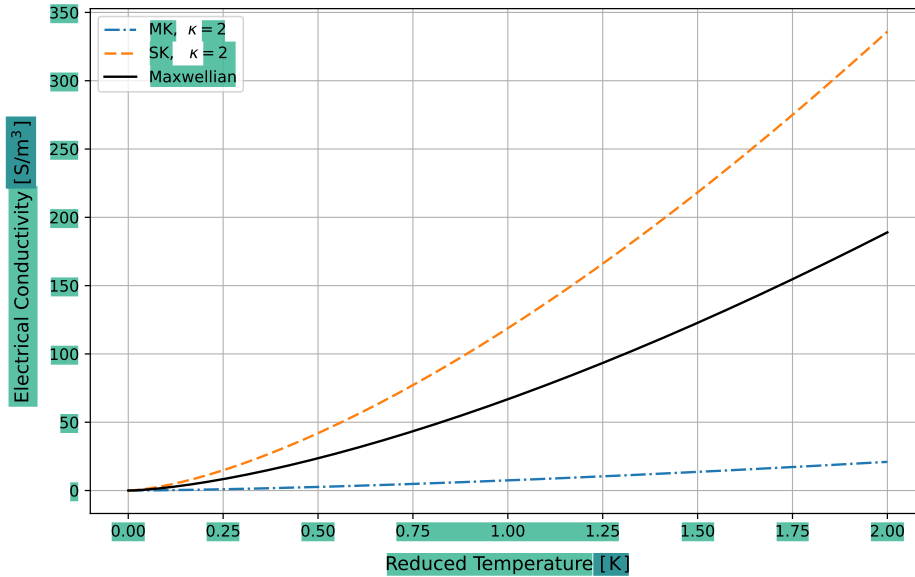


**Figure 10.** The electrical conductivity as a function of reduced temperature  $T_{st}$  for the Maxwellian, modified Kappa, and standard Kappa distributions in case of Coulomb collisions.

For the modified Kappa distribution, the transport coefficients were derived by Jwailes et al. (2025). At first look, we can notice that the  $\kappa$  dependency due to the effective temperature  $T_e^\kappa$ , which appears in both the thermoelectric and diffusion coefficients for the standard Kappa distribution, Eqs. (38) and (40), does not appear in the case of the modified Kappa distribution. Making the thermoelectric coefficient unchanged compared to the Maxwellian case. This behavior arises from the fact that the modified Kappa distribution has the same effective temperature as the Maxwellian distribution.

On the other hand, the remaining transport coefficients in the case of the modified Kappa distribution, similar to the standard Kappa distribution, are influenced through the effective collision frequency. If the collision frequency is independent of particle velocity, the effective collision frequency remains unchanged, and the transport coefficients are not affected by the collision process between the interacting species. For collisions in which the collision frequency depends on particle velocity—such as Coulomb collisions or hard-sphere interactions—the effective collision frequency is affected by the modified Kappa distri-



bution. As a result, the transport coefficients acquire a kappa parameter dependence, where the transport coefficient at small kappa values becomes smaller than in the Maxwellian case. This behavior is opposite to that of the standard Kappa distribution, where, as mentioned earlier, small kappa values increase the transport coefficient relative to the Maxwellian case.

Figure 10 illustrates this difference by plotting the electrical conductivity as a function of the reduced temperature in the case of Coulomb collisions for the Maxwellian, modified Kappa, and standard Kappa distributions. The figure shows that all three distributions exhibit the same general behavior; however, the standard Kappa distribution yields a higher electrical conductivity than the Maxwellian, while the modified Kappa distribution yields a lower value. This difference arises from the redistribution of particle velocities. At low  $\kappa$ , the standard Kappa distribution contains fewer particles in the low-energy core than the Maxwellian, reducing the collision frequency for interactions inversely proportional to velocity, such as Coulomb collisions and hard sphere interactions. This lowers the effective collision frequency at low  $\kappa$ . In contrast, the modified Kappa distribution increases the population of core particles, leading to higher collision frequencies for these interactions.

The results presented in Figure 10 are consistent with those reported in previous studies. In particular, the behavior of the standard Kappa distribution shown in the figure agrees with the findings of Husidic et al. (2021), as also illustrated in Figure 9. For the modified Kappa distribution, similar trends have been reported in earlier work. As discussed in Jwailes et al. (2025), the results are in good agreement with those of Ebne Abbasi et al. (2017). Both studies indicate that plasmas described by a Maxwellian distribution exhibit higher electrical conductivity than those described by a modified Kappa distribution. The reason for this agreement is that Ebne Abbasi et al. (2017) used the Fokker–Planck collision operator, which models Coulomb collisions similarly to the approach used by Jwailes et al. (2025). However, when comparing Jwailes et al. (2025) with the work of Du (2013), the same behavior is not observed. This difference arises because the collision model used in that study is not appropriate for modeling Coulomb collisions. In particular, the simplified approach does not adequately account for the enhanced thermal core of the modified Kappa distribution function; instead, the suprathermal tails dominate the trend of the electric conductivity.

A comparison of the electrical conductivity for three distributions: Maxwellian, modified Kappa, and standard Kappa made by Husidic et al. (2021) reveals a different ordering, as the one shown in Figure 10. The modified Kappa distribution lies between the Maxwellian and the standard Kappa distributions. This is because the simplified Krook-type collision operator does not adequately distinguish between different Kappa distributions. More specifically, it underrepresents the contribution of the enhanced thermal core in the modified Kappa distribution while overemphasizing the role of suprathermal tails. Since the modified Kappa distribution has weaker tails than the standard Kappa distribution but stronger tails than the Maxwellian distribution, its electrical conductivity falls between the two—higher than the Maxwellian case but lower than the standard Kappa case.

Another point of agreement between our results and those of Husidic et al. (2021) concerns the relationship between the electrical conductivity and the mobility coefficient. Specifically, the expressions derived for the electrical conductivity and mobility, given in Eqs. (37) and (41), respectively, for the standard Kappa distribution, satisfy the well-known relation

$$\sigma_e = n_e e \mu_e, \quad (51)$$

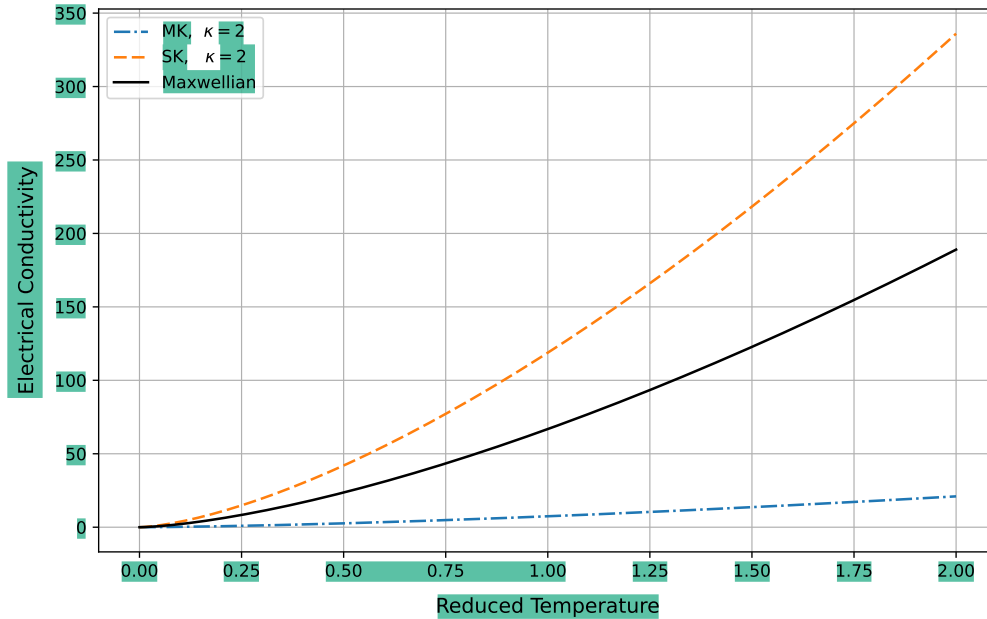


**Figure 10.** The electrical conductivity as a function of reduced temperature  $T_{st}$  for the Maxwellian, modified Kappa, and standard Kappa distributions.

460 Finally, Tables 2, 3 and 4 summarize the main mathematical expressions and low- $\kappa$  physical trends of the collision terms and transport coefficients for the Maxwellian, standard Kappa, and modified Kappa velocity distribution functions for the three types of collisions: Coulomb collisions, hard-sphere interactions, and Maxwell molecule interactions. The tables provide a compact side-by-side comparison of effective collision frequencies, thermalisation rates, momentum and energy exchange, and transport coefficients for both Coulomb collisions and Maxwell molecule interactions, highlighting similarities and differences among the three distributions.

465

500 which also holds for both the modified Kappa distribution and the Maxwellian case. In contrast, the behavior of the thermo-  
electric and diffusion coefficients differs between these distributions. For the modified Kappa distribution and the Maxwellian  
case, these coefficients satisfy the standard Einstein relation,

$$D_e = \frac{k_B T_e}{e} \mu_e. \quad (52)$$

505 However, this relation does not hold for the standard Kappa distribution. Instead, a kappa dependent form of the Einstein  
relation is obtained:

$$D_e = \frac{k_B T_e^\kappa}{e} \mu_e. \quad (53)$$

Here, the influence of the  $\kappa$  parameter appears through the effective temperature. This result is consistent with the findings  
reported in Husidic et al. (2021). Importantly, as the kappa parameter  $\kappa$  approaches infinity, the effective temperature reduces  
to the Maxwellian one, and Eq. (53) reduces to the standard Einstein relation in Eq. (52).

510 The mathematical expressions and the physical trends of the collision terms and transport coefficients for the Maxwellian,  
standard Kappa, and modified Kappa velocity distribution functions for the three types of collisions: Coulomb collisions,  
hard-sphere interactions, and Maxwell molecule interactions, discussed above, are summarized in Tables 2, 3 and 4



**Table 2.** Mathematical and physical comparison between the Maxwellian, standard Kappa, and modified Kappa velocity distribution functions for Coulomb collisions

Feature / Aspect	Maxwellian (M)	Standard Kappa (SK)	Modified Kappa (MK)
Effective collision frequency	$\nu_{st}^{\text{Co}}$	$\nu_{st}^{\text{Co}} \left( \frac{\kappa - 1/2}{\kappa} \right)^2$	$\nu_{st}^{\text{Co}} \left( \frac{\kappa - 1/2}{\kappa - 3/2} \right)^2$
Effective collision frequency behavior at low $\kappa$	Baseline	Lower than Maxwellian	Higher than Maxwellian
Thermalisation rate	$\nu_{ei,T}^{\text{M}} = 2 \frac{m_{ei}}{m_i} \nu_{ei}^{\text{Co}}$	$\nu_{ei,T}^{\text{M}} \left( \frac{\kappa - 1/2}{\kappa} \right)^2$	$\nu_{ei,T}^{\text{M}} \left( \frac{\kappa - 1/2}{\kappa - 3/2} \right)^2$
Thermalisation rate behavior at low $\kappa$	Baseline	Lower than Maxwellian	Higher than Maxwellian
Momentum exchange at low $\kappa$	Baseline	Lower than Maxwellian	Higher than Maxwellian
Energy exchange at low $\kappa$	Baseline	Lower than Maxwellian	Higher than Maxwellian
Thermoelectric coefficient	$\alpha_e^{\text{M}} = -\frac{k_B}{e}$	$\alpha_e^{\text{M}}$	$\alpha_e^{\text{M}}$
Thermoelectric coefficient behavior at low $\kappa$	Baseline	Same as Maxwellian	Same as Maxwellian
Electrical conductivity	$\sigma_e^{\text{M}} = \frac{n_e e^2}{m_e \nu_{ei}^{\text{Co}}}$	$\sigma_e^{\text{M}} \left( \frac{\kappa}{\kappa - 1/2} \right)^2$	$\sigma_e^{\text{M}} \left( \frac{\kappa - 3/2}{\kappa - 1/2} \right)^2$
Electrical conductivity behavior at low $\kappa$	Baseline	Higher than Maxwellian	Lower than Maxwellian
Diffusion coefficient	$D_e^{\text{M}} = \frac{k_B T_e}{m_e \nu_{ei}^{\text{Co}}}$	$D_e^{\text{M}} \left( \frac{\kappa}{\kappa - 1/2} \right)^2$	$D_e^{\text{M}} \left( \frac{\kappa - 3/2}{\kappa - 1/2} \right)^2$
Diffusion coefficient behavior at low $\kappa$	Baseline	Higher than Maxwellian	Lower than Maxwellian
Mobility coefficient	$\mu_e^{\text{M}} = \frac{e}{m_e \nu_{ei}^{\text{Co}}}$	$\mu_e^{\text{M}} \left( \frac{\kappa}{\kappa - 1/2} \right)^2$	$\mu_e^{\text{M}} \left( \frac{\kappa - 3/2}{\kappa - 1/2} \right)^2$
Mobility coefficient behavior at low $\kappa$	Baseline	Higher than Maxwellian	Lower than Maxwellian

**Table 2.** Mathematical and physical comparison between the Maxwellian, standard Kappa, and modified Kappa velocity distribution functions for Coulomb collisions

Feature / Aspect	Maxwellian (M)	Standard Kappa (SK)	Modified Kappa (MK)
Effective collision frequency	$\nu_{st}^{\text{Co}}$	$\nu_{st}^{\text{Co}} \left( \frac{\kappa - 1/2}{\kappa} \right)^2$	$\nu_{st}^{\text{Co}} \left( \frac{\kappa - 1/2}{\kappa - 3/2} \right)^2$
Effective collision frequency behavior at low $\kappa$	Baseline	Lower than Maxwellian	Higher than Maxwellian
Thermalisation rate	$\nu_{ei,T}^{\text{M}} = 2 \frac{m_{ei}}{m_i} \nu_{ei}^{\text{Co}}$	$\nu_{ei,T}^{\text{M}} \left( \frac{\kappa - 1/2}{\kappa} \right)^2$	$\nu_{ei,T}^{\text{M}} \left( \frac{\kappa - 1/2}{\kappa - 3/2} \right)^2$
Thermalisation rate behavior at low $\kappa$	Baseline	Lower than Maxwellian	Higher than Maxwellian
Momentum exchange at low $\kappa$	Baseline	Lower than Maxwellian	Higher than Maxwellian
Energy exchange at low $\kappa$	Baseline	Lower than Maxwellian	Higher than Maxwellian
Thermoelectric coefficient	$\alpha_e^{\text{M}} = -\frac{k_B}{e}$	$\alpha_e^{\text{M}} \left( \frac{\kappa}{\kappa - 3/2} \right)$	$\alpha_e^{\text{M}}$
Thermoelectric coefficient behavior at low $\kappa$	Baseline	Higher than Maxwellian	Same as Maxwellian
Electrical conductivity	$\sigma_e^{\text{M}} = \frac{n_e e^2}{m_e \nu_{ei}^{\text{Co}}}$	$\sigma_e^{\text{M}} \left( \frac{\kappa}{\kappa - 1/2} \right)^2$	$\sigma_e^{\text{M}} \left( \frac{\kappa - 3/2}{\kappa - 1/2} \right)^2$
Electrical conductivity behavior at low $\kappa$	Baseline	Higher than Maxwellian	Lower than Maxwellian
Diffusion coefficient	$D_e^{\text{M}} = \frac{k_B T_e}{m_e \nu_{ei}^{\text{Co}}}$	$D_e^{\text{M}} \left( \frac{\kappa}{\kappa - 3/2} \right) \left( \frac{\kappa}{\kappa - 1/2} \right)^2$	$D_e^{\text{M}} \left( \frac{\kappa - 3/2}{\kappa - 1/2} \right)^2$
Diffusion coefficient behavior at low $\kappa$	Baseline	Higher than Maxwellian	Lower than Maxwellian
Mobility coefficient	$\mu_e^{\text{M}} = \frac{e}{m_e \nu_{ei}^{\text{Co}}}$	$\mu_e^{\text{M}} \left( \frac{\kappa}{\kappa - 1/2} \right)^2$	$\mu_e^{\text{M}} \left( \frac{\kappa - 3/2}{\kappa - 1/2} \right)^2$
Mobility coefficient behavior at low $\kappa$	Baseline	Higher than Maxwellian	Lower than Maxwellian



**Table 3.** Mathematical and physical comparison between the Maxwellian, standard Kappa, and modified Kappa velocity distribution functions for hard sphere interaction

Feature / Aspect	Maxwellian (M)	Standard Kappa (SK)	Modified Kappa (MK)
Effective collision frequency	$\nu_{st}^{\text{HS}}$	$\nu_{st}^{\text{HS}} \left( \frac{\kappa - 1/2}{\kappa} \right)^2$	$\nu_{st}^{\text{HS}} \left( \frac{\kappa - 1/2}{\kappa - 3/2} \right)^2$
Effective collision frequency behavior at low $\kappa$	Baseline	Lower than Maxwellian	Higher than Maxwellian
Thermalisation rate	$\nu_{ei,T}^{\text{M}} = 2 \frac{m_{ei}}{m_i} \nu_{ei}^{\text{HS}}$	$\nu_{ei,T}^{\text{M}} \left( \frac{\kappa - 1/2}{\kappa} \right)^2$	$\nu_{ei,T}^{\text{M}} \left( \frac{\kappa - 1/2}{\kappa - 3/2} \right)^2$
Thermalisation rate behavior at low $\kappa$	Baseline	Lower than Maxwellian	Higher than Maxwellian
Momentum exchange at low $\kappa$	Baseline	Lower than Maxwellian	Higher than Maxwellian
Energy exchange at low $\kappa$	Baseline	Lower than Maxwellian	Higher than Maxwellian
Thermoelectric coefficient	$\alpha_e^{\text{M}} = -\frac{k_B}{e}$	$\alpha_e^{\text{M}}$	$\alpha_e^{\text{M}}$
Thermoelectric coefficient behavior at low $\kappa$	Baseline	Same as Maxwellian	Same as Maxwellian
Electrical conductivity	$\sigma_e^{\text{M}} = \frac{n_e e^2}{m_e \nu_{ei}^{\text{HS}}}$	$\sigma_e^{\text{M}} \left( \frac{\kappa}{\kappa - 1/2} \right)^2$	$\sigma_e^{\text{M}} \left( \frac{\kappa - 3/2}{\kappa - 1/2} \right)^2$
Electrical conductivity behavior at low $\kappa$	Baseline	Higher than Maxwellian	Lower than Maxwellian
Diffusion coefficient	$D_e^{\text{M}} = \frac{k_B T_e}{m_e \nu_{ei}^{\text{HS}}}$	$D_e^{\text{M}} \left( \frac{\kappa}{\kappa - 1/2} \right)^2$	$D_e^{\text{M}} \left( \frac{\kappa - 3/2}{\kappa - 1/2} \right)^2$
Diffusion coefficient behavior at low $\kappa$	Baseline	Higher than Maxwellian	Lower than Maxwellian
Mobility coefficient	$\mu_e^{\text{M}} = \frac{e}{m_e \nu_{ei}^{\text{HS}}}$	$\mu_e^{\text{M}} \left( \frac{\kappa}{\kappa - 1/2} \right)^2$	$\mu_e^{\text{M}} \left( \frac{\kappa - 3/2}{\kappa - 1/2} \right)^2$
Mobility coefficient behavior at low $\kappa$	Baseline	Higher than Maxwellian	Lower than Maxwellian

**Table 3.** Mathematical and physical comparison between the Maxwellian, standard Kappa, and modified Kappa velocity distribution functions for hard sphere interaction

Feature / Aspect	Maxwellian (M)	Standard Kappa (SK)	Modified Kappa (MK)
Effective collision frequency	$\nu_{st}^{\text{HS}}$	$\nu_{st}^{\text{HS}} \left( \frac{\kappa - 1/2}{\kappa} \right)^2$	$\nu_{st}^{\text{HS}} \left( \frac{\kappa - 1/2}{\kappa - 3/2} \right)^2$
Effective collision frequency behavior at low $\kappa$	Baseline	Lower than Maxwellian	Higher than Maxwellian
Thermalisation rate	$\nu_{ei,T}^{\text{M}} = 2 \frac{m_{ei}}{m_i} \nu_{ei}^{\text{HS}}$	$\nu_{ei,T}^{\text{M}} \left( \frac{\kappa - 1/2}{\kappa} \right)^2$	$\nu_{ei,T}^{\text{M}} \left( \frac{\kappa - 1/2}{\kappa - 3/2} \right)^2$
Thermalisation rate behavior at low $\kappa$	Baseline	Lower than Maxwellian	Higher than Maxwellian
Momentum exchange at low $\kappa$	Baseline	Lower than Maxwellian	Higher than Maxwellian
Energy exchange at low $\kappa$	Baseline	Lower than Maxwellian	Higher than Maxwellian
Thermoelectric coefficient	$\alpha_e^{\text{M}} = -\frac{k_B}{e}$	$\alpha_e^{\text{M}} \left( \frac{\kappa}{\kappa - 3/2} \right)$	$\alpha_e^{\text{M}}$
Thermoelectric coefficient behavior at low $\kappa$	Baseline	Higher than Maxwellian	Same as Maxwellian
Electrical conductivity	$\sigma_e^{\text{M}} = \frac{n_e e^2}{m_e \nu_{ei}^{\text{HS}}}$	$\sigma_e^{\text{M}} \left( \frac{\kappa}{\kappa - 1/2} \right)^2$	$\sigma_e^{\text{M}} \left( \frac{\kappa - 3/2}{\kappa - 1/2} \right)^2$
Electrical conductivity behavior at low $\kappa$	Baseline	Higher than Maxwellian	Lower than Maxwellian
Diffusion coefficient	$D_e^{\text{M}} = \frac{k_B T_e}{m_e \nu_{ei}^{\text{HS}}}$	$D_e^{\text{M}} \left( \frac{\kappa}{\kappa - 3/2} \right) \left( \frac{\kappa}{\kappa - 1/2} \right)^2$	$D_e^{\text{M}} \left( \frac{\kappa - 3/2}{\kappa - 1/2} \right)^2$
Diffusion coefficient behavior at low $\kappa$	Baseline	Higher than Maxwellian	Lower than Maxwellian
Mobility coefficient	$\mu_e^{\text{M}} = \frac{e}{m_e \nu_{ei}^{\text{HS}}}$	$\mu_e^{\text{M}} \left( \frac{\kappa}{\kappa - 1/2} \right)^2$	$\mu_e^{\text{M}} \left( \frac{\kappa - 3/2}{\kappa - 1/2} \right)^2$
Mobility coefficient behavior at low $\kappa$	Baseline	Higher than Maxwellian	Lower than Maxwellian



**Table 4.** Mathematical and physical comparison between the Maxwellian, standard Kappa, and modified Kappa velocity distribution functions for Maxwell molecule interactions

Feature / Aspect	Maxwellian (M)	Standard Kappa (SK)	Modified Kappa (MK)
Effective collision frequency	$\nu_{ei}^{MC}$	$\nu_{ei}^{MC}$	$\nu_{ei}^{MC}$
Effective collision frequency behavior at low $\kappa$	Baseline	Same as Maxwellian	Same as Maxwellian
Thermalisation rate	$\nu_{ei,T}^M = 2 \frac{m_{ei}}{m_i} \nu_{ei}^{MC}$	$\nu_{ei,T}^M$	$\nu_{ei,T}^M$
Thermalisation rate behavior at low $\kappa$	Baseline	Same as Maxwellian	Same as Maxwellian
Momentum exchange at low $\kappa$	Baseline	Same as Maxwellian	Same as Maxwellian
Energy exchange at low $\kappa$	Baseline	Higher than Maxwellian	Same as Maxwellian
Thermoelectric coefficient	$\alpha_e^M = -\frac{k_B}{e}$	$\alpha_e^M$	$\alpha_e^M$
Thermoelectric coefficient behavior at low $\kappa$	Baseline	Same as Maxwellian	Same as Maxwellian
Electrical conductivity	$\sigma_e^M = \frac{n_e e^2}{m_e \nu_{ei}^{MC}}$	$\sigma_e^M$	$\sigma_e^M$
Conductivity conductivity behavior at low $\kappa$	Baseline	Same as Maxwellian	Same as Maxwellian
Diffusion coefficient	$D_e^M = \frac{k_B T_e}{m_e \nu_{ei}^{MC}}$	$D_e^M$	$D_e^M$
Diffusion coefficient behavior at low $\kappa$	Baseline	Same as Maxwellian	Same as Maxwellian
Mobility coefficient	$\mu_e^M = \frac{e}{m_e \nu_{ei}^{MC}}$	$\mu_e^M$	$\mu_e^M$
Mobility coefficient behavior at low $\kappa$	Baseline	Same as Maxwellian	Same as Maxwellian

**Table 4.** Mathematical and physical comparison between the Maxwellian, standard Kappa, and modified Kappa velocity distribution functions for Maxwell molecule interactions

Feature / Aspect	Maxwellian (M)	Standard Kappa (SK)	Modified Kappa (MK)
Effective collision frequency	$\nu_{ei}^{MC}$	$\nu_{ei}^{MC}$	$\nu_{ei}^{MC}$
Effective collision frequency behavior at low $\kappa$	Baseline	Same as Maxwellian	Same as Maxwellian
Thermalisation rate	$\nu_{ei,T}^M = 2 \frac{m_{ei}}{m_i} \nu_{ei}^{MC}$	$\nu_{ei,T}^M$	$\nu_{ei,T}^M$
Thermalisation rate behavior at low $\kappa$	Baseline	Same as Maxwellian	Same as Maxwellian
Momentum exchange at low $\kappa$	Baseline	Same as Maxwellian	Same as Maxwellian
Energy exchange at low $\kappa$	Baseline	Higher than Maxwellian	Same as Maxwellian
Thermoelectric coefficient	$\alpha_e^M = -\frac{k_B}{e}$	$\alpha_e^M$	$\alpha_e^M$
Thermoelectric coefficient behavior at low $\kappa$	Baseline	Higher than Maxwellian	Same as Maxwellian
Electrical conductivity	$\sigma_e^M = \frac{n_e e^2}{m_e \nu_{ei}^{MC}}$	$\sigma_e^M \left( \frac{\kappa}{\kappa - 3/2} \right)$	$\sigma_e^M$
Conductivity conductivity behavior at low $\kappa$	Baseline	Same as Maxwellian	Same as Maxwellian
Diffusion coefficient	$D_e^M = \frac{k_B T_e}{m_e \nu_{ei}^{MC}}$	$D_e^M \left( \frac{\kappa}{\kappa - 3/2} \right)$	$D_e^M$
Diffusion coefficient behavior at low $\kappa$	Baseline	Higher than Maxwellian	Same as Maxwellian
Mobility coefficient	$\mu_e^M = \frac{e}{m_e \nu_{ei}^{MC}}$	$\mu_e^M$	$\mu_e^M$
Mobility coefficient behavior at low $\kappa$	Baseline	Same as Maxwellian	Same as Maxwellian



## 5 Conclusions

For a Lorentz plasma described by a standard Kappa distribution, we derive expressions for the transport coefficients: electrical conductivity, thermoelectric, diffusion, and mobility. The analysis begins with a closed system of transport equations for isotropic plasmas within the five-moment approximation. Transport properties are defined relative to the random velocity of each species, with the velocity distribution function expanded in an orthogonal polynomial series about a drifting standard Kappa distribution. By taking only the first term and neglecting higher order moments yields the five-moment approximation. The corresponding momentum and energy collision terms are evaluated via the Boltzmann collision integral for several interaction types, including Coulomb collisions, hard-sphere interactions, and Maxwell molecule collisions. Under suitable assumptions for an unmagnetized, steady-state plasma, explicit expressions for the transport coefficients for the standard Kappa distribution are obtained from the momentum equation.

The methodology adopted in this study is broadly comparable to that of Jwailes et al. (2025), particularly in terms of the formulation of the transport equations, the evaluation of the collision integrals, and the derivation of the transport coefficients. However, a fundamental distinction between the two studies leads to markedly different physical outcomes. While Jwailes et al. (2025) employed a modified Kappa distribution function, the present work is based on the standard Kappa distribution. These two distributions differ substantially in their statistical representation of plasma particle populations, resulting in distinct plasma responses and transport properties. Although the mathematical forms of the governing equations appear similar, the physical interpretation of the quantities involved depends critically on the specific Kappa distribution adopted. This difference motivates the detailed comparative analysis presented in Section 4. That analysis compares three velocity distributions: Maxwellian, standard Kappa, and modified Kappa, across three stages. The first stage examined the effect of the kappa parameter on the effective collision frequency and the thermalisation rate. The second stage focused on how the kappa parameter affects the momentum and energy collision terms for Coulomb collisions. The third stage investigated the impact of the kappa parameter on transport coefficients, including electrical conductivity, diffusion, mobility, and the thermoelectric coefficient. The results of this comparison reveals that the standard Kappa distribution exhibits behavior that is qualitatively different from that of the modified Kappa distribution. For velocity-independent interactions, such as Maxwell molecules, the choice of velocity distribution does not affect the collision frequency or the thermalisation rate. Consequently, the transport coefficients remain identical across all three distributions. In contrast, for velocity-dependent interactions, including Coulomb and hard-sphere collisions, the effects of the kappa parameter become significant. In the standard Kappa distribution, low values of  $\kappa$  lead to a reduction in the effective collision frequency, the number of collisions, and the thermalisation rate. This reduction, in turn, results in enhanced transport coefficients. Conversely, in the modified Kappa distribution, low  $\kappa$  values increase the effective collision frequency and collision rates, which leads to a corresponding reduction in transport coefficients.

While this study advances non-Maxwellian transport theory, it has several limitations. The approach relies on the five-moment approximation, retaining only the first expansion term and neglecting higher-order moments that could affect system behavior. It assumes isotropic plasmas, limiting applicability to real space environments, where magnetization and temperature or pressure anisotropies are common. The Coulomb collision cross-section is simplified using a constant logarithm and

## 5 Conclusions

For a Lorentz plasma described by a standard Kappa distribution, we derive expressions for the transport coefficients: electrical conductivity, thermoelectric, diffusion, and mobility. The analysis begins with a closed system of transport equations for isotropic plasmas within the five-moment approximation. Transport properties are defined relative to the random velocity of each species, with the velocity distribution function expanded in an orthogonal polynomial series about a drifting standard Kappa distribution. By taking only the first term and neglecting higher order moments yields the five-moment approximation. The corresponding momentum and energy collision terms are evaluated via the Boltzmann collision integral for several interaction types, including Coulomb collisions, hard-sphere interactions, and Maxwell molecule collisions. Under suitable assumptions for an unmagnetized, steady-state plasma, explicit expressions for the transport coefficients for the standard Kappa distribution are obtained from the momentum equation.

The methodology adopted in this study is broadly comparable to that of Jwailes et al. (2025), particularly in terms of the formulation of the transport equations, the evaluation of the collision integrals, and the derivation of the transport coefficients. However, a fundamental distinction between the two studies leads to markedly different physical outcomes. While Jwailes et al. (2025) employed a modified Kappa distribution function, the present work is based on the standard Kappa distribution. These two distributions differ substantially in their statistical representation of plasma particle populations, resulting in distinct plasma responses and transport properties. Although the mathematical forms of the governing equations appear similar, the physical interpretation of the quantities involved depends critically on the specific Kappa distribution adopted. This difference motivates the detailed comparative analysis presented in Section 4. That analysis compares three velocity distributions: Maxwellian, standard Kappa, and modified Kappa, across three stages. The first stage examined the effect of the kappa parameter on the effective collision frequency and the thermalisation rate. The second stage focused on how the kappa parameter affects the momentum and energy collision terms for Coulomb collisions. The third stage investigated the impact of the kappa parameter on transport coefficients, including electrical conductivity, diffusion, mobility, and the thermoelectric coefficient. The results of this comparison reveals that the standard Kappa distribution exhibits behavior that is qualitatively different from that of the modified Kappa distribution.

The main distinctions between the results of the standard and modified Kappa distribution functions are summarized as follows: (1) The standard Kappa distribution introduces an explicit dependence on the kappa parameter  $\kappa_s$  through the partial pressure in the five-moment approximation system, whereas this dependence is absent in the modified Kappa distribution. (2) For velocity-independent interactions, such as Maxwell molecules, the choice of velocity distribution does not affect the collision frequency or the thermalization rate. (3) For velocity-dependent interactions, including Coulomb and hard-sphere collisions, low  $\kappa$  values in the standard Kappa distribution reduce the effective collision frequency, the number of collisions, and the thermalization rate, making it suitable for collisionless or weakly collisional environments, while in the modified Kappa distribution, low  $\kappa$  values increase these quantities, indicating its appropriateness for collisional plasmas. (4) As a result, in the case of a Coulomb collision, the standard Kappa distribution leads to weaker momentum and energy exchange compared to the Maxwellian case, whereas the modified Kappa distribution significantly enhances this exchange. (5) The standard Kappa



500 large-velocity approximation, reducing accuracy at low velocities (Fichtner et al., 1996). Additionally, the standard Kappa distribution becomes unphysical for  $\kappa \leq 3/2$ , as the kappa terms D and H diverge, making collision frequency and thermalization rate undefined, so the derived coefficients are valid only for  $\kappa > 3/2$ . Future work should address these limitations by developing a transport theory for the standard Kappa distribution via a generalized polynomial expansion, extending the theory to anisotropic plasmas, incorporating the exact velocity-dependent Coulomb cross-section, and adopting the Regularized Kappa  
505 Distribution (Scherer et al., 2017, 2019) to ensure finite moments and thermodynamic consistency.

*Code availability.* No external or third-party software code was used in this work beyond standard, widely available plotting functions provided by common scientific computing environments. The plotting routines applied in this study consist solely of simple function evaluations and visualizations based directly on the analytical formulas already presented in the paper. All formulas, computational steps, and expressions used to generate the figures are fully described within the paper itself. Because no custom or novel software code was developed and  
510 because the figures can be reproduced entirely from the equations provided, there is no separate software package to archive, cite, or deposit in a public repository.

*Data availability.* This study did not generate or use any external research data. All figures are produced directly from analytical formulas included within the paper, and no numerical datasets were created, collected, or processed. As such, no datasets exist to deposit in a public repository, and no data DOI or persistent URL is applicable.

515 *Author contributions.* M. J. Jwailes proposed the research idea, carried out the theoretical work, derived the framework used to obtain the figures and results, wrote the initial manuscript, and led the discussion of the findings. I. A. Barghouthi supervised the study, verified the validity of the results, and assisted in scientific editing of the manuscript. Q. S. Atawnah contributed to the final revisions of the manuscript.

*Competing interests.* The authors declare that they have no competing interests.

520 *Disclaimer.* The views expressed in this article are solely those of the authors and do not necessarily represent the views of their affiliated institutions.

*Acknowledgements.*

distribution affects transport coefficients through both the effective temperature and the effective collision frequency, while the modified Kappa distribution does so only via the effective collision frequency. (6) In the Coulomb collision case, a plasma described by the standard Kappa distribution exhibits enhanced transport properties as the value of  $\kappa$  decreases. Specifically, lower  $\kappa$  values lead to more efficient electrical conductivity, greater mobility of charged particles in response to electric fields, faster particle diffusion, and a stronger conversion of temperature gradients into electric current compared to the Maxwellian case. In contrast, when the plasma is described by the modified Kappa distribution, decreasing  $\kappa$  produces the opposite effect. Electrical conductivity becomes less efficient, the motion of charged particles under electric fields is more restricted, and particle diffusion is slower than in the Maxwellian case. However, the conversion of temperature gradients into electric current remains unchanged, occurring at the same rate as in the Maxwellian distribution.

While this study advances non-Maxwellian transport theory, it has several limitations. The approach relies on the five-moment approximation, retaining only the first expansion term and neglecting higher-order moments that could affect system behavior. It assumes isotropic plasmas, limiting applicability to real space environments, where magnetization and temperature or pressure anisotropies are common. The Coulomb collision cross-section is simplified using a constant logarithm and large-velocity approximation, reducing accuracy at low velocities (Fichtner et al., 1996). Additionally, the standard Kappa distribution becomes unphysical for  $\kappa \leq 3/2$ , and therefore quantities derived from it, such as the collision frequency, thermalization rate, and transport coefficients, are only physically meaningful for  $\kappa > 3/2$ . This restriction is consistent with the mathematical behavior of the kappa dependent terms D and H, which exhibit divergences: in some cases for  $\kappa \leq 1/2$ , and in others for  $\kappa \leq 3/2$ .

Future work should address these limitations by developing a transport theory for the standard Kappa distribution via a generalized polynomial expansion, extending the theory to anisotropic plasmas, and incorporating the exact velocity-dependent Coulomb cross-section. Alongside these theoretical developments, ongoing research is investigating transport coefficients derived from the regularized Kappa distribution (Scherer et al., 2017, 2019), which ensures finite moments and maintains thermodynamic consistency, including a detailed comparison with the results reported by Husidic et al. (2022). Additionally, comparisons with observational data—particularly from the solar wind—are crucial, with efforts focused on evaluating the predictive accuracy of both the Standard Kappa and Modified Kappa distributions against in-situ measurements.

## Appendix A

The effective collision frequency for Coulomb interactions in the case of a standard Kappa distribution is given by

$$\nu_{st}^{\text{SK}} = \nu_{st} \left( \frac{\kappa - 1/2}{\kappa} \right)^2, \quad (\text{A1})$$

where  $\nu_{st}$  is the effective collision frequency in the Maxwellian case. For Coulomb collisions in a Maxwellian plasma,  $\nu_{st}$  is inversely proportional to the mean free path  $\lambda_{\text{mfp}}$  (Livadiotis, 2019), which represents the average distance a particle travels between successive collisions. Therefore, for a standard Kappa distribution, the effective collision frequency can be expressed



as

$$\nu_{st}^{\text{SK}} \propto \frac{1}{\lambda_{\text{mfp}}} \left( \frac{\kappa - 1/2}{\kappa} \right)^2. \quad (\text{A2})$$

580 The mean free path depends on the Debye length and is proportional to the fourth power of the Debye length divided by the Coulomb logarithm, i.e., (Livadiotis, 2019)

$$\lambda_{\text{mfp}} \propto \frac{\lambda_{\text{D}}^4}{\ln \Lambda}. \quad (\text{A3})$$

Substituting this into the expression for  $\nu_{st}^{\text{SK}}$ , the effective collision frequency scales as

$$\nu_{st}^{\text{SK}} \propto \frac{\ln \Lambda}{\lambda_{\text{D}}^4} \left( \frac{\kappa - 1/2}{\kappa} \right)^2. \quad (\text{A4})$$

585 This scaling can be rewritten in terms of the Debye length for the standard Kappa distribution, as

$$\nu_{st}^{\text{SK}} \propto \frac{\ln \Lambda}{[\lambda_{\text{D}}^{\text{SK}}]^4}, \quad (\text{A5})$$

with  $\lambda_{\text{D}}^{\text{SK}}$  is the Debye length in the case of the standard Kappa distribution, defined as

$$\lambda_{\text{D}}^{\text{SK}} = \lambda_{\text{D}} \left( \frac{\kappa}{\kappa - 1/2} \right)^{1/2}. \quad (\text{A6})$$

Accordingly, the corresponding mean free path in the standard Kappa case is

$$590 \lambda_{\text{mfp}}^{\text{SK}} \propto \frac{[\lambda_{\text{D}}^{\text{SK}}]^4}{\ln \Lambda}. \quad (\text{A7})$$

Thus, the effective collision frequency can also be expressed in the familiar form

$$\nu_{st}^{\text{SK}} \propto \frac{1}{\lambda_{\text{mfp}}^{\text{SK}}}. \quad (\text{A8})$$

This derivation highlights that the kappa-dependent modification of the Debye length is consistent with the results reported in Scherer et al. (2020), providing an independent validation of the physical robustness and internal consistency of the present

595 theoretical framework.

*Code availability.* No external or third-party software code was used in this work beyond standard, widely available plotting functions provided by common scientific computing environments. The plotting routines applied in this study consist solely of simple function evaluations and visualizations based directly on the analytical formulas already presented in the paper. All formulas, computational steps, and expressions used to generate the figures are fully described within the paper itself. Because no custom or novel software code was developed and  
600 because the figures can be reproduced entirely from the equations provided, there is no separate software package to archive, cite, or deposit in a public repository.



*Data availability.* This study did not generate or use any external research data. All figures are produced directly from analytical formulas included within the paper, and no numerical datasets were created, collected, or processed. As such, no datasets exist to deposit in a public repository, and no data DOI or persistent URL is applicable.

605 *Author contributions.* M. J. Jwailes proposed the research idea, carried out the theoretical work, derived the framework used to obtain the figures and results, wrote the initial manuscript, and led the discussion of the findings. I. A. Barghouthi supervised the study, verified the validity of the results, and assisted in scientific editing of the manuscript. Q. S. Atawnah contributed to the final revisions of the manuscript.

*Competing interests.* The authors declare that they have no competing interests.

610 *Disclaimer.* The views expressed in this article are solely those of the authors and do not necessarily represent the views of their affiliated institutions.

*Acknowledgements.* The authors thank the reviewers for their critical reading of the manuscript and for their constructive suggestions, which significantly improved the quality of this work.



## References

- Bittencourt, J.: Fundamentals of Plasma Physics, Springer New York, 3rd ed edn., 2004.
- Collier, M. R. and Hamilton, D. C.: The relationship between kappa and temperature in energetic ion spectra at Jupiter, *Geophysical Research Letters*, 22, 303–306, <https://doi.org/10.1029/94GL02997>, 1995.
- 525 Davis, S., Avaria, G., Bora, B., Jain, J., Moreno, J., Pavez, C., and Soto, L.: Kappa distribution from particle correlations in nonequilibrium, steady-state plasmas, *Physical Review E*, 108, 065 207, <https://doi.org/10.1103/PhysRevE.108.065207>, 2023.
- Du, J.: Transport coefficients in Lorentz plasmas with the power-law kappa-distribution, *Physics of Plasmas*, 20, 092 901, <https://doi.org/10.1063/1.4820799>, 2013.
- 530 Ebne Abbasi, Z. and Esfandyari-Kalejahi, A.: Transport coefficients of a weakly ionized plasma with nonextensive particles, *Physics of Plasmas*, 26, 012 301, <https://doi.org/10.1063/1.5051585>, 2019.
- Ebne Abbasi, Z., Esfandyari-Kalejahi, A., and Khaledi, P.: The collision times and transport coefficients of a fully ionized plasma with superthermal particles, *Astrophysics and Space Science*, 362, 103, <https://doi.org/10.1007/s10509-017-3081-4>, 2017.
- Fichtner, H., Sreenivasan, S. R., and Vormbrock, N.: Transfer integrals for fully ionized gases, *Journal of Plasma Physics*, 55, 95–120, <https://doi.org/10.1017/S0022377800018699>, 1996.
- 535 Formisano, V., Moreno, G., Palmiotto, F., and Hedgecock, P. C.: Solar Wind Interaction with the Earth's Magnetic Field 1. Magnetosheath, *Journal of Geophysical Research (1896-1977)*, 78, 3714–3730, <https://doi.org/10.1029/JA078i019p03714>, 1973.
- Grad, H.: On the kinetic theory of rarefied gases, *Communications on Pure and Applied Mathematics*, 2, 331–407, <https://doi.org/10.1002/cpa.3160020403>, 1949.
- 540 Guo, R. and Du, J.: Transport coefficients of the fully ionized plasma with kappa-distribution and in strong magnetic field, *Physica A: Statistical Mechanics and its Applications*, 523, 156–171, <https://doi.org/10.1016/j.physa.2019.02.011>, 2019.
- Husidic, E., Lazar, M., Fichtner, H., Scherer, K., and Poedts, S.: Transport coefficients enhanced by suprathermal particles in nonequilibrium heliospheric plasmas, *Astronomy & Astrophysics*, 654, A99, <https://doi.org/10.1051/0004-6361/202141760>, 2021.
- Jwailles, M. J., Barghouthi, I. A., and Atawnah, Q. S.: Transport coefficients in modified Kappa distributed plasmas, *Annales Geophysicae*, 43, 783–802, <https://doi.org/10.5194/angeo-43-783-2025>, 2025.
- 545 Lazar, M. and Fichtner, H.: Kappa Distributions: From Observational Evidences via Controversial Predictions to a Consistent Theory of Nonequilibrium Plasmas, *Astrophysics and Space Science Library*, Springer International Publishing, ISBN 9783030826239, <https://books.google.ps/books?id=ZtNSEAAAQBAJ>, 2021.
- Livadiotis, G.: Kappa distributions: Theory and applications in plasmas, Elsevier, 2017.
- 550 Livadiotis, G.: Kappa distributions: Thermodynamic origin and Generation in space plasmas, 1100, 012 017, <https://doi.org/10.1088/1742-6596/1100/1/012017>, 2018.
- Maksimovic, M., Pierrard, V., and Riley, P.: Ulysses electron distributions fitted with Kappa functions, *Geophysical Research Letters*, 24, 1151–1154, <https://doi.org/10.1029/97GL00992>, 1997.
- Marsch, E.: Kinetic Physics of the Solar Corona and Solar Wind, *Living Reviews in Solar Physics*, 3, <https://doi.org/10.12942/lrsp-2006-1>, 2006.
- 555 Mintzer, D.: Generalized Orthogonal Polynomial Solutions of the Boltzmann Equation, *The Physics of Fluids*, 8, 1076–1090, <https://doi.org/10.1063/1.1761357>, 1965.

## References

- Bittencourt, J.: *Fundamentals of Plasma Physics*, Springer New York, 3rd ed edn., 2004.
- 615 Chapman, S. and Cowling, T.: *The Mathematical Theory of Non-uniform Gases: An Account of the Kinetic Theory of Viscosity, Thermal Conduction and Diffusion in Gases*, Cambridge Mathematical Library, Cambridge University Press, 1990.
- Collier, M. R. and Hamilton, D. C.: The relationship between kappa and temperature in energetic ion spectra at Jupiter, *Geophysical Research Letters*, 22, 303–306, <https://doi.org/10.1029/94GL02997>, 1995.
- 620 Collier, M. R., Hamilton, D. C., Gloeckler, G., Bochsler, P., and Sheldon, R. B.: Neon-20, oxygen-16, and helium-4 densities, temperatures, and suprathermal tails in the solar wind determined with WIND/MASS, *Geophysical Research Letters*, 23, 1191–1194, <https://doi.org/https://doi.org/10.1029/96GL00621>, 1996.
- Davis, S., Avaria, G., Bora, B., Jain, J., Moreno, J., Pavez, C., and Soto, L.: Kappa distribution from particle correlations in nonequilibrium, steady-state plasmas, *Physical Review E*, 108, 065 207, <https://doi.org/10.1103/PhysRevE.108.065207>, 2023.
- Du, J.: Transport coefficients in Lorentz plasmas with the power-law kappa-distribution, *Physics of Plasmas*, 20, 092 901, <https://doi.org/10.1063/1.4820799>, 2013.
- 625 Ebne Abbasi, Z. and Esfandyari-Kalejahi, A.: Transport coefficients of a weakly ionized plasma with nonextensive particles, *Physics of Plasmas*, 26, 012 301, <https://doi.org/10.1063/1.5051585>, 2019.
- Ebne Abbasi, Z., Esfandyari-Kalejahi, A., and Khaledi, P.: The collision times and transport coefficients of a fully ionized plasma with superthermal particles, *Astrophysics and Space Science*, 362, 103, <https://doi.org/10.1007/s10509-017-3081-4>, 2017.
- 630 Fichtner, H., Sreenivasn, S. R., and Vormbrock, N.: Transfer integrals for fully ionized gases, *Journal of Plasma Physics*, 55, 95–120, <https://doi.org/10.1017/S0022377800018699>, 1996.
- Formisano, V., Moreno, G., Palmiotto, F., and Hedgecock, P. C.: Solar Wind Interaction with the Earth's Magnetic Field 1. Magnetosheath, *Journal of Geophysical Research (1896-1977)*, 78, 3714–3730, <https://doi.org/10.1029/JA078i019p03714>, 1973.
- Grad, H.: On the kinetic theory of rarefied gases, *Communications on Pure and Applied Mathematics*, 2, 331–407, <https://doi.org/10.1002/cpa.3160020403>, 1949.
- 635 Guo, R. and Du, J.: Transport coefficients of the fully ionized plasma with kappa-distribution and in strong magnetic field, *Physica A: Statistical Mechanics and its Applications*, 523, 156–171, <https://doi.org/10.1016/j.physa.2019.02.011>, 2019.
- Husidic, E., Lazar, M., Fichtner, H., Scherer, K., and Poedts, S.: Transport coefficients enhanced by suprathermal particles in nonequilibrium heliospheric plasmas, *Astronomy & Astrophysics*, 654, A99, <https://doi.org/10.1051/0004-6361/202141760>, 2021.
- 640 Husidic, E., Scherer, K., Lazar, M., Fichtner, H., and Poedts, S.: Toward a Realistic Evaluation of Transport Coefficients in Non-equilibrium Space Plasmas, *The Astrophysical Journal*, 927, 159, <https://doi.org/https://doi.org/10.3847/1538-4357/ac4af4>, 2022.
- Jwailes, M. J., Barghouthi, I. A., and Atawnah, Q. S.: Transport coefficients in modified Kappa distributed plasmas, *Annales Geophysicae*, 43, 783–802, <https://doi.org/10.5194/angeo-43-783-2025>, 2025.
- Lazar, M. and Fichtner, H.: *Kappa Distributions: From Observational Evidences via Controversial Predictions to a Consistent Theory of Nonequilibrium Plasmas*, *Astrophysics and Space Science Library*, Springer International Publishing, ISBN 9783030826239, <https://link.springer.com/book/10.1007/978-3-030-82623-9>, 2021.
- 645 Lazar, M., Fichtner, H., and Yoon, P. H.: On the interpretation and applicability of  $\kappa$ -distributions, *A & A*, 589, A39, <https://doi.org/10.1051/0004-6361/201527593>, 2016.



- Olbert, S.: Summary of Experimental Results from M.I.T. Detector on IMP-1, in: *Physics of the Magnetosphere*, edited by Carovillano, R. L., McClay, J. F., and Radoski, H. R., pp. 641–659, Springer Netherlands, Dordrecht, ISBN 978-94-010-3467-8, [https://doi.org/10.1007/978-94-010-3467-8\\_23](https://doi.org/10.1007/978-94-010-3467-8_23), 1968.
- 560 Pierrard, V. and Lazar, M.: Kappa Distributions: Theory and Applications in Space Plasmas, *Solar Physics*, 267, 153–174, <https://doi.org/10.1007/s11207-010-9640-2>, 2010.
- Pierrard, V., Maksimovic, M., and Lemaire, J.: Core, Halo and Strahl Electrons in the Solar Wind, *Astrophysics and Space Science*, 277, 195–200, <https://doi.org/10.1023/A:1012218600882>, 2001.
- 565 Qureshi, M. N. S., Pallochia, G., Bruno, R., Cattaneo, M. B., Formisano, V., Reme, H., Bosqued, J. M., Dandouras, I., Sauvaud, J. A., Kistler, L. M., Möbius, E., Klecker, B., Carlson, C. W., McFadden, J. P., Parks, G. K., McCarthy, M., Korth, A., Lundin, R., Balogh, A., and Shah, H. A.: Solar Wind Particle Distribution Function Fitted via the Generalized Kappa Distribution Function: Cluster Observations, *AIP Conference Proceedings*, 679, 489–492, <https://doi.org/10.1063/1.1618641>, 2003.
- Scherer, K., Fichtner, H., and Lazar, M.: Regularized  $\kappa$ -distributions with non-diverging moments, *Europhysics Letters*, 120, 50002, <https://doi.org/10.1209/0295-5075/120/50002>, 2017.
- 570 Scherer, K., Lazar, M., Husidic, E., and Fichtner, H.: Moments of the Anisotropic Regularized  $\kappa$ -distributions, *The Astrophysical Journal*, 880, 118, <https://doi.org/10.3847/1538-4357/ab1ea1>, 2019.
- Schunk, R. and Nagy, A.: *Ionospheres: Physics, Plasma Physics, and Chemistry*, Cambridge Atmospheric and Space Science Series, Cambridge University Press, 2009.
- 575 Schunk, R. W.: Mathematical structure of transport equations for multispecies flows, *Reviews of Geophysics*, 15, 429–445, <https://doi.org/10.1029/RG015i004p00429>, 1977.
- Tsallis, C.: Nonadditive entropy  $S_q$  and nonextensive statistical mechanics: Applications in geophysics and elsewhere, *Acta Geophysica*, 60, 502–525, <https://doi.org/10.2478/s11600-012-0005-0>, 2012.
- Vasyliunas, V. M.: A Survey of Low-Energy Electrons in the Evening Sector of the Magnetosphere with OGO 1 and OGO 3, *Journal of Geophysical Research (1896-1977)*, 73, 2839–2884, <https://doi.org/10.1029/JA073i009p02839>, 1968.
- 580 Wang, L. and Du, J.: The diffusion of charged particles in the weakly ionized plasma with power-law kappa-distributions, *Physics of Plasmas*, 24, 102305, <https://doi.org/10.1063/1.4996775>, 2017.

- Lazar, M., Poedts, S., and Fichtner, H.: Destabilizing effects of the suprathermal populations in the solar wind, *A&A*, 582, A124, <https://doi.org/10.1051/0004-6361/201526509>, 2015.
- 650
- Lima, J. A. S., Silva, R., and Plastino, A. R.: Nonextensive Thermostatistics and the  $H$  Theorem, *Phys. Rev. Lett.*, 86, 2938–2941, <https://doi.org/10.1103/PhysRevLett.86.2938>, 2001.
- Livadiotis, G.: Introduction to special section on Origins and Properties of Kappa Distributions: Statistical Background and Properties of Kappa Distributions in Space Plasmas, *Journal of Geophysical Research: Space Physics*, 120, 1607–1619, <https://doi.org/https://doi.org/10.1002/2014JA020825>, 2015.
- 655
- Livadiotis, G.: *Kappa distributions: Theory and applications in plasmas*, Elsevier, 2017.
- Livadiotis, G.: Kappa distributions: Thermodynamic origin and Generation in space plasmas, 1100, 012 017, <https://doi.org/10.1088/1742-6596/1100/1/012017>, 2018.
- Livadiotis, G.: Collision frequency and mean free path for plasmas described by kappa distributions, *AIP Advances*, 9, 105 307, <https://doi.org/10.1063/1.5125714>, 2019.
- 660
- Maksimovic, M., Pierrard, V., and Riley, P.: Ulysses electron distributions fitted with Kappa functions, *Geophysical Research Letters*, 24, 1151–1154, <https://doi.org/10.1029/97GL00992>, 1997.
- Marsch, E.: Kinetic Physics of the Solar Corona and Solar Wind, *Living Reviews in Solar Physics*, 3, <https://doi.org/10.12942/lrsp-2006-1>, 2006.
- 665
- Mintzer, D.: Generalized Orthogonal Polynomial Solutions of the Boltzmann Equation, *The Physics of Fluids*, 8, 1076–1090, <https://doi.org/10.1063/1.1761357>, 1965.
- Olbert, S.: Summary of Experimental Results from M.I.T. Detector on IMP-1, in: *Physics of the Magnetosphere*, edited by Carovillano, R. L., McClay, J. F., and Radoski, H. R., pp. 641–659, Springer Netherlands, Dordrecht, ISBN 978-94-010-3467-8, [https://doi.org/10.1007/978-94-010-3467-8\\_23](https://doi.org/10.1007/978-94-010-3467-8_23), 1968.
- 670
- Pierrard, V. and Lazar, M.: Kappa Distributions: Theory and Applications in Space Plasmas, *Solar Physics*, 267, 153–174, <https://doi.org/10.1007/s11207-010-9640-2>, 2010.
- Pierrard, V., Maksimovic, M., and Lemaire, J.: Core, Halo and Strahl Electrons in the Solar Wind, *Astrophysics and Space Science*, 277, 195–200, <https://doi.org/10.1023/A:1012218600882>, 2001.
- Qureshi, M. N. S., Palloccchia, G., Bruno, R., Cattaneo, M. B., Formisano, V., Reme, H., Bosqued, J. M., Dandouras, I., Sauvaud, J. A., Kistler, L. M., Möbius, E., Klecker, B., Carlson, C. W., McFadden, J. P., Parks, G. K., McCarthy, M., Korth, A., Lundin, R., Balogh, A., and Shah, H. A.: Solar Wind Particle Distribution Function Fitted via the Generalized Kappa Distribution Function: Cluster Observations, *AIP Conference Proceedings*, 679, 489–492, <https://doi.org/10.1063/1.1618641>, 2003.
- 675
- Scherer, K., Fichtner, H., and Lazar, M.: Regularized  $\kappa$ -distributions with non-diverging moments, *Europhysics Letters*, 120, 50002, <https://doi.org/10.1209/0295-5075/120/50002>, 2017.
- 680
- Scherer, K., Lazar, M., Husidic, E., and Fichtner, H.: Moments of the Anisotropic Regularized  $\kappa$ -distributions, *The Astrophysical Journal*, 880, 118, <https://doi.org/10.3847/1538-4357/ab1ea1>, 2019.
- Scherer, K., Husidic, E., Lazar, M., and Fichtner, H.: The  $\kappa$ -cookbook: a novel generalizing approach to unify  $\kappa$ -like distributions for plasma particle modelling, *Monthly Notices of the Royal Astronomical Society*, 497, 1738–1756, <https://doi.org/10.1093/mnras/staa1969>, 2020.
- Schunk, R. and Nagy, A.: *Ionospheres: Physics, Plasma Physics, and Chemistry*, Cambridge Atmospheric and Space Science Series, Cambridge University Press, 2009.
- 685



- Schunk, R. W.: Mathematical structure of transport equations for multispecies flows, *Reviews of Geophysics*, 15, 429–445, <https://doi.org/10.1029/RG015i004p00429>, 1977.
- Tsallis, C.: Nonadditive entropy  $S_q$  and nonextensive statistical mechanics: Applications in geophysics and elsewhere, *Acta Geophysica*, 60, 502–525, <https://doi.org/10.2478/s11600-012-0005-0>, 2012.
- 690 Vasyliunas, V. M.: A Survey of Low-Energy Electrons in the Evening Sector of the Magnetosphere with OGO 1 and OGO 3, *Journal of Geophysical Research (1896-1977)*, 73, 2839–2884, <https://doi.org/10.1029/JA073i009p02839>, 1968.
- Wang, L. and Du, J.: The diffusion of charged particles in the weakly ionized plasma with power-law kappa-distributions, *Physics of Plasmas*, 24, 102 305, <https://doi.org/10.1063/1.4996775>, 2017.
- Yoon, P. H.: Electron kappa distribution and quasi-thermal noise, *Journal of Geophysical Research: Space Physics*, 119, 7074–7087, <https://doi.org/https://doi.org/10.1002/2014JA020353>, 2014.
- 695